Quantitative assessment of exposure risks due to oil spills from shipping in Western Port Bay

Revision 2 – 06/05/2013

Prepared for:
Victorian National Parks Association

Document control form:

Revision	*Originated*	*Edit & review*	*Authorised*	*Date*
Rev A - Issued for internal review	*M. Zapata* *S. Langtry*			*20/12/12*
Rev 0 – Issued for client review		*S. Langtry*		*6/1/12*
Rev 1- Issued with clarifications		*S. Langtry*		
Rev 2- Issued with revisions		*S. Langtry*		*6/5/13*

Document name: J0149 – VNPA Western Port Bay Rev 2

APASA Project Number: J0149

APASA Project Manager: Scott Langtry

Contact Details:

Asia-Pacific Applied Science Associates

ABN: 79 097 553 734

Physical Address: Level 1, 87 Brown Street

East Perth WA 6004

Telephone: +61-8-9221 2911

Facsimile: +61-8-9221 2910

Contents

Figures

Tables

EXECUTIVE SUMMARY

A quantitative oil spill risk assessment was undertaken for spills of fuel oils that would be carried by vessels operating from the Port of Hastings, within Western Port Bay, Victoria, Australia. The assessment was undertaken via numerical modelling, applying a number of advances in sophistication and expected accuracy over previous modelling assessments. This assessment applied:

- a three dimensional hydrodynamic model of Western Port Bay and approaches, applying a fine resolution (80 m) bathymetric grid and representation of the tidal wetting and drying of the intertidal habitats;

- validation of the skill of the hydrodynamic model to represent tidal fluctuations as well as current magnitudes and directions;

- a three-dimensional oil trajectory and weathering model, with capability to model the fate of spilled oil as floating, entrained and dissolved components;

- stochastic modelling of defined spill scenarios, which involved repeated simulating the same scenario given different time-sequences of wind and current conditions. These sequences were selected at random from a 3-year dataset by random selection of spill starting times.

The spill assessment examined three spill scenarios related to shipping operations within Western Port Bay and at the Port of Hastings:

1. A 200 Metric Tonne (MT) spill of Heavy Fuel Oil (HFO) at Long Island Point Jetty, involving an initial release of 100 MT over the first 12 hours with the remaining volume leaking over the next 60 hours (total spill duration of 72 hours).
2. A 200 MT spill of HFO at McHaffie’s Reef, also involving an initial release of 100 MT over the first 12 hours with the remaining volume leaking over the next 60 hours (total spill duration of 72 hours).
3. An 80 m^3 (66 MT) spill of diesel occurring over less than 20 minutes at Long Island Point Jetty.

These scenarios involve conservative volumes of fuel oil compared to volumes that have been spilled in the past from shipping operations in Australia, and could be lost in the future due to ship groundings or collisions with other ships or infrastructure. Diesel fuels tend to be used by support and work vessels, while heavy fuel oils are used as fuel by larger ships.

The hydrodynamic modelling highlighted the exchange of water that occurs between different segments of Western Port Bay, via the connecting channels, the large variations in tidal current speeds that occur spatially and the large fluctuations in the area of inundated seabed that occurs as the intertidal zones wet and dry over tidal cycles.

The spill modelling indicated that oil spilled under any of the spill scenarios has a high probability of spreading widely throughout the estuary system. Spills of Heavy Fuel oil will undergo limited evaporation (< 20%) and the residual oil will tend to remain floating on the water surface, where it will spread and undergo transport under the influence of the prevailing wind and water currents unless the oil strands on shorelines. Fluctuations of the tidal flow will result in oscillations in the flow directions of the floating slicks over periods of around 12 hours, and subsequent flooding tides have the potential to re-float some of the previously stranded oil, resulting in ongoing spread over days to weeks. These processes will increase the areas of intertidal and shoreline habitat that receive exposure to this oil type.

Stochastic simulations of HFO spills indicate that over 80% of the oil mass from an HFO spill could wash ashore over periods of days to a few weeks. Because HFO has a tendency to entrain water to form a highly viscous emulsion, the volume of oily waste may be 50% or greater than the spilled volume. Spills of HFO at Long Point Jetty are most likely to result in oil grounding within Lower and upper North Arm, the shorelines around the confluence zone of the North and East Arm, and the East Basin but could strand on shorelines of most segments of the wider estuary system at > 1 g/m^2 at 1% probability. Spills of HFO at McHaffie's Reef will also present relatively high probability (> 40%) of stranding on shorelines within Lower and Upper arm, but present an increased probability of exposure to the Western Entrance Channel, East Basin habitats, East Arm and the ocean coastline of Port Phillip island and the surrounding mainland, with the west entrance channel being the most likely exit. The north-eastern coastline of Phillip Island is indicated to have a very high probability of accumulating HFO spilled at this location.

Exposure to local shorelines could occur within minutes, if prevailing winds are directly onshore from spill sites at Long Point Island Jetty or McHaffie's Reef, while designated marine reserves and national parks in Western Port Bay could be exposed within less than 6 hours, providing a short time for shoreline protection or other response actions to be put into practice. Booming operations may also be difficult because the high current speeds that typically occur along the main channels may exceed the capability of existing boom designs to contain the oil, resulting in the oil entraining under booms.

Spills of Diesel at Long Point Jetty are indicated to present a high probability of exposure to shorelines within Lower and Northern Arm if they occur during summer and increased probability of exposure to shorelines of the Confluence Zone and East Basin if they occur during winter. Spills of diesel also present a high probability of exposure to the subtidal habitats, because a higher probability of the diesel will mix into the water column as entrained oil droplets. Highest concentrations can be expected at highest probability within Lower North Arm for a spill from Long Point Jetty.

1 INTRODUCTION

Western Port Bay is recognised as a unique feature on the coastline of Victoria in terms of the complex and unusual geometry of this waterway, the wide range of valued habitats that occur closely together in the bay and the extraordinary diversity of wildlife that use these habitats (Melbourne Water 2011).

A detailed review of the physical setting, hydrodynamic patterns, water quality, ecological systems, ecosystem processes and biota of the bay, which was recently undertaken by agencies of the Victorian government, described the many natural assets of the bay and discussed threats that they face due to urban and industrial development of the catchment and waterway (Melbourne Water 2011). Among these threats they listed the introduction and spread of contaminants.

Among the industrial activities that occur within the bay is the operation of commercial and naval shipping, with the major activity centres being Cribb Point and Port Hastings, located on the western shoreline and a shipping channel has been dredged to allow access of deep draft vessels from the western entrance as far upstream as Port Hastings. The Port of Hastings currently handles international and domestic shipping, including import and export of crude oil, Liquid Petroleum Gas, Unleaded Petrol and various bulk cargos (http://www.portofhastings.com/projectupdates.html). Consequentially, ships using these channels and facilities carry substantial loads of oil either as fuel or cargo. Associated tugs and service vessels also carry hydrocarbon fuels of various grades, with regular refuelling operations required at the port. These activities bring with them the potential for oil spills due to collisions, ship groundings, fuel transfer spills or other accidents. Table 1-1 list some of the larger oil spills that have been occurred in Australian waters over the last 4 decades due to shipping operations. Many smaller spills have occurred and many near misses and grounding events have occurred that had the potential to result in significant oil losses. For example, on 4th January 2006, a fully laden oil tanker (114,000 dwt) ran aground while sailing under pilotage into the adjacent Port Phillip, resulting in holing of the forepeak tanks and water ballast tanks (http://www.bluewedges.org.au/index.php?mact=News,cntnt01,detail,0&cntnt01articleid=7&cntnt01returnid=66). A dredging vessel spilled 900 litres of hydraulic oil into Port Phillip Bay in 2008 (http://www.theage.com.au/victoria/dredging-firm-fined-for-oil-spill-20100816-126y2.html). In 2012, the *Lady Cheryl*, a 27m commercial fishing vessel sank in Port Phillip Bay after it hit a submerged reef, leaking an large proportion of the 30 tons of diesel on board (*Lady Cheryl*).

The environmental threat posed by oil spills from shipping operations has been raised by community groups for a number of decades (Brian Cuming, Westernport and Peninsula Protection Council, Pers. Comm.) and efforts have been made to simulate the trajectory of oil spills that might arise from shipping accidents related to the existing operations. These included a number of modelling assessments using general particle-transport models as well as specifically developed oil spill trajectory and fates models (e.g. Greilach, 1993, and unpublished assessments by Jon Hinwood & Tim Pollock of Monash University; Professor Alan Easton, Swinburne Institute of Technology; Dr Kerry Black, Victorian Institute of technology, and others) which lent credence to the potential for widespread exposure of environmentally areas within the bay if a spill were to occur at point sources within the shipping areas. These investigations have been included in submissions to government organisations and numerous committees of enquiry. At a later stage, Asia-Pacific Applied Science Associates (APASA) were commissioned by the Marine Safety Victoria to undertake a modelling study to quantify exposure risks associated with ship-based spills, specifically to assess the net environmental benefits of applying oil dispersants onto oil slicks generated along the shipping channel of at Port Hastings. This study, which used a purposely developed, 3-dimensional, oil spill behaviour model indicated that spilled oil could become widely spread within the bay by tidal and wind forces and that chemical treatment would likely have a net negative impact – likely increasing exposure to subtidal habitats over a wider area at higher concentrations while not substantially reducing the likelihood of exposure to intertidal and shoreline habitats (Zigic *et. al*. 2011). These past modelling efforts all used relatively coarse representations of circulation within the bay and, therefore, although these studies indicated consistent outcomes, the veracity of the studies might be subject to challenge.

The Victorian Government has now committed to expansion of shipping operations within Western Port Bay, with plans to establish the port as a major container terminal with the expectation that container movements into and out of Victoria will quadruple over the next 30 years leading to over-ingestion at the neighbouring Port of Melbourne (http://www.portofhastings.com/). This development would result in increased shipping traffic along the channel and within the port as well as increases in support vessel operations, increasing the opportunities for oil spills within or approaching the port.

The Victorian National Parks Association (VNPA) commissioned APASA to undertake a quantitative assessment of exposure risks to the natural resources of Western Port Bay, Victoria (Figure 1-1) if oil spills were to occur from shipping operations associated with the Port of Hastings applying more sophisticated hydrodynamic and oil spill modelling techniques.

VNPA identified 3 spill scenarios for investigation that might occur from shipping operations either at the Port of Hastings or along the shipping channel that vessels would traverse to and from the port:

4. A 200 Metric Tonne (MT) spill of Heavy Fuel Oil (HFO) at Long Island Point Jetty, involving an initial release of 100 MT over the first 12 hours with the remaining volume leaking over the next 60 hours (total spill duration of 72 hours).

5. A 200 MT spill of HFO at McHaffie's Reef, also involving an initial release of 100 MT over the first 12 hours with the remaining volume leaking over the next 60 hours (total spill duration of 72 hours).

6. An 80 m^3 (66 MT) spill of diesel occurring over less than 20 minutes at Long Island Point Jetty.

Scenario 1 and 2 are indicative of conservative volumes of fuel oil that might leak from ships due to accidental damage to fuel tanks, such as might result from a ship grounding or collision with another ship or with the port infrastructure. The volumes assumed are considered conservative compared with the magnitude of many spills that have previously occurred from shipping operations in Australian waters (Table 1-1). The initial pulse specified in these scenarios is to represent the initially fast loss as the head of pressure in fuel tanks reduced, while the latter phase is to represent ongoing leakage at a reduced rate. Scenario 3 is indicative of fuel leakage from smaller support vessels, such as tugs and crew boats.

The oil spill modelling was performed using the SIMAP three-dimensional spill trajectory and weathering model (French *et. al*. 1994, 1997, 1999, French 2000, French McCay 2004), which is designed to simulate the transport, spreading and weathering of specific oil types under the influence of changing meteorological and oceanographic forces in order to determine potential exposure to natural resources. SIMAP is a development of the Natural Resource Damage Assessment model (French *et. al*. 1996) and has been applied widely in Australia and other countries to assess risks associated with oil handling operations, support oil spill response and to hind-cast the outcomes of real spill events.

The SIMAP model uses the unique physical and chemical properties of an oil type to calculate rates of evaporation, spreading and changes in density and viscosity, including the tendency to form oil-in-water emulsions, if appropriate for the oil type. Moreover, the unique transport and dispersion of surface slicks and in-water components (entrained and dissolved) are modelled separately. Thus, the model can be used to understand the wider potential consequences of a spill, including direct contact to slick oil for surface features as well as exposure to entrained oil droplets and/or dissolved hydrocarbons for organisms in the water column.

Oil spills, by their nature, are unpredictable in terms of their timing relative to prevailing conditions, hence there will tend to be a wide range of possible conditions and hence a wide range of outcomes of an accidental spill, in terms of the locations that are affected by oil, the degree of weathering of the oil at the point of arrival, what concentrations are involved and how long exposure persists. It is therefore necessary to consider a wide range of the potential conditions that might prevail immediately before, during and after an accidental spill, in order to objectively quantify the probability of particular outcomes. A stochastic modelling scheme was followed in this study to capture the variability in potential spill outcomes and identify the more likely outcomes. SIMAP was applied to repeatedly simulate the defined spill scenarios using different samples of current and wind data. These data samples were selected randomly from a historic time series of wind and current data representative of the study area. The results of the replicate simulations were then statistically analysed and mapped to define contours of risk around the release point.

Transport of floating oil will be affected by a combination of the forces exerted by the prevailing water current (acting on the underside of the slick) and the prevailing wind (acting on the oil surface), while the transport of entrained and dissolved components will be affected solely by the prevailing water currents at the depth where these components are located.

To provide a suitably robust sample of the range of potential conditions, an archive of spatially-variable wind and current data spanning 3 continuous years (2009-2011, inclusive) was assembled for the study region. Current data consisted of three-dimensional current fields that were generated using a detailed (80 m resolution), three-dimensional hydrodynamic model of Western Port Bay that represented the tidal wetting and drying of the extensive intertidal zones. Wind data were historic measurements of the wind speed and direction over the data period from the Cerberus and Rhyll Meteorological Stations.

Analysis of wind conditions over Western Port Bay highlighted the reversal of prevailing wind conditions between the summer (November to February) and winter (May to August) months. To avoid averaging out the probabilities of contact that would result from these seasonal differences and to highlight risks in each of the major seasons, modelling was carried out using current and wind data sampled from the data archive for periods commencing in both Summer and Winter by random selection of the spill starting time. Simulations were run to represent the fate of each replicate spill for 10 days, using 10-day long sequences of wind and current data sampled at random from the longer run data archive. Outcomes were analysed separately for simulations commencing in each seasonal period, to differentiate risks of contact at surrounding locations for spills commencing during each period. The modelled scenarios are summarised in Table 1-2.

Table 1-1: History of major oil spills since 1970 resulting from shipping operations in Australian waters (Sources: Australian maritime Safety Authority and Australian Transport Safety Bureau)

Date	Vessel	Location	Spill estimate
03/03/1970	*Oceanic Grandeur*	Torres Strait QLD	1,100 tonnes
26/05/1974	*Sygna*	Newcastle, NSW	700 tonnes
14/07/1975	*Princess Anne Marie*	Offshore, WA	14,800 tonnes
10/09/1979	*World Encouragement*	Botany Bay NSW	95 tonnes
29/10/1981	*Anro Asia*	Bribie Island QLD	100 tonnes
22/01/1982	*Esso Gippsland*	Port Stanvac SA	unknown
03/12/1987	*Nella Dan*	Macquarie Island	125 tonnes
06/02/1988	*Sir Alexander Glen*	Port Walcott, WA	450 tonnes
20/05/1988	*Korean Star*	Cape Cuvier WA	600 tonnes
28/07/1988	*Al Qurain*	Portland VIC	184 tonnes
21/05/1990	*Arthur Phillip*	Cape Otway VIC	unknown
14/02/1991	*Sanko Harvest*	Esperance WA	700 tonnes
21/07/1991	*Kirki*	WA	17,280 tonnes
30/08/1992	*Era*	Port Bonython SA	300 tonnes
10/07/1995	*Iron Baron*	Hebe Reef TAS	325 tonnes
28/06/1999	*Mobil Refinery*	Port Stanvac SA	230 tonnes
26/07/1999	*MV Torungen*	Varanus Island, WA	25 tonnes
03/08/1999	*Laura D'Amato*	Sydney NSW	250 tonnes
18/12/1999	*Sylvan Arrow*	Wilson's Promontory VIC	<2 tonnes
02/09/2001	*Pax Phoenix*	Holbourne Island, QLD	~ 1000 tonnes
25/12/2002	*Pacific Quest*	Border Island , QLD	>70 km slick
24/01/2006	*Global Peace*	Gladstone, QLD	25 tonnes
11/03/2009	*Pacific Adventurer*	Cape Moreton, QLD	270 tonnes
03/04/2010	*Shen Neng1*	Great Keppel Island QLD	4 tonnes
09/01/2012	*MV Tycoon*	Christmas Island	102 tonnes
2011-2012	*GL Lan Xiu*	Hamilton, Brisbane, QLD	5 tonnes
2011-2012	Tug *Terlak*	Mackay Harbour, QLD	2 tonnes

Table 1-2: Summary of modelled scenarios.

ID	Oil Type	Spilled Volume (MT)	Location	Release Depth	Spill Duration	Simulation Duration (days)	Season
1	Heavy Fuel Oil	200	Long Point jetty	Surface	3 days	10	Summer
							Winter
2	Heavy Fuel Oil	200	McHaffie's Reef	Surface	3 days	10	Summer
							Winter
3	Diesel	66	Long Point jetty	Surface	<20 min	10	Summer
							Winter

The SIMAP spill modelling accounted for the unique physical and chemical properties of specific oil types. These properties included the density and viscosity of the whole oil mixture, the breakdown by boiling point and the proportion of the oil mass represented by soluble aromatic compounds. The model also accounted for the release conditions specified in the scenario. For scenarios involving discharge onto the water surface, the model accounted for the spreading of surface films and the varying evaporation rates of volatile and semi-volatile components, leading to changes in the physical and chemical properties of the remnant oil that will affect their subsequent weathering and response to physical forces.

It is important to note that the modelling results presented in this document relate to the predicted outcomes once a spill event has occurred and, therefore, the results should be viewed as a guide to the likely outcomes should such an event occur. The probability of occurrence of a spill event must also be considered when assessing the overall risk to environmental resources.

Furthermore, the study does not attempt to quantify the environmental consequences of exposure, which should consider the potential for the reported concentrations to cause harm to the resources. This assessment provides guidance for such an assessment taking account of the sensitivity of particular resources.

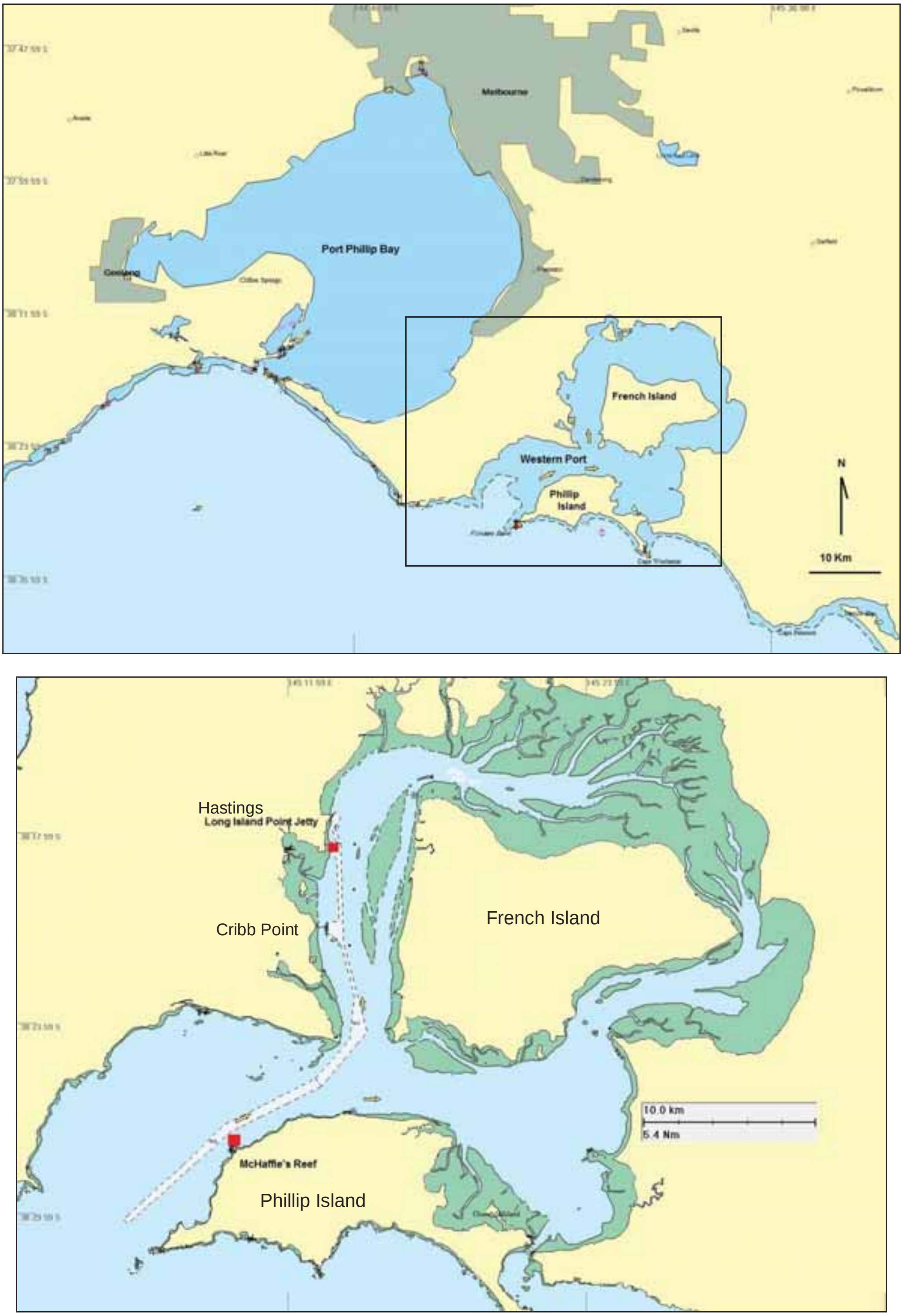

Figure 1-1: Setting for the risk assessment - Western Port Bay, Victoria. The upper image shows the regional setting on the Victorian coastline. The lower image shows the general waterway at Lowest Astronomical Tide (LAT) level in blue with the extent to Highest Astronomical Tide (HAT) shown in green. Red markers indicate the hypothetical spill locations applied in the study. The existing shipping channel from the western entrance to the Port of Hastings is shown in pale blue with a hatched outline.

2 BACKGROUND TO THE STUDY REGION

2.1 Circulation patterns

Western Port Bay is a complex embayment with an area of approximately 680 km^2, of which two-fifths (an estimated 270 km^2) consists of highly channelised intertidal mudflats. The bay connects to Bass Straight through two entrances of unequal size and includes two major islands that effectively create a complex channel network for tidal flow. The total length of coastline, including French and Phillip Islands, is about 263 km (CSIRO 2003) but with a large variation in the effective coastline depending upon the state of the tide.

The hydrodynamic processes within Western Port Bay have been the subject of a number of studies described in Harris (1979), Marsden (1979), Sternberg (1979), Hinwood and Jones (1979), Hancock (2001) and EPA (2011). The waters of the bay have previously been divided into several functional segments based upon physical characteristics, particularly the topography and flow characteristics (Marsden *et al* 1979; Figure 2-1). These segments are:

- Lower North Arm, bounded by the Sandy Point constriction in the south and Eagle Rock constriction in the north-east
- Upper North Arm, bounded by Eagle Rock constriction in the west and Stockyard Point constriction in the east
- Corinella, bounded by the Stockyard Point constriction in the north and the Settlement Point constriction in the south
- Rhyll, bounded by the Settlement Point constriction in the north and the Cowes confluence zone in the west
- Western Entrance Zone, bounded by Flinders Point on the Bass Strait entrance and the Sandy Point constriction in the north-east

One of the more influential morphological features of Western Port Bay is the arrangement of channels leading from the deep ocean entrances to the large expanse of intertidal wetlands and mud banks at the back of the bay. Tides flooding through the larger western channel divide around French Island to form two estuary arms that flood through braided channels to meet over the extensive mudflats over the north-eastern sector of the bay, a region referred to as the Embayment Head; Figure 2-1. Ebbing tides then recede through the braided channels in the opposite directions to expose the mudflats.

The Victorian government review of Western Port Bay (Melbourne Water, 2011) highlighted the importance of water-circulation patterns within the bay in affecting the exchange of nutrients, sediment, larvae and contaminants and listed among the priority requirements for improved understanding and management of human impacts on Western Port Bay the further development of calibrated hydrodynamic models to represent accurate water movement. An understanding of the circulation processes in Western Port Bay is also essential in determining the expected movement of hydrocarbons within the bay.

A number of hydrodynamic models have been developed for Western Port Bay since the 1970's. Early models of the bay were simplistic, spatially-coarse, two-dimensional, models that assumed a fixed coastline (not changing with tidal inundated; Hinwood & O'Brien 1974, Hinwood 1979). While these models represented the general circulation under the influence of tide and wind forcing with some skill, they lacked suitable realism. The coarse scale (square grid cells of several hundreds of metres) of these models meant that they could only represent general flow patterns over highly-smoothed representations of the bathymetry. Thus, they could not show variations of flow in response to finer bathymetric details such as small banks and channels. Being two-dimensional, they also produced depth-averaged estimates of the current flows that would vary from those at specific depths of interest, such as the surface layer, or near-bed layer. By assuming a fixed coastline they did not allow for the full exchange of water due to the filling and draining of the water-shed provided by tidally inundated areas, leading to underestimation of tidal current speeds through the channels. Moreover, these models could not represent the drying out of the large extent of shallow intertidal areas at low tide, particularly over the north-eastern section of the bay, which results in marked variations in local flow patterns with tidal state.

Later, more sophisticated, models that were developed to investigate exchange between the land catchment and the bay waters also applied relatively coarse, two-dimensional hydrodynamic models of Western Port Bay on the assumption that 2-dimensional models were adequate for systems that are not strongly density stratified (EPA 2011). However, this ignored the depth-varying influence of wind shear (acting on the surface) and frictional drag (acting at the seabed) that will be relevant when modelling for substances that would occupy particular depth levels, such as spilled oil.

The most sophisticated hydrodynamic model that has been developed for Western Port Bay to date is a model developed by ASR Ltd for the Victorian EPA to inform the Better Bays and Waterways Water Quality Improvement Plan (EPA 2011, Melbourne Water 2011). This model, which has been titled the Receiving Water Quality Model (RWQM), was designed to investigate a wide range of water quality phenomena and is a 3-dimensional hydrodynamic model built on a more detailed and accurate bathymetric model of the bay and includes specification of density and thermal stratification with atmospheric heating and cooling. The net circulation patterns produced by this model more closely resembles the observed circulation within the bay and reveals the effect of channels in affecting circulation within and among the sub-basins. This model also better represents the complex tidal flooding and draining that occurs in the north-eastern section of the bay. While earlier models indicated a net movement of the water in the bay that was clockwise around French Island (Figure 2-2), residual flows calculated by the more detailed RWQM model indicates that circulation patterns are more complex, with both clockwise and anticlockwise flows along each estuary. This more detailed model also better represents the periodic flooding and draining at the Embayment Head, as well as the regular extension and retraction of other intertidal areas due to tidal fluctuations (Figure 2-3).

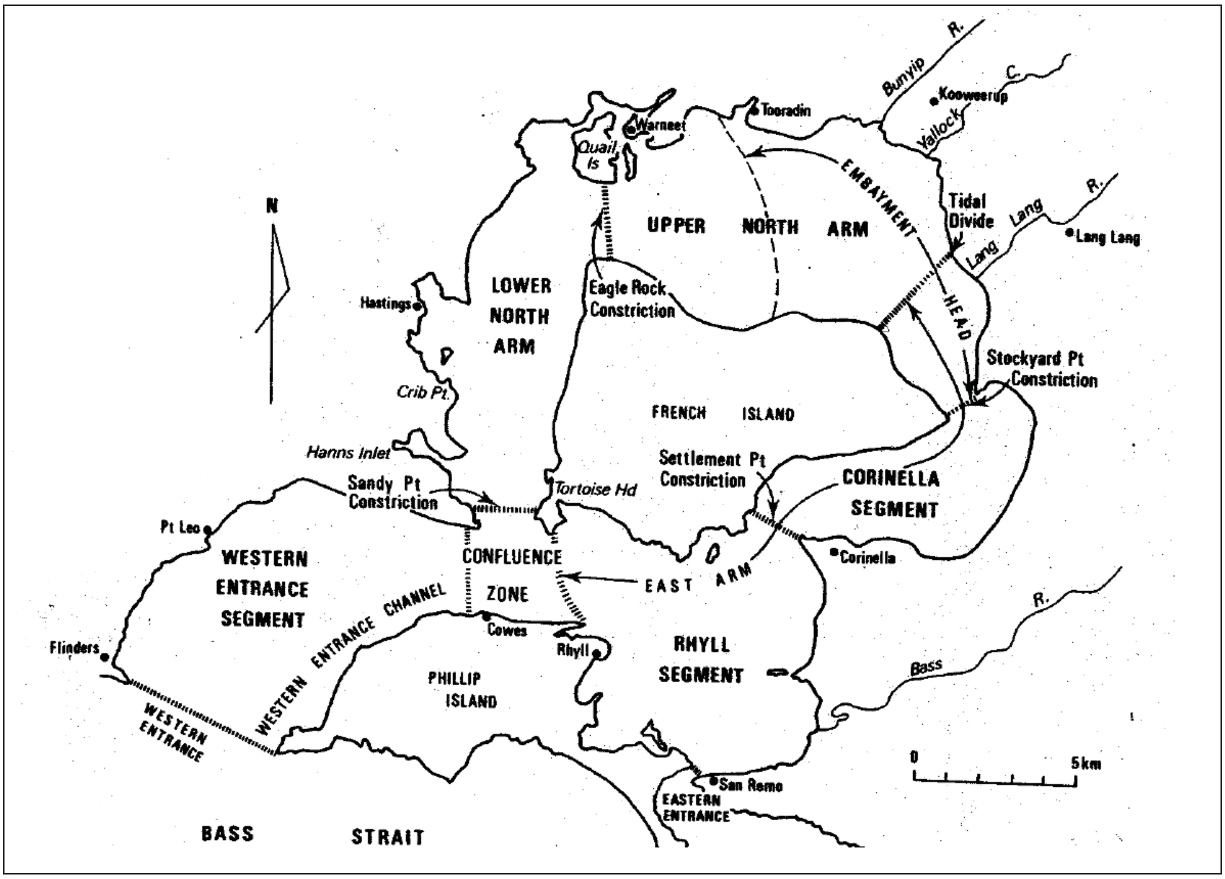

Figure 2-1: Regional distinctions of Western Port Bay (from Marsden et al., 1979).

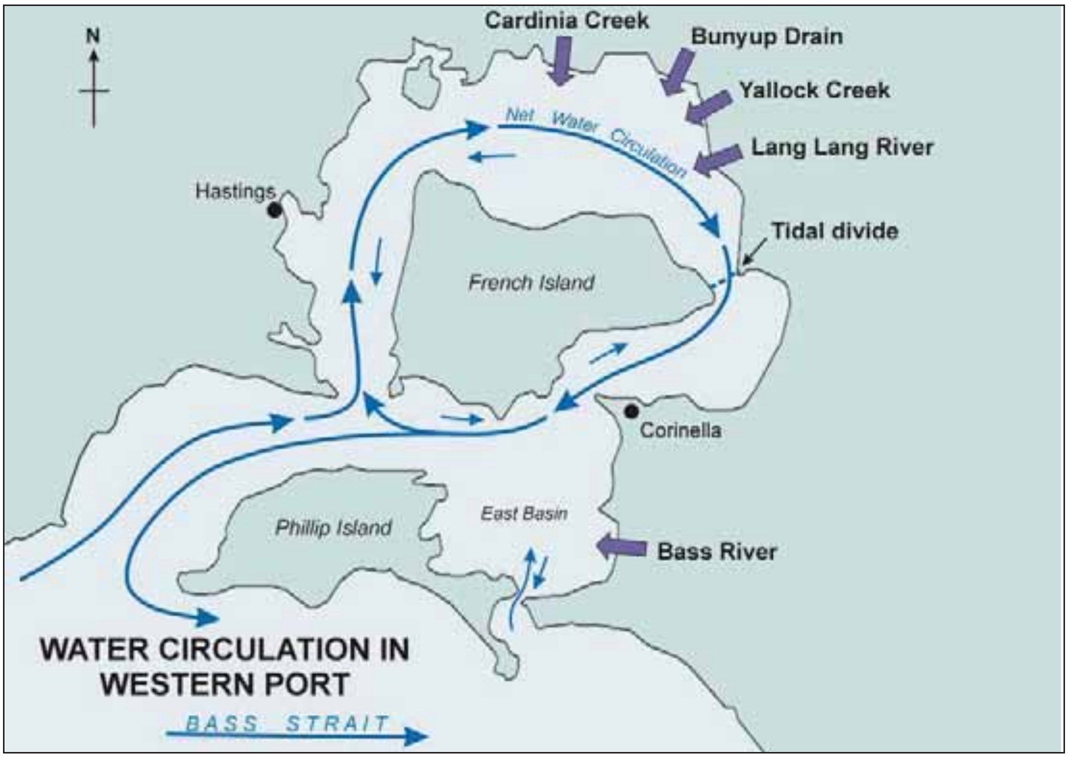

Figure 2-2: Residual water circulation in Western Port Bay according to Hancock et al. (2001).

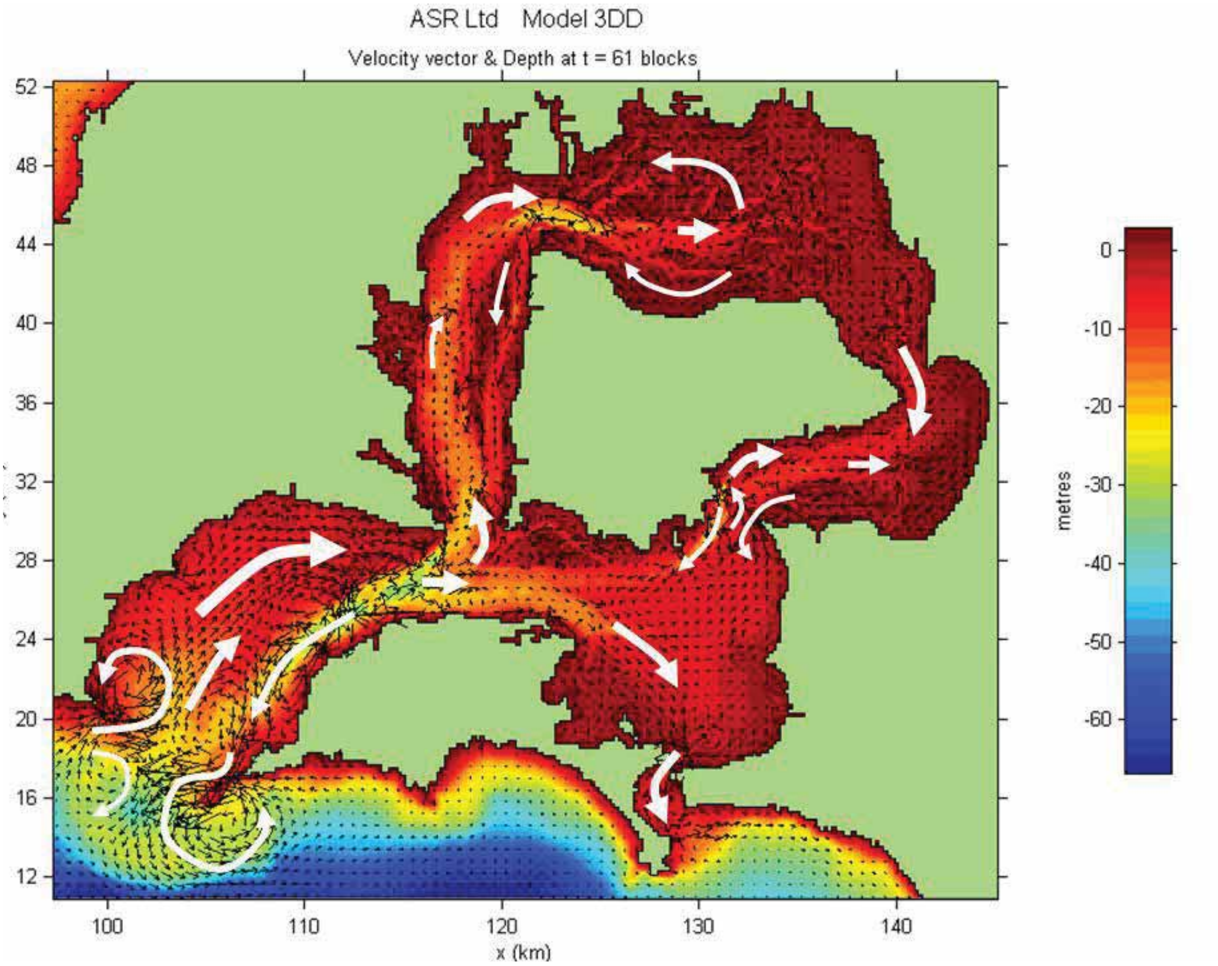

Figure 2-3: Improved representation of residual water circulation in Western Port Bay, according to the RWQM (EPA 2011, Melbourne Water 2011).

Hydrodynamic models are best prepared for their intended purpose and findings from the RWQM model, in particular, provided good guidance for the effective representation of circulation within Western Port Bay necessary for oil spill modelling.

Water movement within the bay is complexly affected by the bathymetry of the waterway with circulation dominated by tidal exchange with the ocean, indicating that the model should be defined on a high resolution grid (< 100 m scale) with good representation of the bathymetry at this scale. Further, the model domain should extend seaward into the open ocean a suitable distance to best represent tidal exchange. Accurate representation of tidal waves entering the boundaries of the model domain would be necessary to accurately represent variation in tidal exchange over tidal and lunar (spring-neap) cycles. There would also be a requirement for accurate representation of the watershed volume necessary to accurately represent tidal propagation through the bay, indicating that it is also critical to represent tidal wetting and drying across the intertidal zone rather than assume a fixed coastline. Representation of tidal wetting and drying is also necessary to realistically represent the interaction of oil with the intertidal areas of the bay. Observations and experiments with the RWQM model reveal seasonal as well as short-term response to wind forcing that vary across the waterway and are stronger outside of the channels (EPA 2011) and large effects of the wind would be expected at the water surface, where the wind effect is directly exerted, indicating the requirements for both detailed representation of wind forcing at high frequency and calculation of depth-varying (3-dimensional) current fields that account for the propagation of wind-shear and seabed drag vertically.

Although salinity differences are set up by evaporation over the shallow mudflats and heating and cooling have been shown experimentally to have periodic effects on circulation in some areas, efforts to calibrate to these forces have not been highly successful despite considerable effort (EPA 2011). Moreover, the influence of circulation due to these effects on the fate of spilled oil was assumed to be low, compared to wind and tidal forcing, indicating that stratification effects could be ignored in the hydrodynamic model without compromising forecasts for the trajectory of spilled oil, particularly if at the water surface.

2.2 Habitat distributions

An important detail for the assessment of risk and consequence of particular oil spill scenarios within Western Port Bay is the distribution of sensitive environmental resources within the estuary system. The review of the Western Port Bay Environment undertaken by agencies of the Victorian Government (Melbourne Water 2011) mapped the distribution of a number of habitats that would be sensitive to oil exposure.

Mangrove and saltmarshes occur along the margins and embayments of the west and north coasts of Lower North Arm and Upper North Arm, along the north and west coastline of French island and within Rhyll inlet on the north-eastern end of Phillip Island (Figure 2-4; See Figure 2-1 for location details). Significant coverage of saltmarshes also occur on the east and west coastlines of the East Basin (Figure 2-2). The vertical distribution of these habitats, ranging from the upper intertidal to supratidal (Melbourne Water 2011), indicates that the lower growing assemblages might be exposed to floating, entrained or dissolved oil that arrives at higher tidal levels, while the higher growing assemblages, including the saltmarshes, would require coincidence of oil arrival with high spring tides, except where small drainage channels provide entry points for oil arriving at lower tidal levels.

A number of species of seagrasses occur over a wide area of the Western Entrance Segment, along Lower and Upper North Arm and around the Eastern Basin (Rhyll Segment) extending along the eastern shoreline of the Corinella Segment past Corinella (Figure 2-5; see Figures 2-1 and 2-2 for locational references). The vertical distribution of these seagrasses extends from the upper intertidal to the shallow subtidal, with large areas of seagrass exposed at low tide levels (Melbourne Water 2011). This range of vertical distributions places seagrass beds at risk of exposure to floating, entrained and dissolved oil arriving at any tidal level, with exposure to different vertical zones varying as the tide level changes. The potential for stranding of oil on exposed seagrass beds and the unconsolidated mud banks, being trapped in shallow pools that occur on the exposed areas as the tide recedes, and of oil mixing down into the sediment and invertebrate burrows within these habitats is also presented. Oil that does not bind to the sediments will tend to be redistributed as the tide rises again, potentially contaminating other areas, while oil that enters the sediment may remain as a persistent source of hydrocarbon contamination for years to decades.

Rocky intertidal and subtidal reefs are mostly confined to the offshore coastline on the western side of the West Entrance and the eastern side of the East Entrance, but also represent a large part of the coastline along the east and south coasts of Phillip Island (Figure 2-6; see Figures 2-1 and 2-2 for locational references). Smaller areas of intertidal platforms also occur further along the estuary, mostly at local points where they extend into the waterway beyond the soft sediments. The vertical distribution of the intertidal reefs places them at risk of exposure to floating, entrained and dissolved oil. Floating oil can strand onto exposed reefs, or pool in local rock pools, with this exposure migrating vertically as the tide changes. If waves are present, floating oil that is washed ashore has the potential to be mixed into the water column, exposing sections of the reef that are below the tide level to entrained and dissolved oil. The subtidal reefs will not be at risk of exposure to floating oil but shallow subtidal reefs (< ~ 3 m below MSL) have the potential for exposure to entrained oil that is mixed into the water column by wave action, as well as to oil compounds that are dissolved into the water column.

Large areas of Western Port Bay are important feeding areas for wading, roosting and other aquatic birds, both migratory and resident (Figure 2-7). These areas largely correspond with the areas occupied by intertidal seagrasses, unvegetated sediment and saltmarsh within Lower and North Arm, and along East Arm to the Embayment Head, as well as the intertidal zones surrounding the East Basin. Exposure of these areas by oil arriving as slicks presents direct risks to waterbirds in the effected locations, through physical contact and contamination of their feathers, leading to hypothermia, drowning, physical impairment or poisoning through ingestion of oil when effected birds attempt to preen (AMSA undated). Longer term risks from the arrival of slick oil into these habitats may include reduction of food sources, through effects on prey species that live in the sediments or intertidal waters as well as behavioural changes and reductions in breeding success due to longer term exposure to toxic hydrocarbons that leach from contaminated sediments (e.g. Andres 1999).

Roosting areas occur at high tide levels over this distribution (Melbourne Water 2011) indicating that direct exposure of roosting areas would be restricted to conditions where floating oil arrives at high spring tides. However, adult birds that become contaminated in exposed areas can be vectors for the transfer of oil to juveniles in the roosting areas.

The open waters of Western Port Bay and approaches are also important feeding areas for marine birds and mammals, including colonies of Little Penguins, Terns, Shearwaters, Penguins, Cormorants, Gulls and other piscivores that feed over the port waters (Melbourne Water 2011). A large colony of Fur Seals use the western entrance to Western Port Bay, but are thought to mostly remain outside of the bay entrance. The distribution of these fauna would indicate that they are at greatest risk of direct exposure from floating oil slicks, with longer term effects from any impacts on their prey sources.

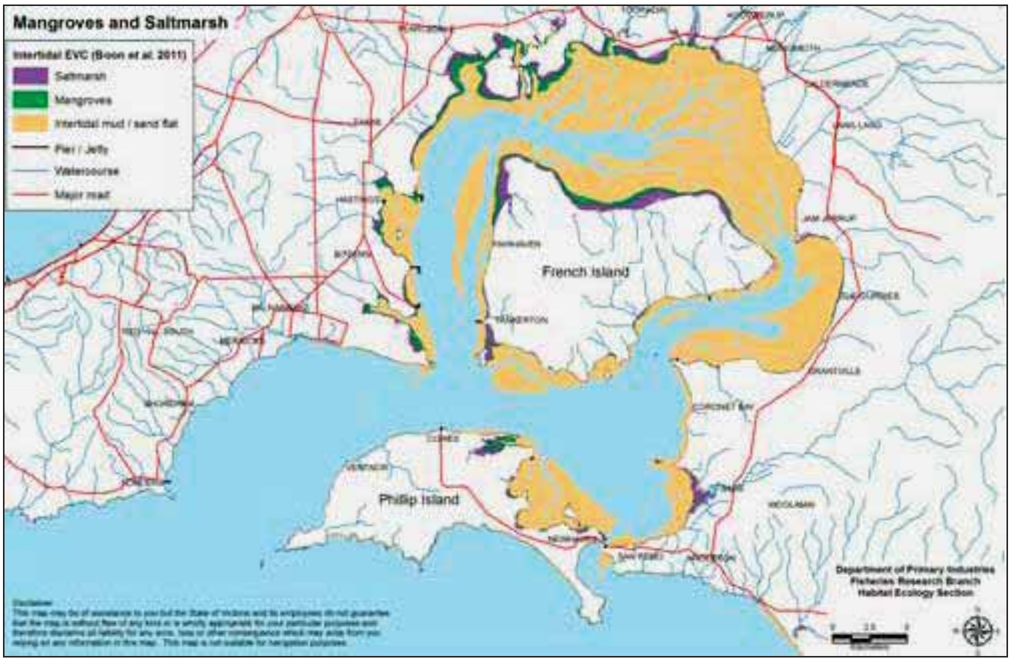

Figure 2-4: Known distribution of saltmarsh and mangroves in Western Port Bay. Reproduced from Melbourne Water 2011.

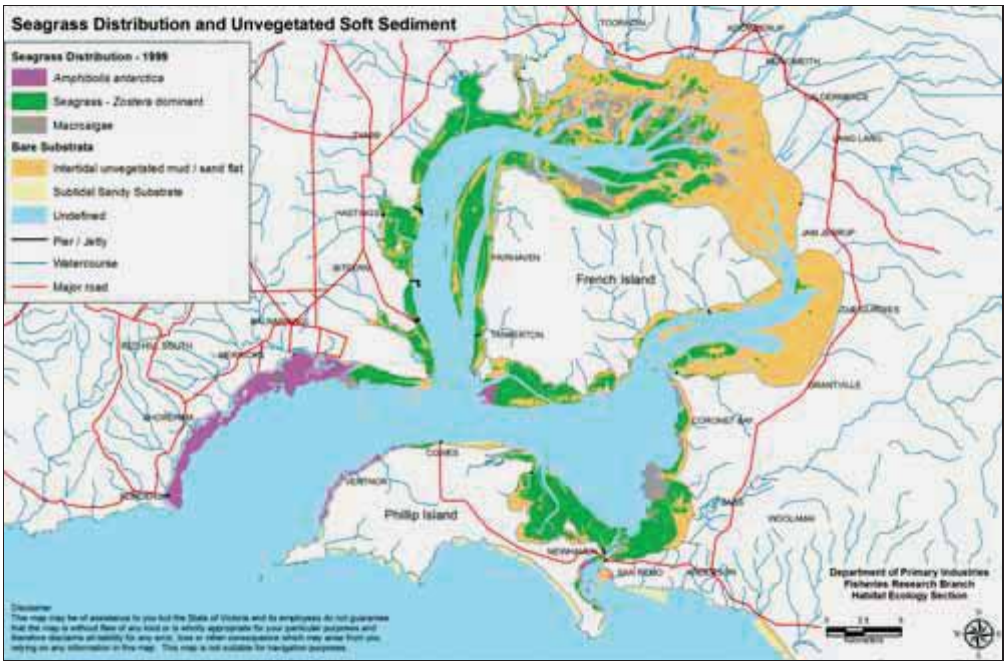

Figure 2-5: Known distribution of seagrass in Western Port Bay. Reproduced from Melbourne Water 2011.

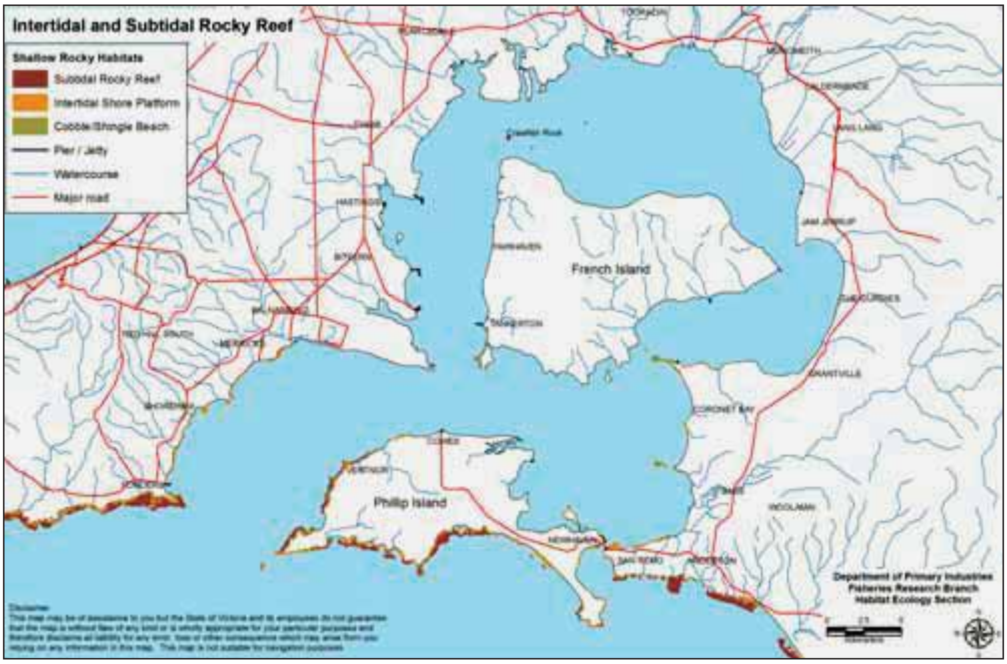

Figure 2-6: Known distribution of reefs in Western Port Bay. Reproduced from Melbourne Water 2011.

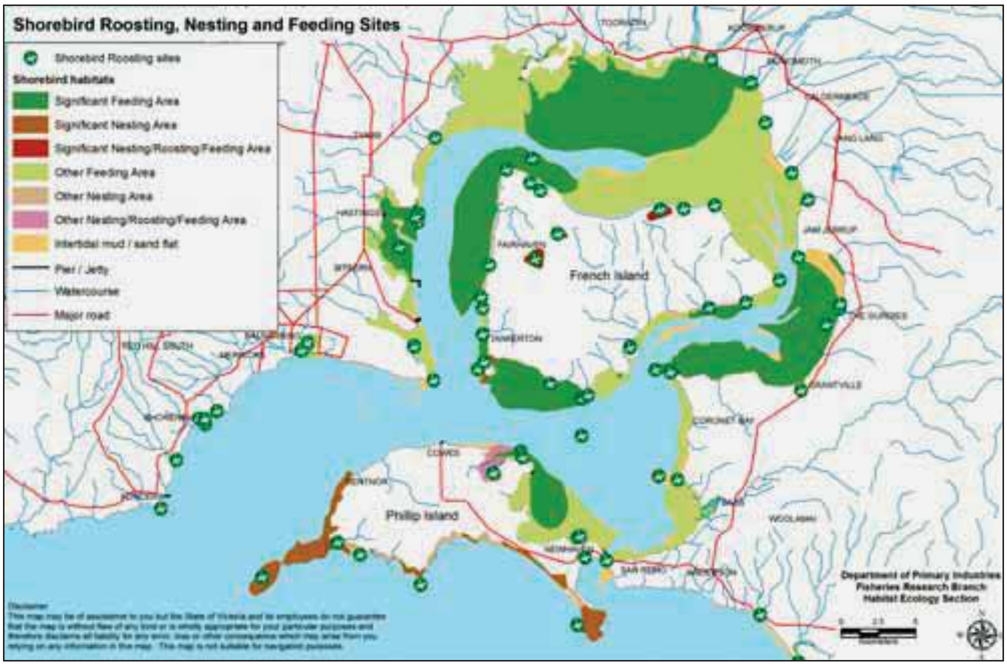

Figure 2-7: Known distribution of habitats used by shorebirds in Western Port Bay. Reproduced from Melbourne Water 2011.

3 STUDY METHODS

3.1 Development of a circulation model for Western Port Bay

A three-dimensional circulation model was developed for Western Port Bay and approaches using the model Delft3D-FLOW, which is the hydrodynamic component of the Delft3D suite of modelling products (Gerritsen *et. al.* 2007). Delft3D-FLOW is a multidimensional (2D or 3D) hydrodynamic and transport model which can calculate non-steady flow and transport phenomena resulting from tidal, meteorological and baroclinic (density) forcing. Delft3D-FLOW can be implemented on a rectilinear or curvilinear grid system, and uses either a σ-coordinate (layer thickness varying proportional to the depth) or z-coordinate (constant thickness) vertical layering approach. The model solves the non-linear Reynolds-averaged Navier-Stokes equations for fluid momentum, and can used in either hydrostatic or non-hydrostatic mode.

Delft3D-FLOW has been used for a vast array of applications all over the world, and is considered to be a reliable and robust model for oceanic, coastal, estuarine, riverine and flooding applications. The model also adheres to the International Association for Hydro-Environment Engineering and Research guidelines for documenting the validity of computational modelling software, closely replicating an array of analytical, laboratory, schematic and real-world data (Gerritsen *et. al.* 2007).

Some of the common applications of Delft3D-FLOW include:

- Tide and wind-driven flow resulting from space and time varying wind and atmospheric pressure.
- Density driven flow and salinity intrusion.
- Horizontal transport of matter on large and small scales.
- Hydrodynamic impact of engineering works such as land reclamation, breakwaters, dikes.
- Hydrodynamic impact of hydraulic structures such as gates, weirs, barriers and floating structure.
- Spreading of waste water discharges from coastal outfalls.
- Hydrostatic and non-hydrostatic flow.
- Small scale current patterns near harbour entrances.
- Flows resulting from dam breaks.

This hydrodynamic model is ideally suited to application within Western Port Bay, as it allows for accurate three-dimensional representations of tidal and wind-driven flows in topographically complex macro-tidal environments, including the representation of tidal wetting and drying of intertidal zones. Another important feature of this model for the present study was that the Delft3D-FLOW model can be set up efficiently to model over a relatively large area while also allowing high spatial resolution of current variations over sub-areas of highest interest.

3.1.1 Model Domain and Computational Grid

Modelling the tides and tidal currents within Western Port Bay and approaches required a model domain that could accurately define the bathymetry and channelized mudflats within the complex embayment. A minimum horizontal grid size of ~80 m was required in order to resolve the complex coastline and bathymetric features.

The Delft3D-FLOW model was applied over a simple rectangular grid made up of cells with a uniform spatial resolution of 80m x 80m in the horizontal. The grid was extended up to 20 km seaward to ensure that the ocean boundaries overlapped with tidal data available from the Topex Poseidon tidal database (TPX 7.2), which provides specifications of the amplitude and phase of individual tidal constituents that are derived from satellite observations over decades (NASA).

Bathymetric data for the model region was compiled from nautical charts obtained from the Australia Hydrographic Service (AUS 150 and AUS 151), which are based on naval charts, supplemented with spot soundings from the C-MAP database and digitised contours from ENC charts. The amalgamated bathymetric database was converted from chart datum to approximately mean sea level (MSL) by adding 1.7 m, which is the approximate chart datum MSL around Western Port Bay (varying along the estuaries). The bathymetric database was then interpolated onto the Delft3D model grid, using a triangulated interpolation method (Delaunay Triangulation). No smoothing was applied to the bathymetry.

A map displaying the model grid over the available bathymetric data (before interpolation) is presented in Figure 3-1.

Figure 3-2 shows the three-dimensional model developed after spatial interpolation of the bathymetric data over the model grid.

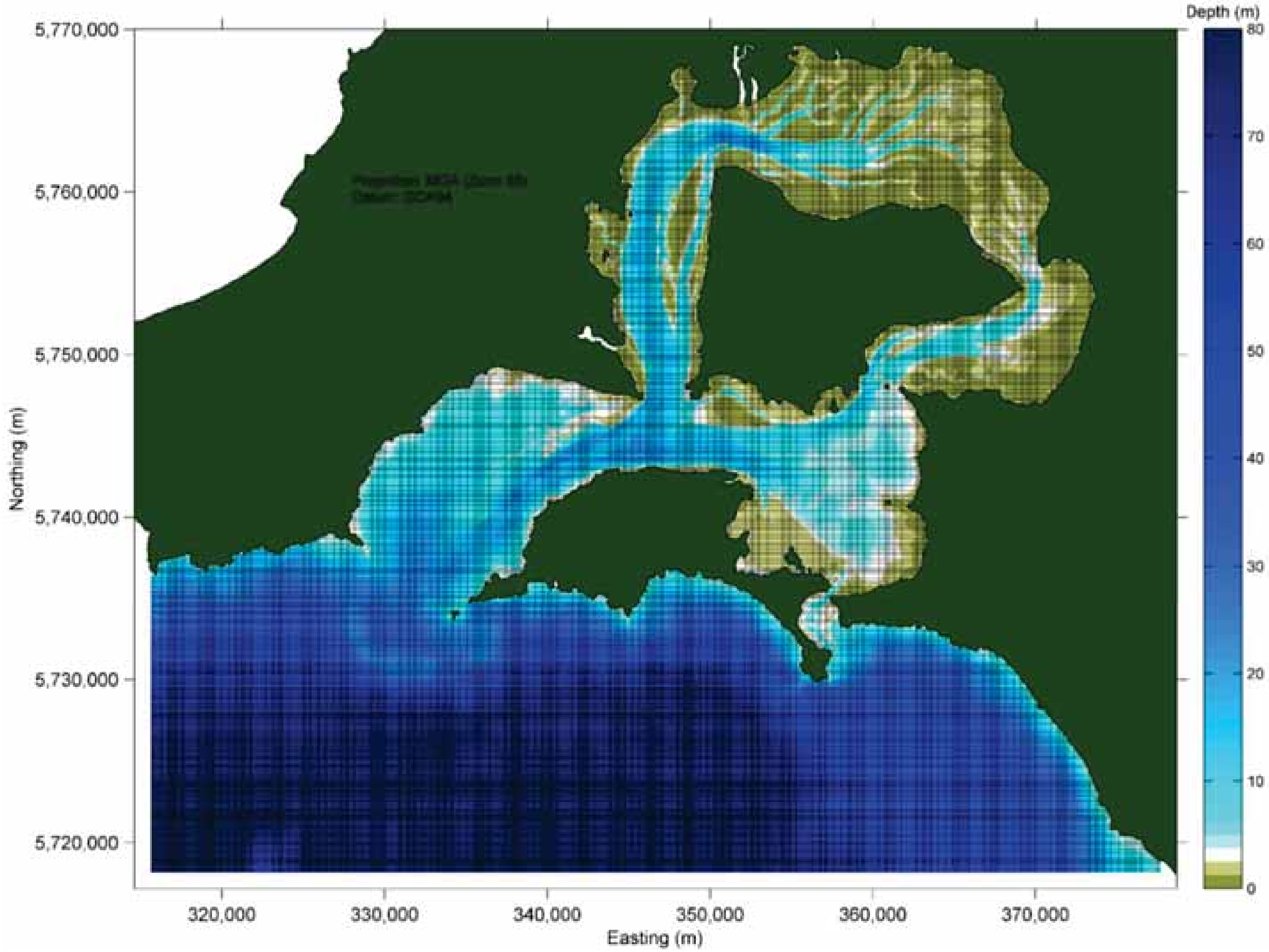

Figure 3-1: Map showing the model grid established for the study, consisting of square cells of uniform size 80 m x 80 m overlaying the bathymetric data available for the study area

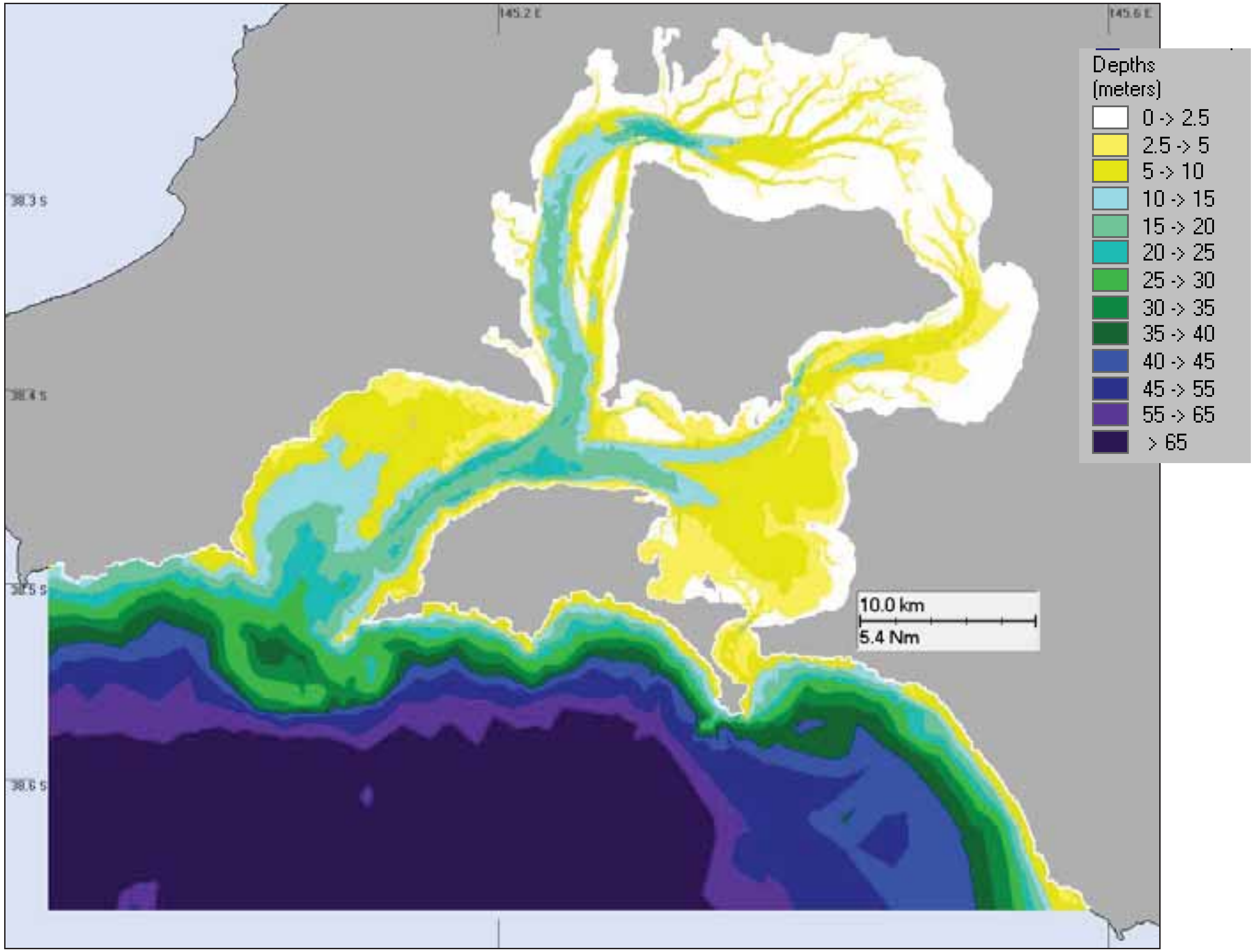

Figure 3-2: Map showing the bathymetric model refined for the study after spatial interpolation of the available bathymetric data. Depths are relative to Mean Sea Level (MSL).

3.2 Model Forcing and Boundary Conditions

3.2.1 Water Levels

The open boundaries of the outer model grid (grid0) were forced with a time-series of tidal water levels calculated from the TPXO7.2 global tidal model (Egbert and Erofeeva 2002). This model is essentially a database of tidal harmonic constituents, derived from satellite altimetry data from the TOPEX/Poseidon and Jason satellites. The tides are provided as complex amplitudes of earth-relative sea-surface elevation for eight primaries (M_2, S_2, N_2, K_2, K_1, O_1, P_1, Q_1), two long periods (M_f, M_m) and 3 non-linear (M_4, MS_4, MN_4) harmonic constituents, on a ¼° resolution grid for the full globe.

The open boundary of the model grid was subdivided into a number of segments, and the tidal time series was calculated at each segment using the TPXO7.2 database. Tide elevations are interpolated linearly along each boundary segment for a local time datum (UTC+8). The model then used calculations for the elevation of the water levels along the boundary to calculate the propagation of individual tidal waves into Western Port Bay.

Because the study area includes large areas of mudflats that wet and dried with the tide level, with water tending to flood and ebb through branching channels cut through the mudflats, it was critical to configure the model so that the coastline varied with the tidal level. This was essential to correctly represent the changing volume of the bay with tidal level, and hence correctly represent current speeds within the channels. Further, this was necessary so that the spill model could calculate interactions with the shoreline for oil arriving at different states of the tide. The hydrodynamic model was configured to dynamically wet and dry over the bathymetric grid in response to the calculated volume of water within the domain at each time step, thus representing the change in the coastline over tidal cycles (Figure 3-3).

A time sequence of model forecasts over one example tidal cycle, commencing at high tide (Figure 3-4) reveals high spatial variability in current speeds, with the strongest flows directed through the channels that are present along the estuaries and at local constriction points. Considerable differences are also noted in the timing of the various tidal phases within the port, with some areas beginning to receive flooding tides while other areas are still draining. The time-sequence also reveals the ebb and flood of water through the two estuary arms around French Island, with weak flows meeting at peak tides over the mudflats on the north-east side of the island. A portion of the tide flooding past Phillip Island can be seen to divert southward to fill the Rhyll basin, where relatively weak tides are indicated. Strong tidal currents within the eastern entrance are revealed as localised flows.

3.2.2 Model Configuration

A number of choices regarding physics and numerical schemes can be invoked within Delft3D-FLOW, additional to specifying hydrodynamic parameters.

The base hydrodynamic model was run in a barotropic (physically driven), three-dimensional, mode to capture variations in current speed with location and depth. In this mode, temperature and salinity gradients were assumed to have negligible influence on circulation due to the high level of mixing energy. The discretisation of the vertical coordinate with purely physical forcing is still important for oil spill modelling to represent current variability in the vertical due to conservation of mass, the influence of seabed drag at the bottom of the water column and the shear force generated by wind at the water surface. Application in three-dimensional mode is also important to avoid errors due to depth-averaging of current speeds.

The “cyclic” advection schemes for momentum and transport were selected, which generally give the most accurate solution compared to other schemes (Deltares 2011). The κ-ε turbulence closure scheme was selected for the vertical eddy viscosity and diffusivity formulation, with background values set to 0 m^2/s. Non-zero values of background vertical eddy viscosity and diffusivity are only required for highly stratified flows to account for sub-grid-scale internal waves which would be absent from the system under study.

The quadratic friction law was applied to simulate local shear-stress at the seabed, using the bottom roughness length scale, z_0 (m), as the parameter to quantify the frictional effects of the seabed. The model uses a formulation to convert z_0 into a Chézy coefficient, which is used in the quadratic formulation. The roughness length scale z_0 was a calibration parameter. Typical values for z_0 range from 0.2 mm for a smooth mud, to 0.4 mm for unrippled sand, and 6 mm for rippled sand (Soulsby 1997). A bottom roughness ‘sponge layer’ was employed on the open boundary, with a buffer zone of higher-bottom roughness to smooth out transient instabilities.

The drag force due to wind on the free surface boundary layer was parameterised with a linear scheme, which scales between $C_D = 0.00063$ at $U_{10} = 0$ m/s, to $C_D = 0.00723$ at $U_{10} =$ 100 m/s.

For the σ-coordinate vertical system, 5 equally proportioned layers were specified. This is adequate to reproduce the vertical profiles of barotropic currents in the region, while maintaining computational efficiency.

The model time-step was set to 15 seconds, which met the stability criteria of Courant numbers less than 10 for the entire model domain.

Sub-grid scale turbulence in the horizontal plane was parameterised by horizontal eddy viscosity and diffusivity parameters, which were considered as calibration parameters. The parameters can be specified as constant values or can be set as a dynamic quantity using a sub-grid-scale model known as Horizontal Large Eddy Simulation (HLES). If the parameters are set as constants, there is no clearly defined way of establishing exactly what values of eddy viscosity and diffusivity to use for a given model simulation. The general rule for hydrodynamic modelling is that the values should be proportional to the grid resolution. In the case of viscosity, the value should be no greater than what is required to establish model stability. Appropriate diffusivity values can be established from field experiments with tracer dyes, and estimates can be found in the literature. For detailed models where much of the details of the flow are resolved by the grid (grid sizes typically tens of metres or less), appropriate values for the eddy viscosity and the eddy diffusivity will typically be in the range of 1 to 10 m^2/s (Deltares 2011) However, for representation of large tidal areas with a coarser grid (grid sizes of hundreds of metres or more), the coefficients typically range from 10 to 100 m^2/s. The use of the HLES model calculated the effective eddy viscosity and diffusivity of horizontal flows subjected to bed friction by adding a dynamic component to the background values the user sets, potentially providing a more realistic model simulation.

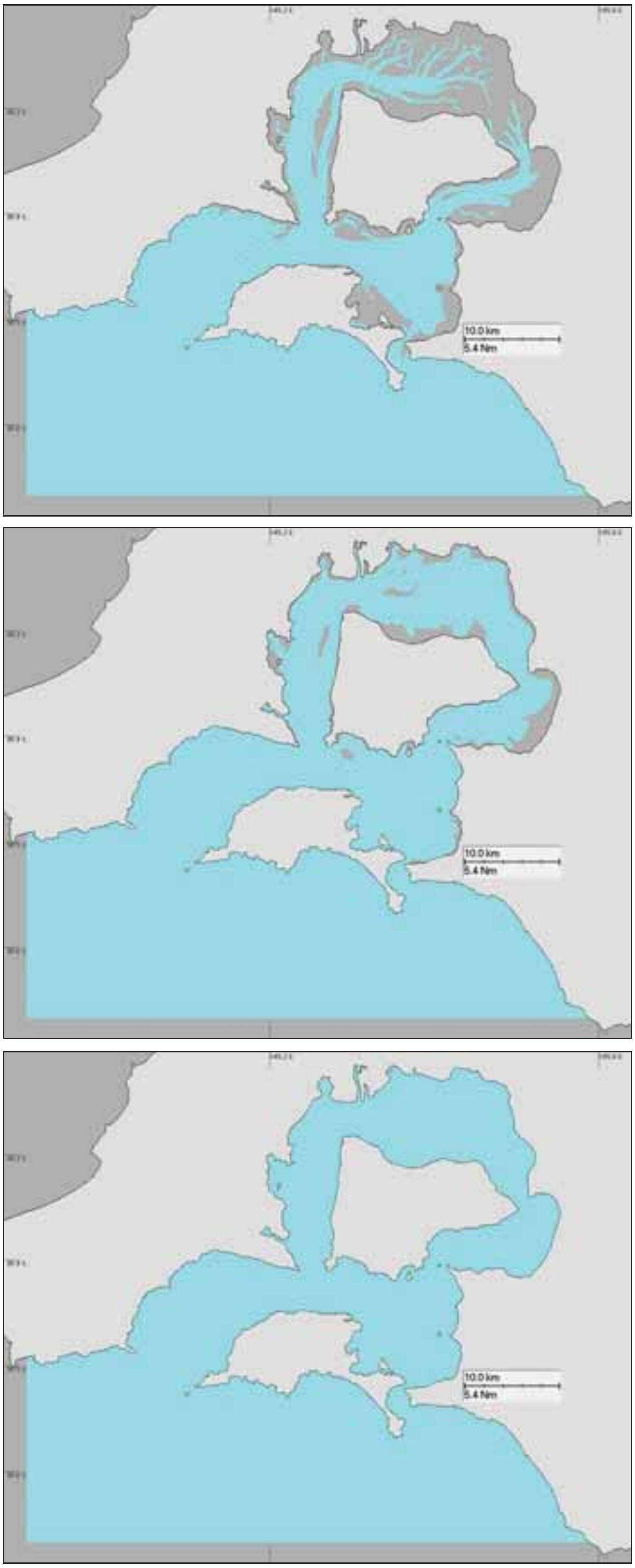

Figure 3-3: Example of the changing coastline represented by tidal wetting and drying within the model, showing lowest astronomical tide, mean sea level and highest astronomical tide.

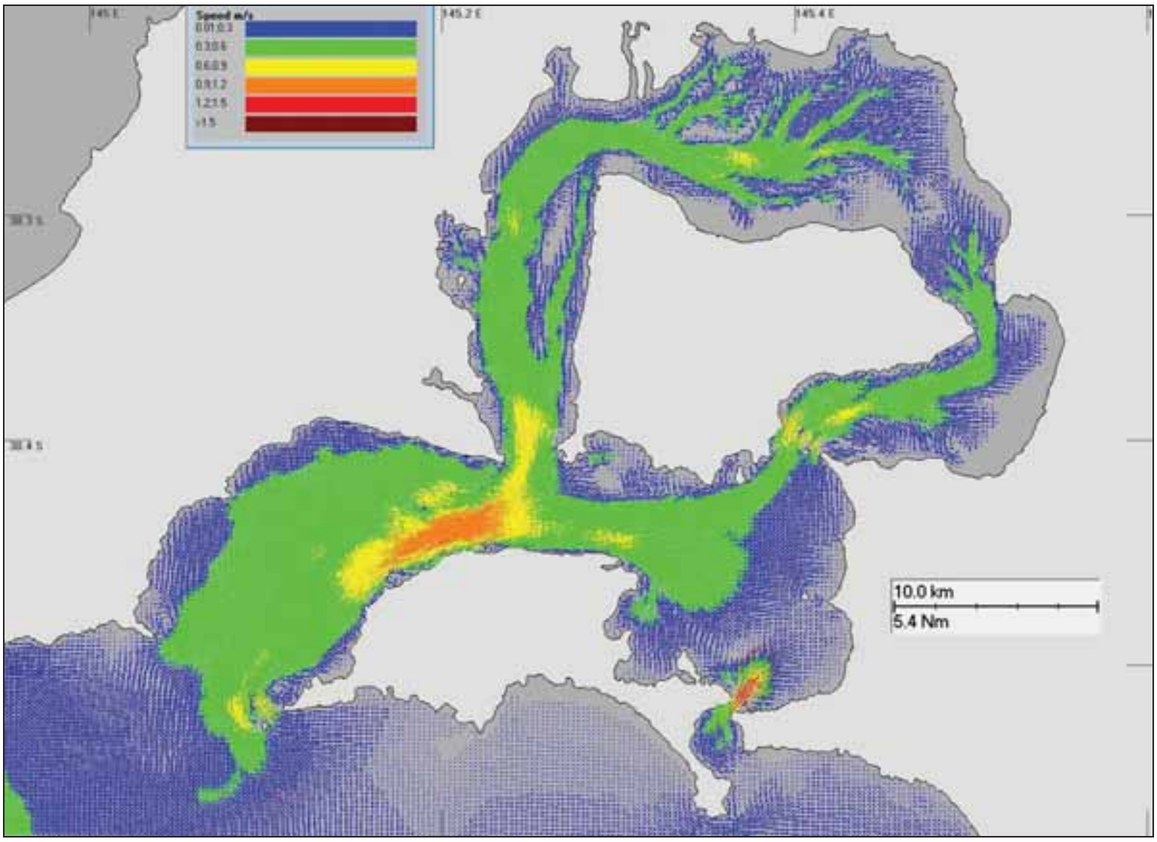

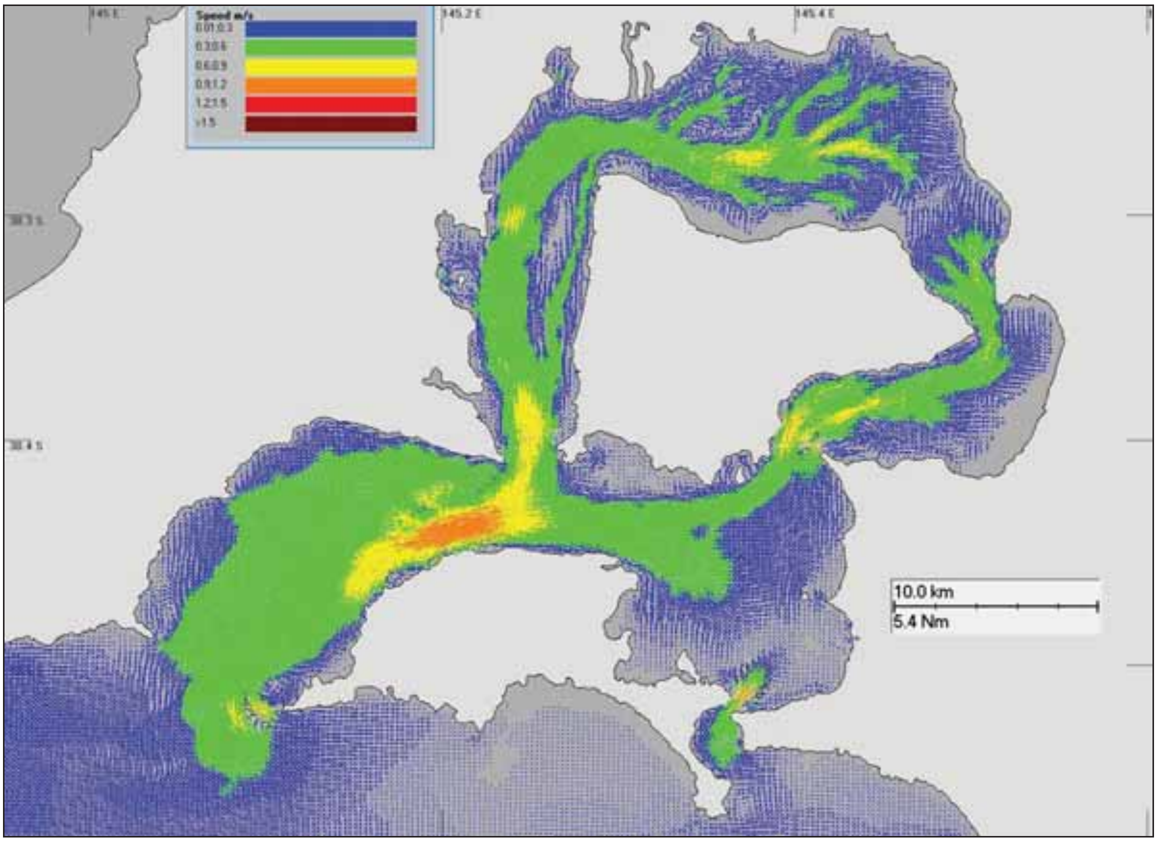

Figure 3-4: Time sequence of current speeds forecasted over the domain for one tidal cycle. Images are at hourly time intervals commencing on a flooding tide. Current magnitudes are colour coded.

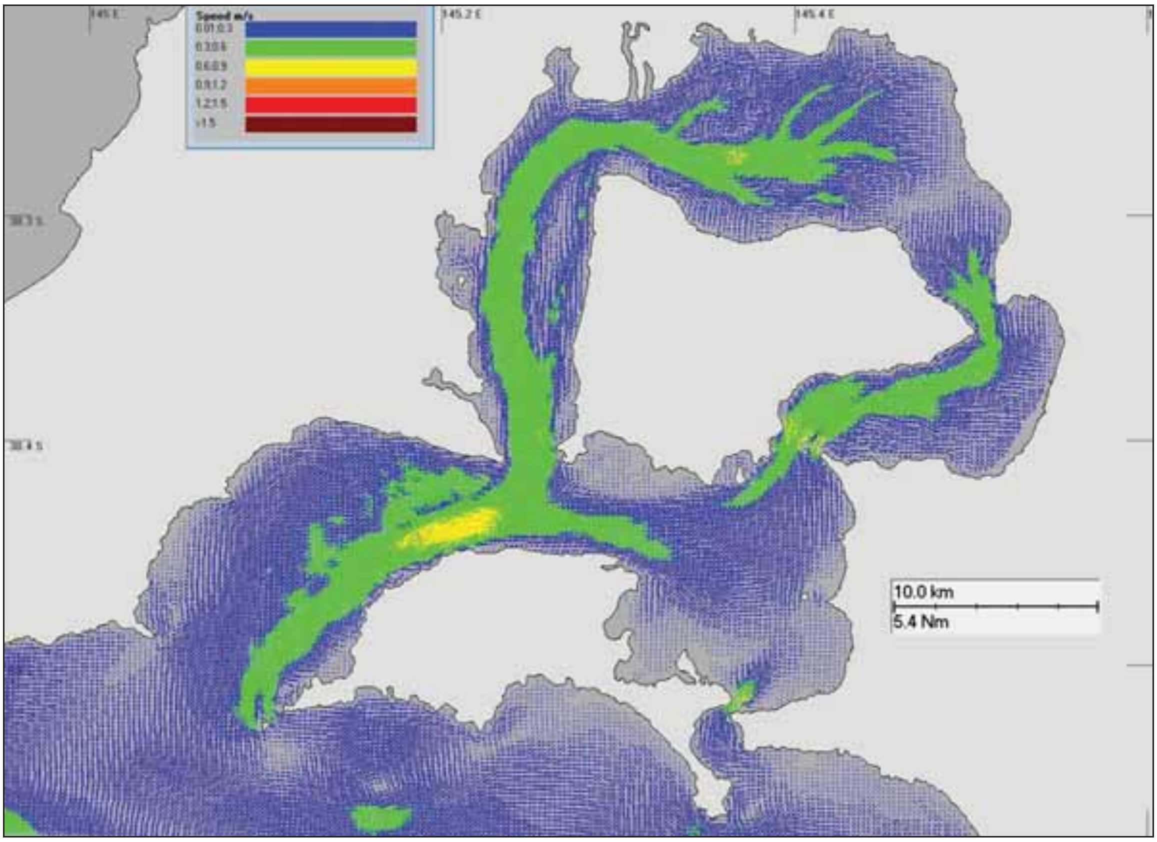

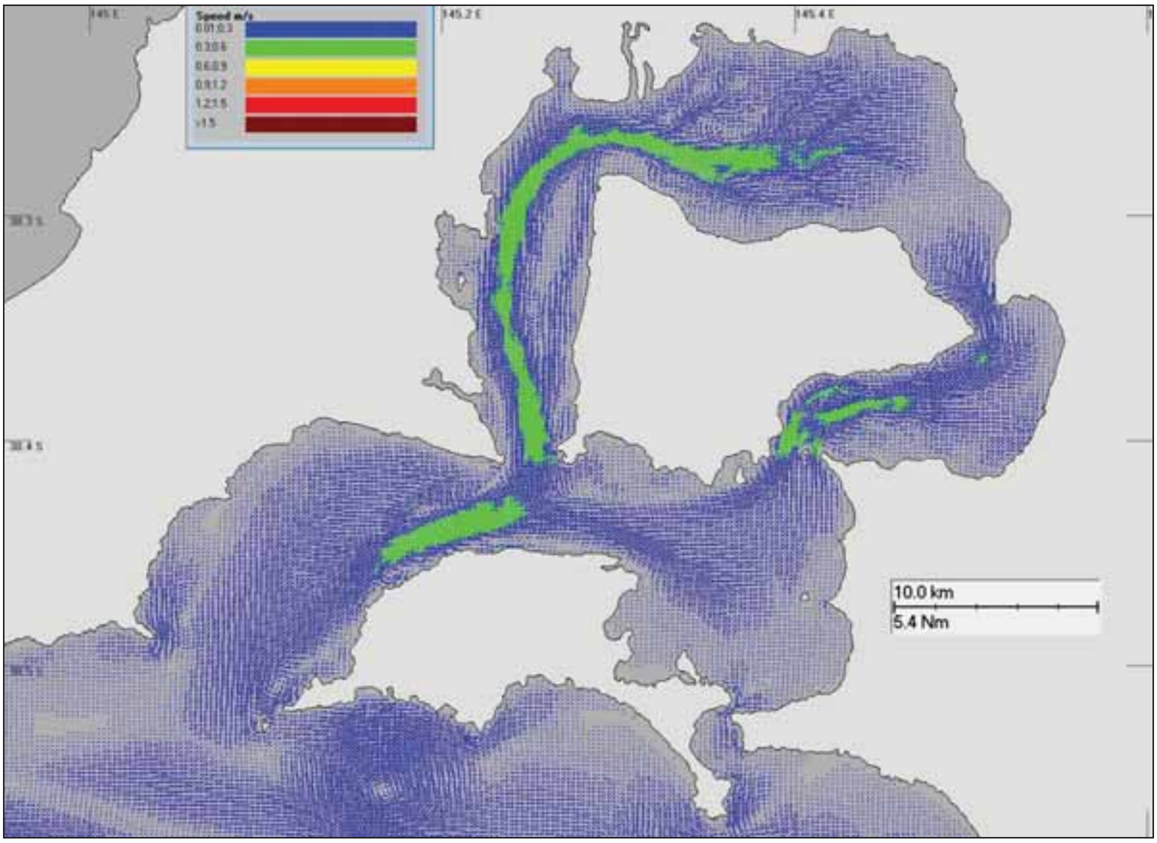

Figure 3-4 (Continued)

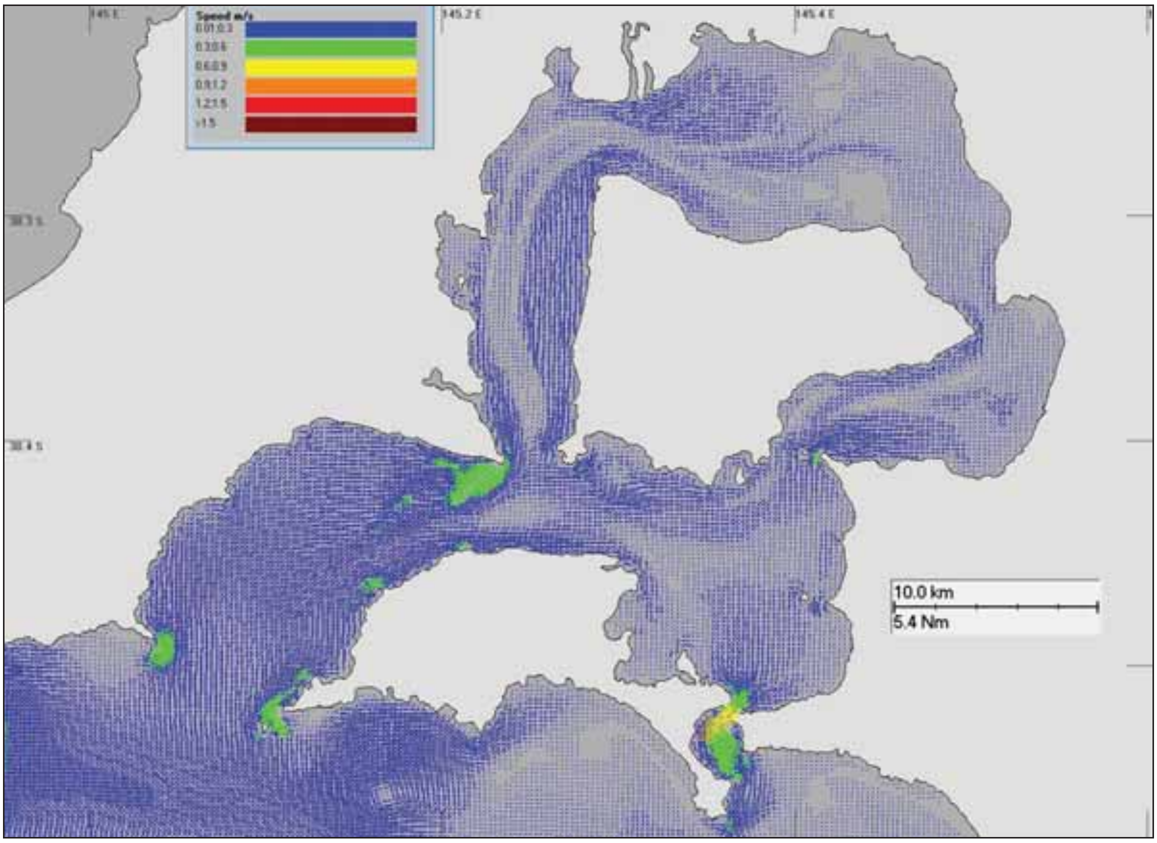

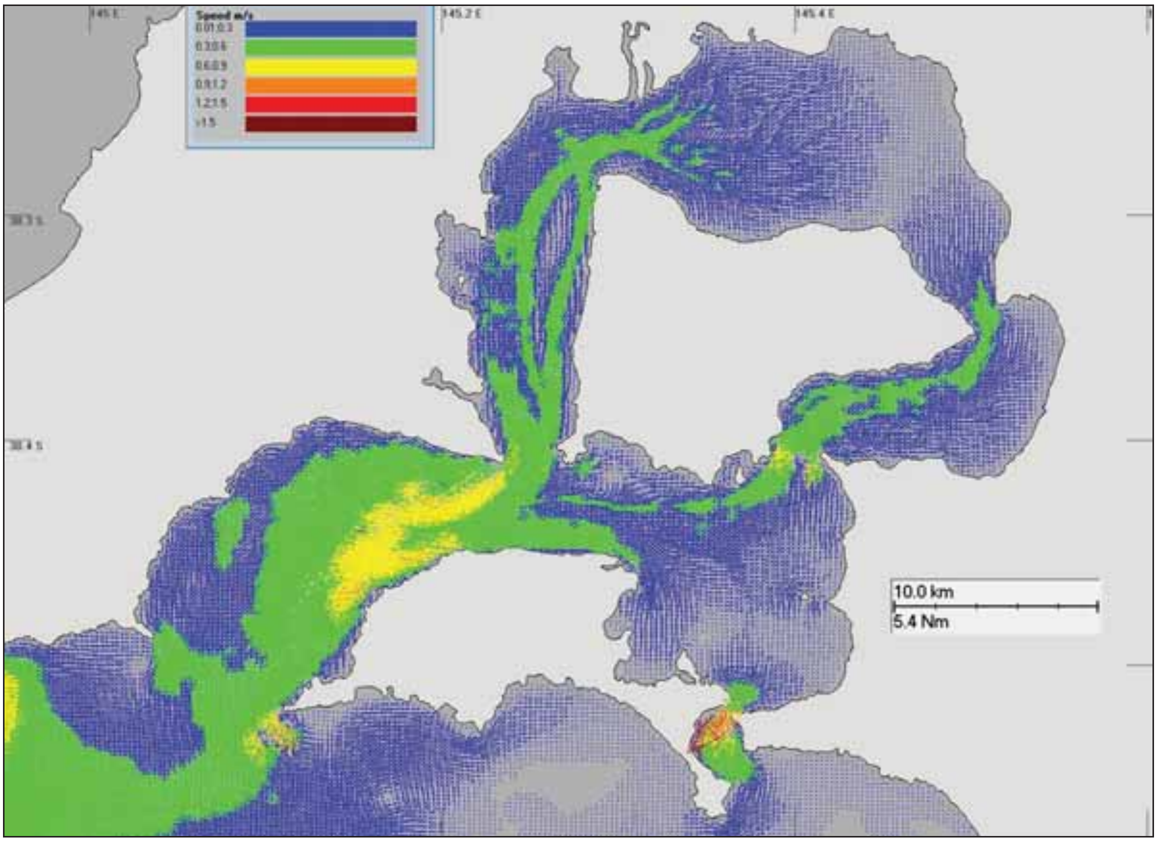

Figure 3-4 (Continued)

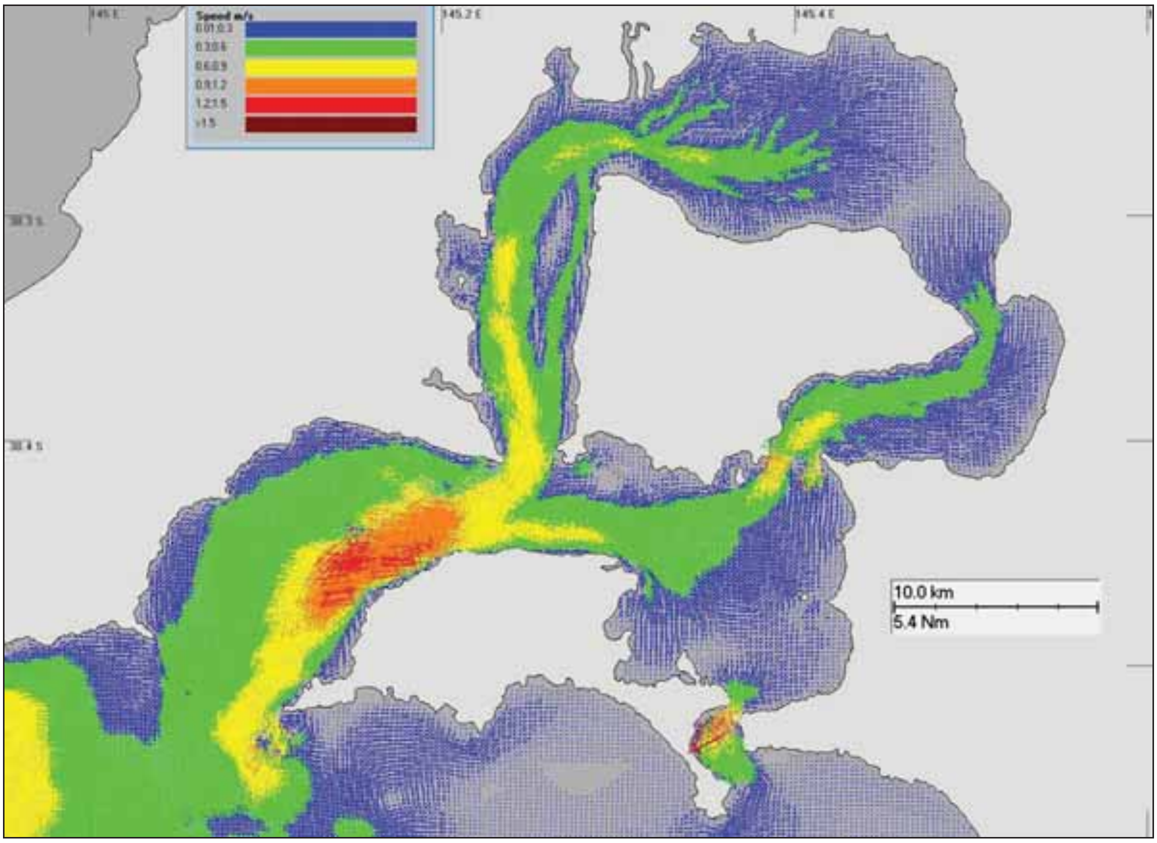

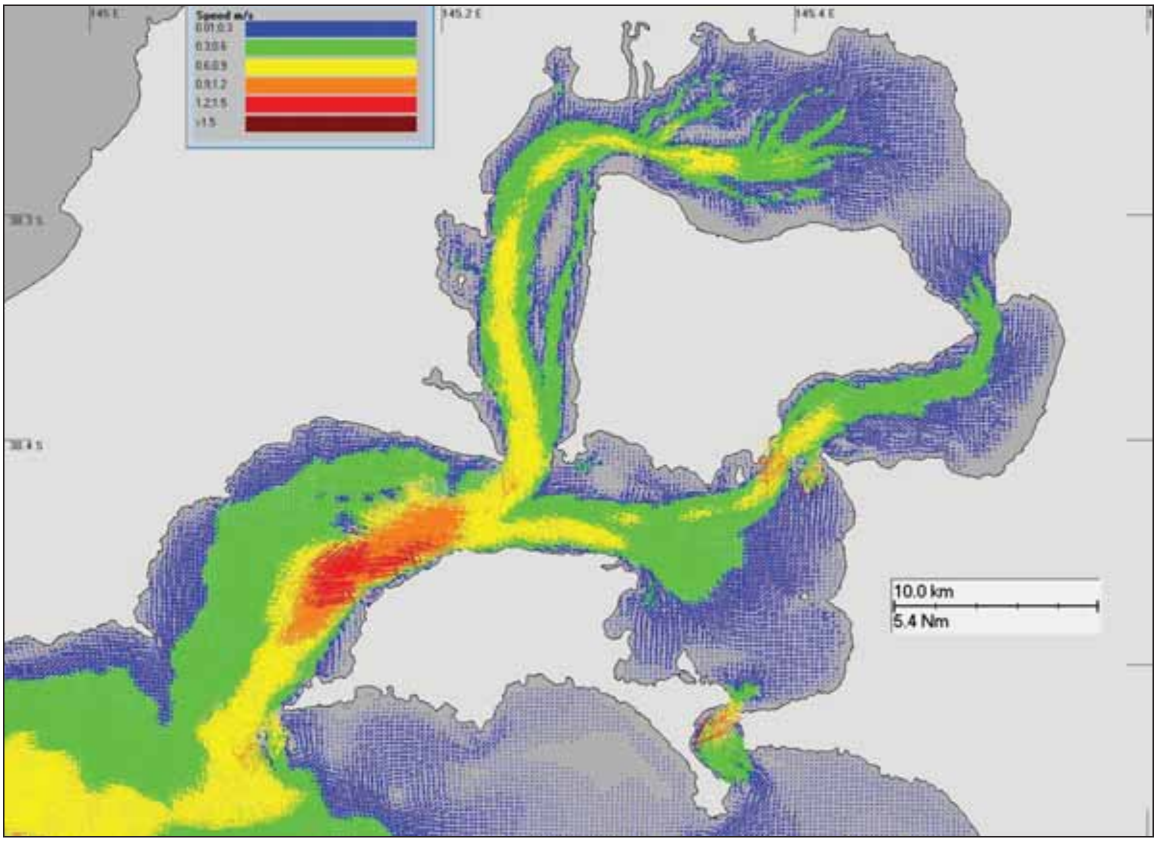

Figure 3-4 (Continued)

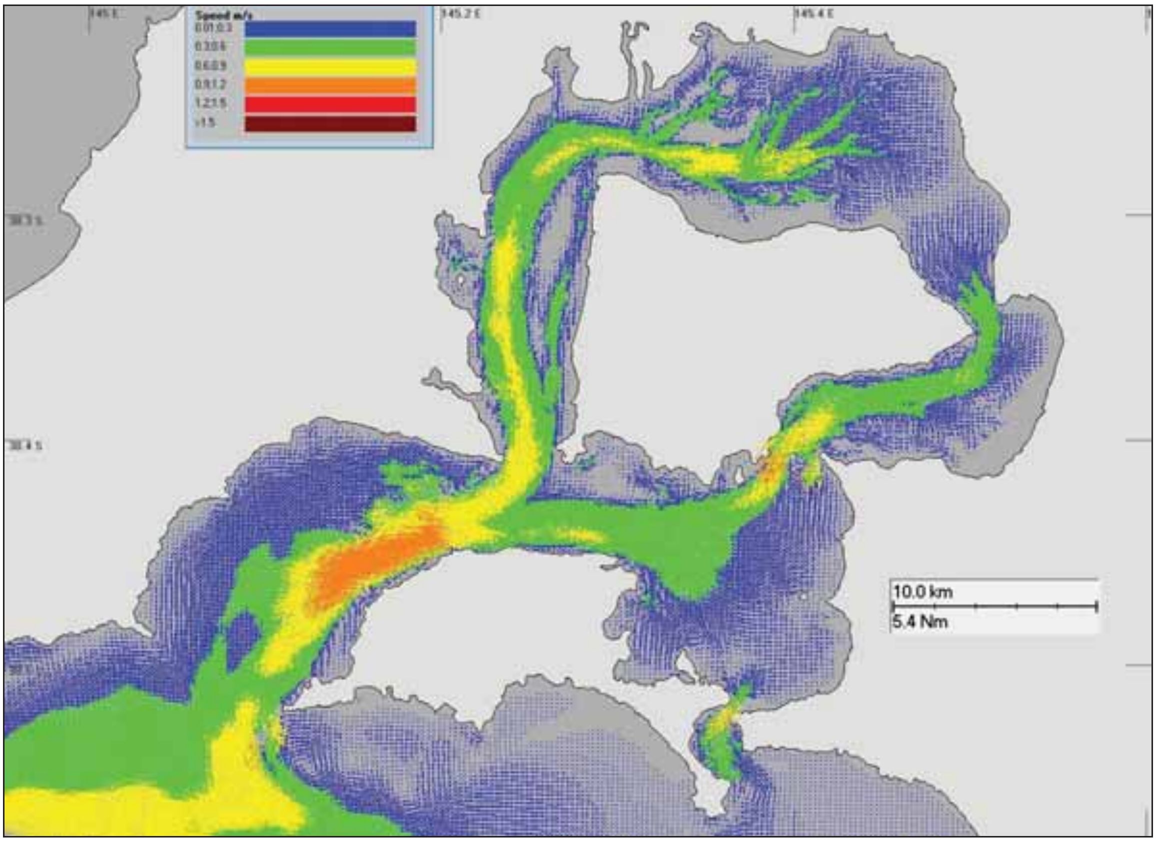

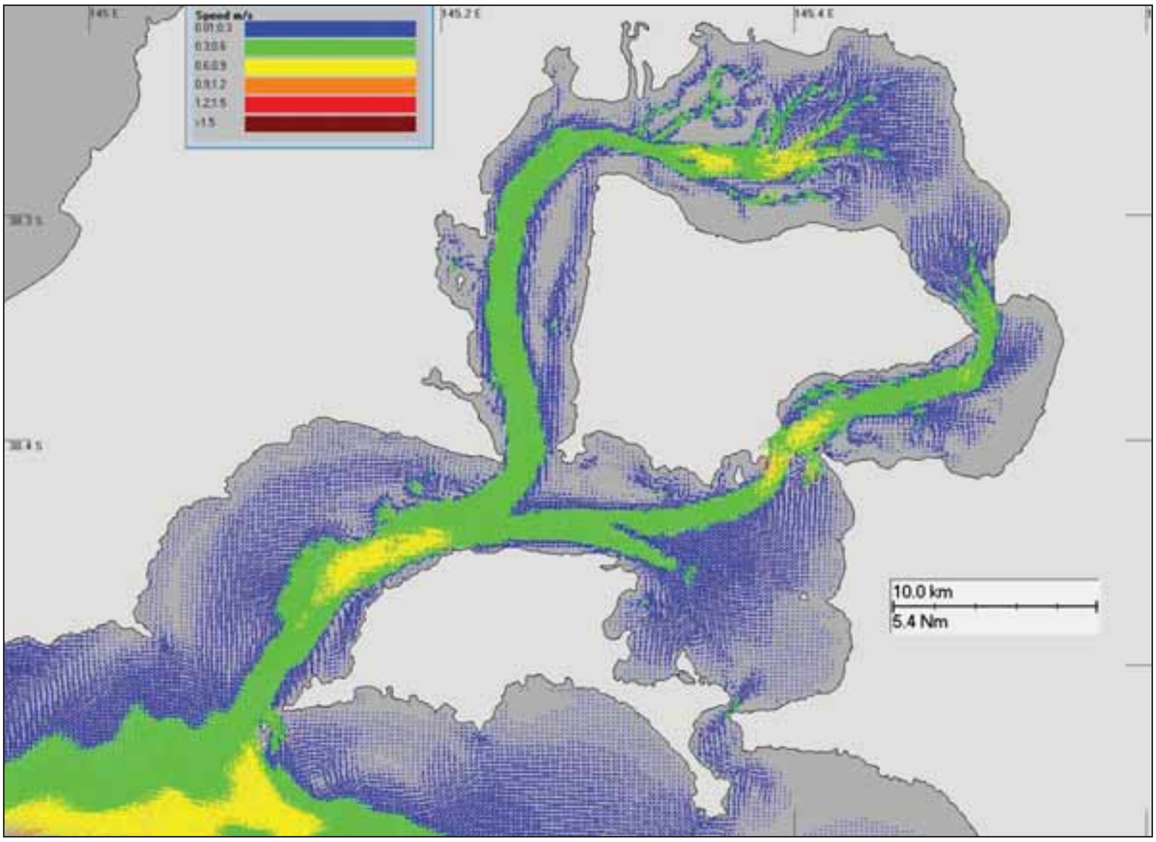

Figure 3-4 (Continued)

3.2.3 Wind and Pressure

Two sources of wind and pressure were tested and used for forcing the hydrodynamic model. Both sources were obtained from the Bureau of Meteorology (BOM) and consisted of raw time-series measured wind data from the H.M.A.S Cerberus Naval Base (Cerberus) and Rhyll Weather Station.

As an example of the wind patterns affecting the bay, frequency analysis of long term (10 year duration) records of wind speed and direction at Cerberus Meteorological Station indicate that wind patterns are highly variable but with overriding seasonal distributions. Winds from the southern sector (mostly south-west to south) are most common during Summer, while winds from the northern and north-western sector are most common during the Winter. Patterns during the Autumn and Spring indicate a transition between the Summer and Winter patterns with similar frequencies from the north and south, which were applied using distance weighting to represent wind fields over the model domains.

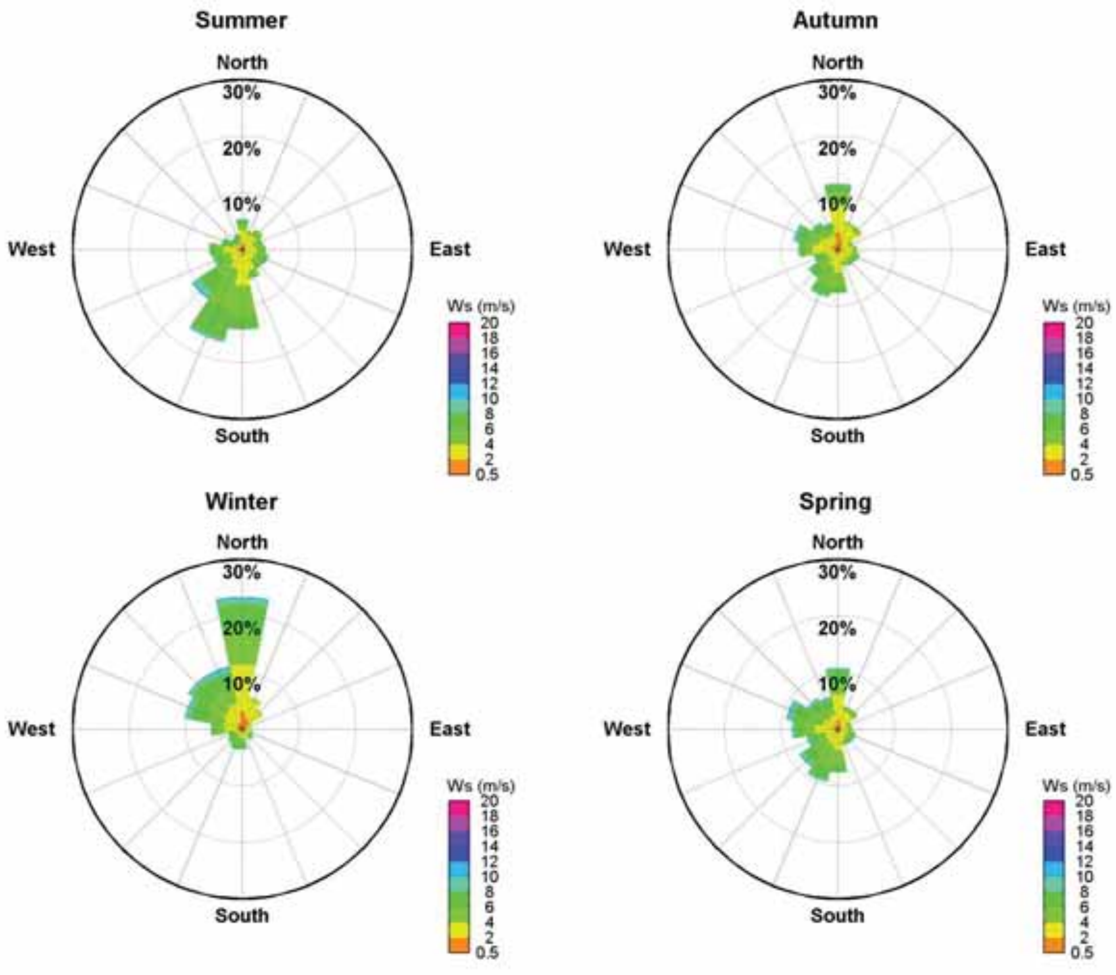

Figure 3-5: Wind roses (direction from) for Cerberus measured data (Jan 2002 – Sep 2012) – Summer (top left), Autumn transition (top right), Winter (bottom left) and Spring transition (bottom right). The sectors point towards the direction that the wind came from following meteorological convention.

3.2.4 Model Calibration

The model performance was refined through repeatedly re-running the model and altering input data and parameters, and then comparing the model output to measured data in the form of current drogues deployed at two locations at different states of the tidal phase. For each model configuration, the model was run for two 5 day periods to allow comparison against the drogue measurements, with the chosen periods corresponding with those of the drogue measurements.

The wind data was one calibration input considered. The model was run using the hourly records of wind speed and direction measured at Cerberus applied uniformly across the domain, and another run was made using the winds measured at Rhyll. It was difficult to establish any difference in model skill using either wind data source, due to the winds being relatively light, and currents in the region being very tidally dominated on the droguing occasions. As a consequence, distance weighted interpolation was applied to estimate winds spatially based on concurrent records from both sources. As an average, a coefficient of 3% of the wind speed was assumed for the influence of the wind in affecting surface slicks.

The bottom roughness length scale, z_0 (m), was another important calibration parameter. Initially a value of 0.2 mm was used, which represents the drag typical of a sandy bottom, but this slightly overestimated the current speeds at surface in some areas. A value of z_0= 6 mm, which represents a rippled sandy bottom, improved the results but led to a slight under-estimation of currents. A value of 3 mm provided the best match to observed currents and was therefore applied to the final model configuration.

3.2.5 Validation of Model Skill

To provide a statistical measure of the performance of the model in forecasting current speeds and directions, once calibrated, the Index of Agreement (IOA - Willmott 1981) and the Mean Absolute Error (MAE – Willmott, 1982, and Willmott and Matsuura, 2005) were used.

The MAE is simply the average of the absolute values of the difference between the observed and modeled value. It is a more natural measure of the average error (Willmott and Matsuura, 2005) and is more readily understood.

The Index of Agreement (IOA) is determined by:

$$\mathrm{IOA} = 1 - \frac{\sum |X_{\mathrm{model}} - X_{\mathrm{obs}}|^2}{\sum \left(|X_{\mathrm{model}} - \overline{X_{\mathrm{obs}}}| + |X_{\mathrm{obs}} - \overline{X_{\mathrm{obs}}}|\right)^2}$$

where X represents the variable being compared and $\overline{X}$ the time mean of that variable.

A perfect agreement exists between the model and field observations if the index gives an agreement value of 1 and complete disagreement will produce an index measure of 0 (Wilmott, 1981). Willmott et al (1985) also suggests that values meaningfully larger than 0.5 represent good model performance. Clearly, a greater IOA and lower MAE represent a better model performance.

One important point to note regarding both measures, and in fact most measures of model performance, is that slight phase differences in the data series can result in seemingly poor statistical comparisons, which is particularly evident in tidally dominated signals where tidal direction or water elevation changes rapidly. Small, uniform, differences in the phase (i.e. miss-timing) between actual and modelled currents are insignificant for application to stochastic modelling because the model is tasked with representing realistic time sequences from randomly selected times, and not from a specific time. It is therefore always important to consider both the statistical approach and the visual representation of the comparison to detect discrepancies purely to small time offsets (Willmott *et al*, 1985).

3.2.6 Skill in forecasting water levels

For the purpose of verification of the tidal predictions, in terms of the timing and magnitude of tidal waves through the modelled region, forecasts of the water levels produced by the model were compared to independent predictions of tides using the XTide database (Flater, 1998). Only one tidal station (Stony Point) occurs within the model domain.

Time-series comparisons were completed for a two month period from June to July 2012. The statistics are summarised in Table 3-1and indicate excellent model performance. On average, the model predictions are within 0.2 m of XTide predictions based on known constituent data at any point in time. Water elevation time series are shown in Figure 3-4 (top) for one month within the period (June 2012). The comparison shows that the model produces a very good match to the known tidal behaviour for a wide range of tidal amplitudes and clearly represents the varying semi-diurnal nature of the tidal signal.

Table 3-1: Statistics for time series comparisons of Delft3D and XTide predictions (June 2012).

Station Name	Long.	Lat.	CC	IOA	RMSE (m)	MAE (m)
Stony Point	145.2195	-38.363	0.97	0.98	0.19	0.16

Notes: *CC Correlation Coefficient – values close to 1 represent very good correlation.*
IOA Index of Agreement – values close to 1 represent a high level of agreement.
RMSE Root Mean Square Error – the lower the value, the smaller the error.
MAE Mean Absolute Error – the lower the value, the smaller the error.

The performance of the model was also evaluated through a comparison of the predicted and observed tidal constituents, derived from an analysis of model predicted time-series at each location. The comparison data is summarised in Table 3-2, while Figure 3-6 shows the results graphically for the amplitude and phase of the five dominant tidal constituents (S_2, M_2, N_2, K_1 and O_1). The red line on each plot shows the 1:1 line, which would indicate a perfect match between the modelled and observed data. Note that the data is generally closely aligned to the 1:1 line demonstrating the high quality of the model performance.

Table 3-2: Comparison of tidal constituents derived from model results and observed data at Stony Point. Note that the Phase is measured as compass bearings (0-360°). Amplitude is in metres.

Constituent:				M_2		S_2		K_1		O_1		N_2		Q_1	
Station Name	Long.	Lat.	Data	Amp. (m)	Phase (°)	Amp. (m)	Phase (°)	Amp. (m)	Phase (°)	Amp. (m)	Phase (°)	Amp. (m)	Phase (°)	Amp. (m)	Phase (°)
Stony Point	141.2195	-38.363	Obs.	0.92	351.51	0.23	136.63	0.23	76.7	0.15	42.99	0.17	309.04	0.04	24.28
			Mod.	0.92	6.13	0.14	147.98	0.29	81.8	0.15	44.09	0.16	314.69	0.04	25.54

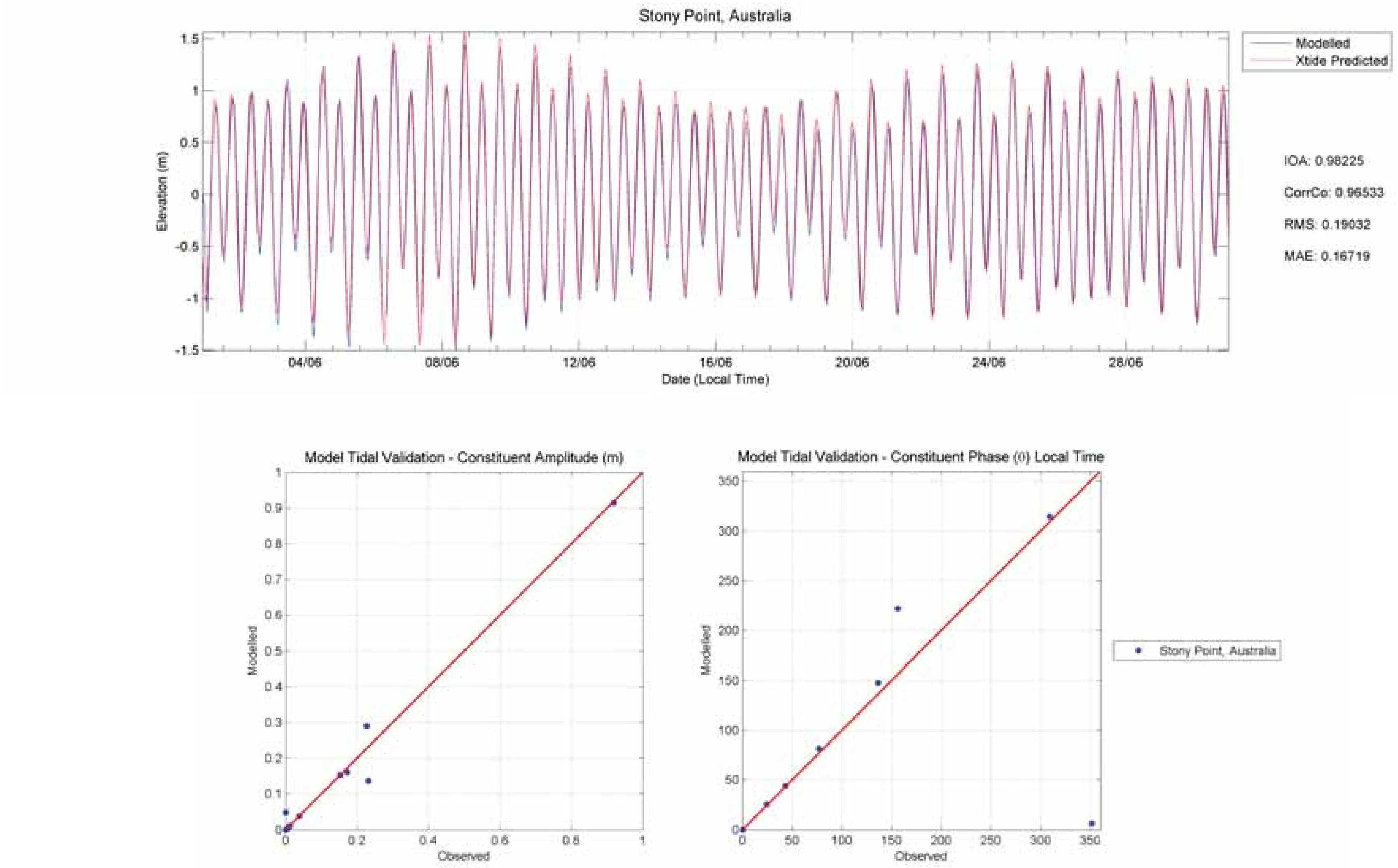

Figure 3-6: Comparisons between the predicted (blue line) and observed (green line) surface elevation variations (top) and comparison between modelled and observed tidal constituent amplitudes and phases (bottom) at Stony Point for June 2012.

3.2.7 Skill in forecasting current speeds and directions

A drogue deployment was undertaken by VNPA on two occasions: the 13th June 2012 and 8th July 2012, to test the models skill in forecasting current speeds and directions. The drogues were constructed from large (2 m x 2 m) squares of foam carpet underlay with portable GPS (global positioning system) devices mounted in low profile containers at their centre (Figure 3-7). The drogue configuration was designed to follow the movement of water at the water surface as closely as possible.

Multiple drops were undertaken with up to three simultaneously released drogues released at the same positions to measure variations in trajectory over time. Experiments on the 13 June 2012 were carried out during an ebb tide while experiments on the 8 July 2012 occurred during the flooding tide.

Figure 3-7: Current drogues deployed in Western Port Bay.

Delft3D was configured to reproduce currents for the same time intervals using the observed wind data for the period. Forecasts for the water currents were applied as input to a Lagrangian particle model (Delft3D Drogue) to forecast the trajectory of particles representing the drogues. Maps showing comparisons between the measured and modelled drogue tracks are presented in Figure 3-8 and Figure 3-9. These results also show excellent fit between the observed and modelled data. The model accurately predicts the speed of the currents, as indicated by the match between the lengths of the trajectories over the sampling durations. The models skill in predicted variations in the currents is indicated by the conformation of the shape of the tracks, accurately predicting variations over space and time including the turn of the tides.

Collectively, the validation studies indicated that the hydrodynamic model, as configured would provide suitable representation of current fields within Western Port Bay for use in the spill modelling. On this basis the hydrodynamic model was applied to simulate for the full 3 year sample period (1 January 2009 – 31 December 2011).

Table 3-3: Characteristics of water currents in Western Port Bay estimated from the results of drogue experiments; June and July 2012 field campaign.

Date	Release Number	Time	Distance (m)	Max Speed (km/h)
13/06/12 Ebb tide	1	8:58 AM – 10:27 AM	1,050	1.5
	2	10:32 AM – 11:55 AM	2,053	4.0
8/07/12 Flood tide	3	9:20 AM – 10:39 AM	4,830	7.8

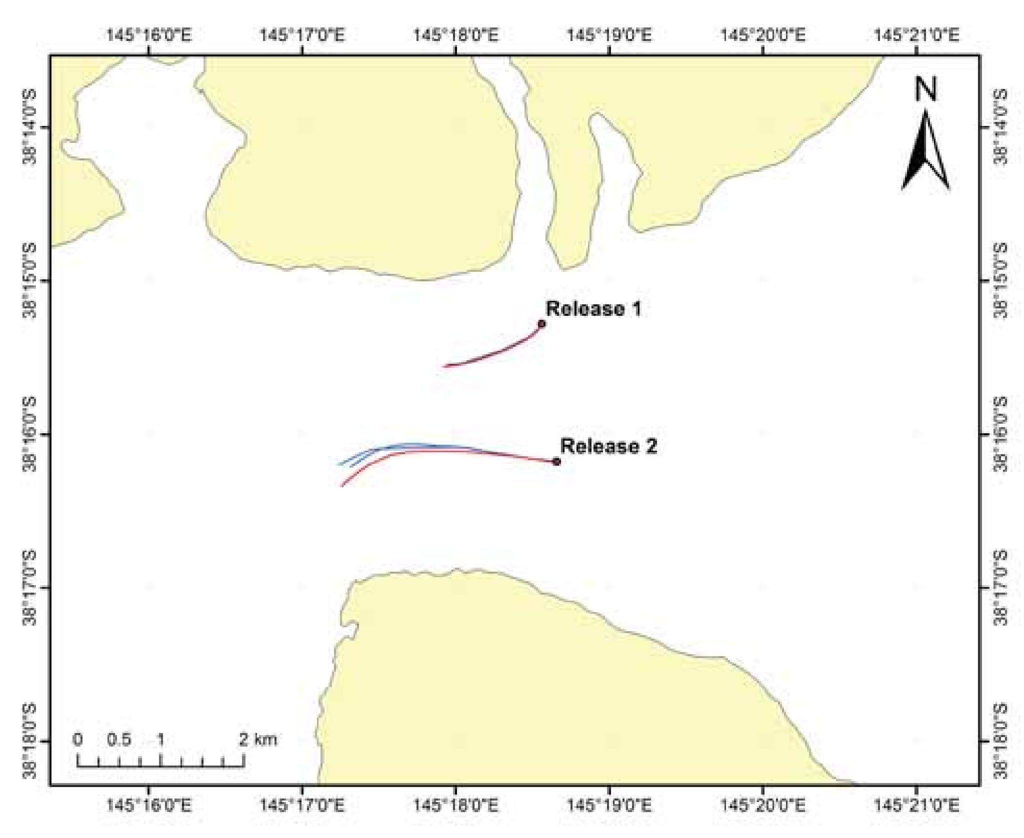

Figure 3-8: Observed (blue) versus predicted (red) drogue tracks for 13 June 2012 releases.

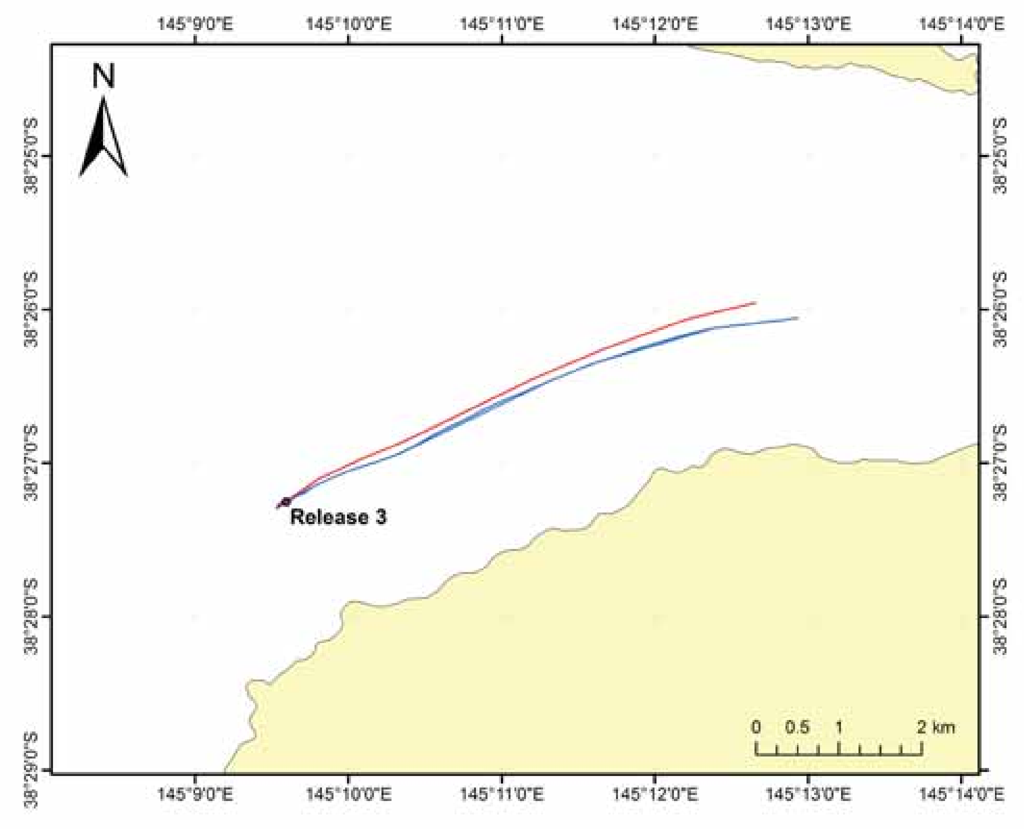

Figure 3-9: Observed (blue) versus predicted (red) drogue tracks for 8 July 2012 release.

3.3 Calculation of Exposure Risks due to defined oil spill scenarios

3.3.1 Overview

The spill modelling was carried out using the purpose-developed oil spill trajectory and fates model, SIMAP (Spill Impact Mapping & Assessment Program), which is an evolution of the US EPA Natural Resource Damage Assessment model (French & Rines, 1997; French, 1998; French *et al*, 1999) and is designed to simulate the transport and weathering processes that affect the outcomes of hydrocarbon spills to the sea, accounting for the spill depth, the specific oil type that is spilled, the spill volume and duration of the spill (hence, total volume), prevailing sea and air temperatures, wind and current patterns and ocean turbulence, which collectively affect the transport, spreading and weathering of the oil.

The SIMAP model is a three-dimensional spill model and considers the exchange of oil components between the water surface, the water column and the atmosphere. Transport of oil is calculated by representing the spilled volume by a large number of particles, each representing a proportion of the spilled volume. Evaporation rates vary over space and time dependent on the prevailing sea temperatures, wind and current speeds, the surface area of the slick and entrained droplets that are exposed to the atmosphere as well as the state of weathering of the oil. Evaporation rates will decrease over time, depending on the calculated rate of loss of the more volatile compounds. By this process, the model can differentiate between the fates of different oil types.

Entrainment, dissolution and emulsification rates are correlated to wave energy, which is accounted for by estimating wave heights from the sustained wind speed, direction and fetch (i.e. distance downwind from land barriers) at different locations in the domain. Dissolution rates are dependent upon the proportion of soluble, short-chained, hydrocarbon compounds, and the surface area at the oil/water interface of slicks. Dissolution rates are also strongly affected by the level of turbulence. For example, they will be relatively high at the site of the release for a deep-sea discharge at high pressure. In contrast, the release of hydrocarbons onto the water surface will not generate high concentrations of soluble compounds. However, subsequent wave action will enhance dissolution from surface slicks. Because the compounds that have high solubility also have high volatility, the processes of evaporation and dissolution will be in dynamic competition. Technical descriptions of the algorithms used in SIMAP and validations against real spill events are provided in e.g. French *et al* (1999) and French (1998).

Input specifications for oil types include the density, viscosity, pour-point, distillation curve (volume of oil distilled off versus temperature) and the aromatic/aliphatic component ratios within given boiling point ranges. The model calculates a distribution of the oil by mass into the following components:

- Surface bound oil;
- Entrained oil (non-dissolved oil droplets that are physically entrained by wave action);
- Dissolved hydrocarbons (principally the aromatic and short-chained aliphatic compounds);
- Evaporated hydrocarbons;

- Sedimented hydrocarbons;
- Decayed hydrocarbons.

The transport and weathering of each particle is calculated independently over discrete time steps. For floating oil, transport is calculated as a vector due to the local wind speed and direction, a vector due to the local current speed and direction and a vector due to random variation – representing horizontal dispersion due to turbulence. For oil that is in the water column, the model separately calculates the transport of particles representing entrained oil droplets and dissolved oil compounds in solution (the water-soluble fraction), as a vector only of the local current at the depth occupied by the particles plus vectors due to random variation in both the horizontal and the vertical – representing turbulent mixing.

Fate calculations interact with the transport calculations and allow for all processes that are known to significantly affect changes in spilled oil over time, including interactions with suspended sediments and shorelines. The physical transport algorithms calculate transport and spreading by physical forces, including surface tension, gravity and wind and current forces for both surface slicks and oil within the water column. The fates algorithms calculate all of the weathering processes known to be important for oil spilled to marine waters. These include droplet and slick formation, entrainment by wave action, emulsification, dissolution of soluble components, sedimentation, evaporation, bacterial and photo-chemical decay and shoreline interactions. These algorithms account for the specific oil type being considered

A stochastic modelling approach was applied to gain quantitative estimates of exposure probability for surrounding locations, given variations in the prevailing wind and current fields that would affect the trajectory and weathering of oil spilled under different spill scenarios. This involves repeated simulation of each scenario, using different samples of metocean conditions each time. To affect an objective and statistically representative selection of these conditions, a set of times and dates are selected at random from within the period of the long-run data set (i.e. 1997-2006 inclusive). The sequence of metocean conditions that follow these times are then applied to unique spill simulations. To stratify risks of exposure separately for the summer and winter, a separate batch of spill simulations were undertaken with start times commencing in the summer (November to February) and winter (May to August) months.

This stochastic sampling approach provides an objective measure of the possible outcomes of a spill, because environmental conditions will be selected at a rate that is proportional to the frequency that these conditions have occurred over the study region. More simulations will tend to use the most commonly occurring conditions, while conditions that are more unusual will be represented less frequently. The approach assumes that wind and current patterns that have occurred over the recent past will be representative of risks over future years.

During each simulation, the SIMAP model records the location (by latitude, longitude and depth) of each of the particles (representing a given mass of oil) on or in the water column, at regular time steps. For any particles that contact a shoreline, the model records the accumulation of oil mass that arrives on each section of shoreline over time, less any mass that is lost to evaporation and/or subsequent removal by current and wind forces.

Accumulation is also limited to realistic limits based on the shoreline type (width of intertidal area and absorbance) and oil viscosity following empirical observations.

The collective records from all simulations are then analysed by dividing the study region into a 3-dimensional grid. For oil particles that are classified as being at the water surface (floating oil), the sum of the mass in all oil particles located within a grid cell, divided by the area of the cell provides estimates of the concentration of oil in that grid cell, at each time step. For entrained and dissolved oil particles, concentrations are calculated at each time step by summing the mass of particles within a grid cell and dividing by the volume of the grid cell.

The concentrations of oil calculated for each grid cell, at each time step, are then analysed to determine whether concentration estimates exceed defined threshold concentrations.

Risks are then summarised as follows:

- The probability of exposure to a location is calculated by dividing the number of spill simulations where contact occurred above a specified threshold at that location divided by the total number of replicate spill simulations. For example, if contact occurred at the location (above a specified threshold) during 21 out of 100 simulations, a probability of exposure of 21% is indicated;

- The minimum potential time to a shoreline location is calculated by the shortest time over which oil was calculated to travel from the source to the location in any of the replicate simulations;

- The maximum potential concentration of oil forecasted for each shoreline section is the highest mass per m^2 of shoreline calculated to strand at any location within that section during any of the replicate simulations;

- The mean expected maximum concentration of oil forecasted to potentially accumulate on each shoreline section is calculated by determining the highest mass per m^2 of shoreline during each of the replicate simulations and calculating an average.

Thus, the minimum time to shoreline and the maximum potential concentration estimates indicate the worst potential outcome of the spill scenario for each section of shoreline. However, the mean expected maximum presents an average of the potential outcomes, in terms of oil that could strand. Note also that results quoted for sections of shoreline or shoal are derived for any individual location within that section or shoal, as a conservative estimate. Locations will represent shoreline lengths of the order of ~ 1 km, while sections will represent shorelines spanning tens to hundreds of km and we do not imply that the maximum potential concentrations quoted will occur over the full extent of each section. We therefore warn against multiplying the maximum concentration estimates by the full area of the section because this will overestimate the total volume expected on that section.

3.3.2 Dispersion Coefficients

A horizontal dispersion coefficient of 1 m^2/s was used to account for dispersive processes acting at the surface that are below the scale of resolution of the input current field, based on typical values for estuaries. Dispersion rates within the water column (applicable for entrained and dissolved plumes of hydrocarbons) were also specified at 1 m^2/s, based on empirical data for the dispersion of hydrocarbon plumes in coastal wasters (King & McAllister, 1998).

3.3.3 Contact Thresholds

The SIMAP model will track oil concentrations to very low levels. Hence, it is useful to define minimum threshold concentrations for recording contact by oil at meaningful concentrations at locations during the simulations.

The judgement of meaningful levels is complicated and will depend upon the mode of action (smothering, ingestion, absorbance of toxic soluble compounds etc.), sensitivity of the biota contacted, the duration of the contact and the particular toxicity of the compounds that are represented in the oil. The latter factor is further complicated by the change in the composition of an oil type over time due to weathering processes. Without specific testing of the oil types, at different states of weathering against a wide range of the potential local receptors, a conservative approach was followed whereby contact by different components of spilled oil (the floating, entrained and dissolved components) was judged for a number of screening-level threshold concentrations, commencing at levels expected to be conservatively low with regards to the potential for lethal effects. These thresholds are summarised in Table 3-4 and are discussed below.

Table 3-4: Summary of the thresholds applied in this study.

	Surface Oil (g/m^2)	Entrained oil (ppb)	Aromatic oil (ppb)	Entrained Oil Dosage (ppb.hr)	Dissolved Aromatic Oil Dosage (ppb.hr)
Thresholds	1 (Rainbow Sheen)	10	40	960	576
	10 (Dull Metallic Colours)	100	100	9,600	4,800
	50 (Dull Metallic Colours)	500	500	48,000	38,400

3.3.3.1 Floating Oil

Surface oil concentrations of oil floating on the surface are relevant to describing the risks of oil coating emergent reefs, vegetation in the littoral zone and shoreline habitats, as well as the risk to wildlife found on the water surface, such as marine mammals, reptiles and birds. Floating oil is also visible at relatively low concentrations (> ~ 0.05 g/m^2). Hence, the area affected by visible oil, which might trigger social or economic impacts, will be larger than the area where biological impacts might be expected.

Thresholds for registering contact by surface slicks onto surface waters were assessed at indicative concentrations, based on the relationship between slick thickness and visible appearance as described in the Bonn Agreement (BA, 2003; Table 3-5, Figure 3-11).

Estimates for the minimal thickness of floating oil that might result in harm to seabirds through ingestion from preening of contaminated feathers, or the loss of the thermal protection of their feathers, has been estimated by different researchers at approximately 10 g/m^2 (French 2000) to 25 g/m^2 (Koops *et al*. 2004). Oil films exceeding 0.1 mm (~ 100 g/m^2) have been suggested as sufficient to smother epifauna on hard substrates (Owens and Sergy 1994), while films > 1 mm (1 kg/m^2) have been shown to impact marsh and mangrove plants by smothering (French 2009). Hence, the lowest (1 g/m^2) threshold is applied as a conservative level in terms of environmental harm and is likely to be more indicative of the perceived area of effect of a spill that might trigger economic and social impacts, such as the temporary closure of local fisheries as a precautionary measure. The higher thresholds (10 g/m^2 and 50 g/m^2) indicate higher potential for environmental harm.

It is important to note that real spill events generate surface slicks that break up into multiple patches of higher concentration, typically surrounded by thinner sheen and separated by areas of open water. Therefore, calculation of concentrations requires careful definition. When considered over a defined area, concentrations will be the average of the patches, sheens and open areas within the defined area. Concentration defined in this way will be lower than the concentrations within the patches.

For this assessment, water surface concentrations have been calculated as the average concentration (total mass of oil/area) within grid cells of 500 m x 500 m.

Table 3-5: The Bonn Agreement Oil Appearance Code.

Appearance (following Bonn visibility descriptors)	Mass per Area (g/m^2)	Thickness (μm)	Volume per Area (L/km^2)
Continuous true oil colour	> 200	> 200	> 200,000
Discontinuous true oil colours	50 - 200	50 - 200	50,000 - 200,000
Dull metallic colours	5 - 50	5 - 50	5,000 - 50,000
Rainbow sheen	0.30 - 5.0	0.30 - 5.0	300 - 5,000
Silver sheen	0.04 - 0.30	0.04 - 0.30	40 - 300

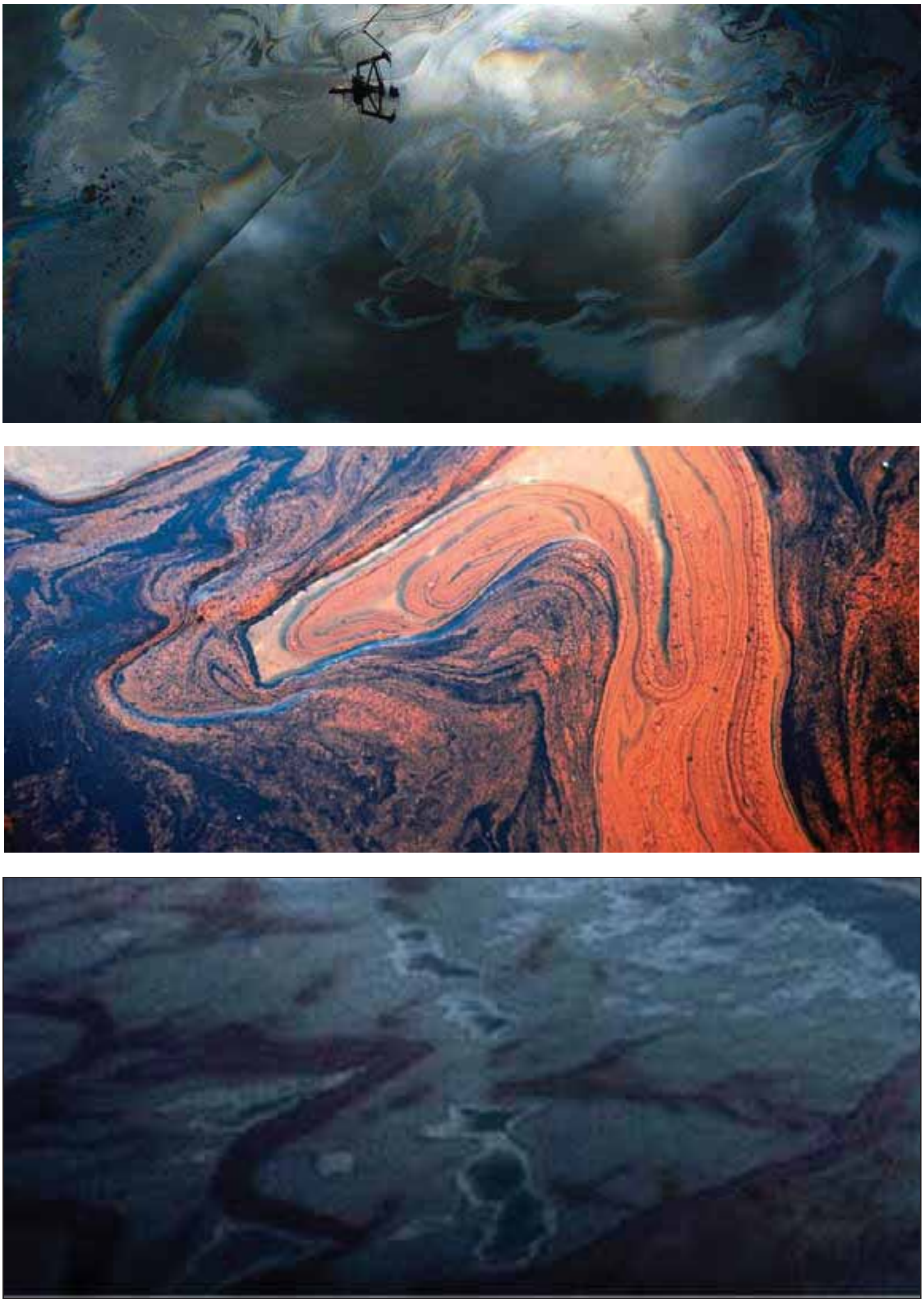

Figure 3-10: Photographs of oil film appearance on the water surface. Top panel indicates continuous true oil colour, middle image represents bands of emulsified oil and non-emulsified oil as a continuous true-oil colour, the lower image indicates bands of true oil colour among rainbow and silver sheen. (Goodman, 2007).

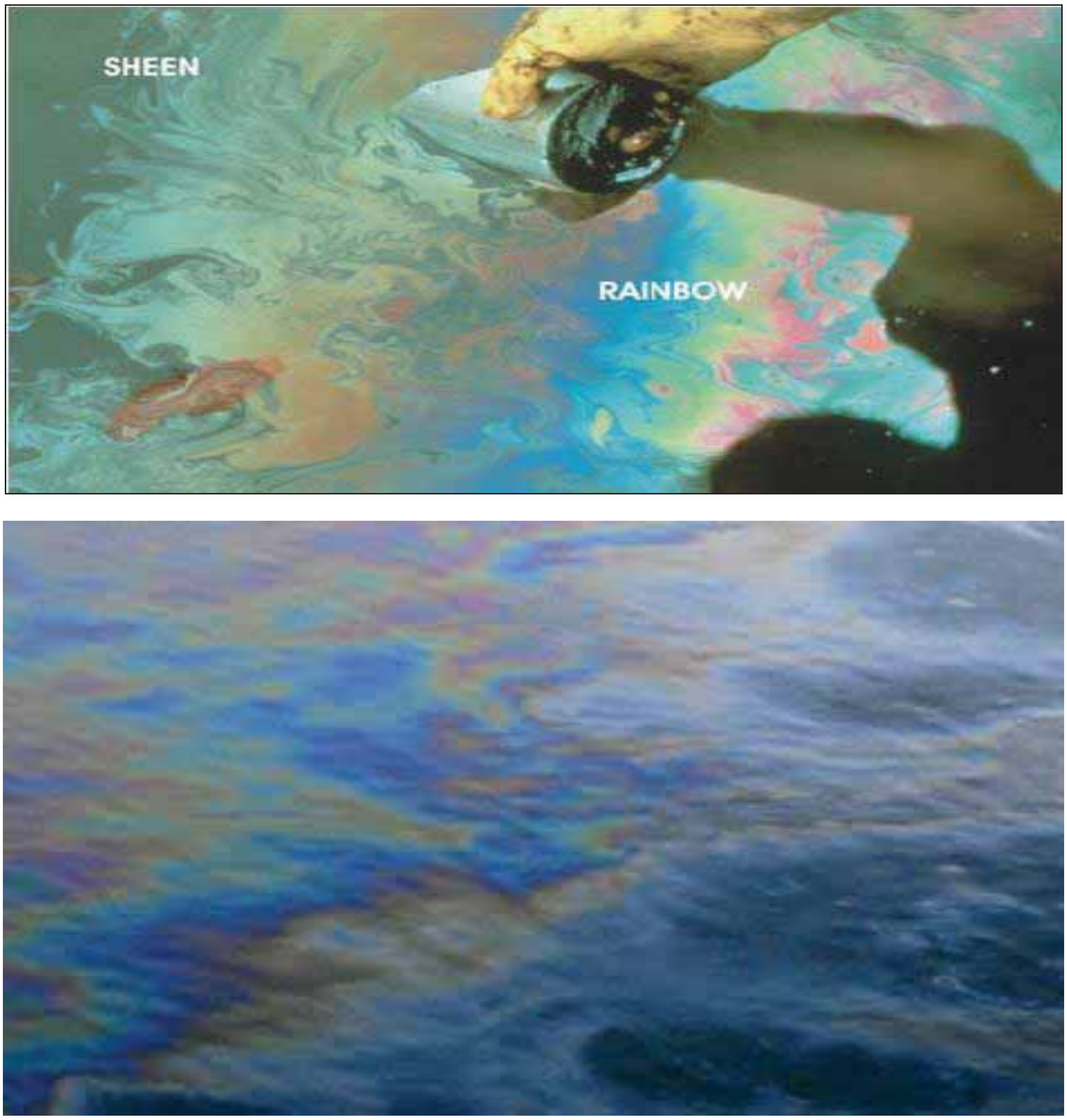

Figure 3-11 (continued): Photographs of oil film appearance on the water surface. Top panel indicates bands of dull metallic colour surrounded by rainbow and silver sheen, for a spill of oil. Lower panel indicates rainbow sheen thinning to silver sheen generated by a diesel spill (Goodman, 2007).

3.3.3.2 Entrained Oil

Oil can be entrained into the water column from surface slicks due to wind and wave-induced turbulence or generated underwater by pressurised discharge at depth. Entrained oil presents a number of possible mechanisms for exerting exposure. The entrained oil droplets may contain soluble compounds, hence have the potential for generating elevated concentrations of dissolved hydrocarbons (e.g. if mixed by breaking waves against a shoreline). Physical and chemical effects of the entrained oil droplets have also been demonstrated through direct contact with organisms, for example through physical coating of gills and body surfaces, and through accidental ingestion (NRC, 2005).

A review of the concentrations of physically entrained oil that has been demonstrated to have harmful effects in laboratory studies (NRC, 2005) shows wide variation depending on the test organisms and the initial oil mixture. For mortality of molluscs, reported LC_{50} values range from 500 ppb to 2 ppm with 96 hr exposure. Wider exposure sensitivities are displayed by species of crustaceans (100 ppb to 258,000 ppm) with 96 hr exposure, while marine fish larvae appear more sensitive again with LC_{50} values as low 45 ppb after 24 hr exposure.

As indications of increasing potential impact on different receptors, thresholds for concentrations of entrained oil were defined at 10 ppb, 100 ppb and 500 ppb (Table 3-4). The lowest threshold is considered a conservatively low estimate of the lowest concentration that may be harmful to sensitive marine organisms with relatively long exposure (tens of hours; French, 2000). Because of the requirement for relatively long exposure times, this threshold is more meaningful for larvae and organisms that might be entrained (and therefore moving) within the oil plumes. The higher thresholds are more relevant to short duration (acute) exposure to organisms or fixed habitats affected by the dynamically varying plume.

Predicted concentrations of entrained oil have been calculated as the average over volumes of 500 m x 500 m in the horizontal x 3 m in the vertical.

3.3.3.3 Dissolved Aromatic Hydrocarbons

Most of the toxic effects of oil on biota have been attributed to the toxicity induced by the uptake of soluble hydrocarbon compounds released into the water column and taken up by the tissues of plants and animals. The mode of action of soluble hydrocarbons is a narcotic effect that interferes with cell functions. This effect is additive, increasing with exposure concentration or with time of exposure (French, 2000; NRC, 2005) For many oil mixtures, the concentration of aromatic hydrocarbons, and specifically the 2-3 ring poly-aromatic hydrocarbons, in the water soluble fraction is the best predictor of the toxicity of the oil.

Reviews of the body of data available from toxicity tests where marine and estuarine biota have been exposed to the water soluble fractions of a wide range of oils indicate different toxicity levels will be generated from different oil types, due to variations in their constituent compounds, and a wide range in the tolerance of individual species and life-stages of organisms. French (2002) compiled comparisons for many oil types and organisms and suggested a lowest lethal effect concentration of around 60 ppbb given 96 hrs exposure, for the more sensitive species exposed to the more toxic soluble mixtures, with higher concentrations required for short term exposures.

Two assessment approaches were followed for the magnitude of exposure to the soluble aromatic hydrocarbons. Firstly, we assessed for exceedence of threshold concentrations at any one time step for concentrations of 40 ppb, 100 ppb and 500 ppb. The time step in the model was one hour, hence exceedence occurred if any location was calculated to have a local concentration exceeding these thresholds for at least one hour.

Because exposure times may be short (< 1-2 hr) in the case of a slick passing over a fixed habitat (such as a reef or seagrass bed), due to fluctuations in the plume location with changing weather and current conditions, and because marine and estuarine organisms can typically tolerate concentrations of toxic hydrocarbons that are two or more orders of magnitude higher over such short durations (French, 2000; Pace *et al*, 1995), we also calculated for exposure dosage at each location. Exposure dosage is calculated as the average concentration experienced multiplied by the duration of the exposure, in hours. Three levels of exposure dosage were defined – 576 ppb.hrs, representing the equivalent of 6 ppb (average) for 96 hrs of exposure; 4,800 ppb.hrs, representing the equivalent of 50 ppb (average) for 96 hrs of exposure; and 38,400, representing the equivalent of 400 ppb (average) for 96 hrs of exposure. Based on the findings of French (2002), the lower dosage exposure threshold is considered to be indicative for sub-lethal effects, while the higher thresholds would indicate increased likelihood of direct mortality.

3.3.4 Oil Properties and Weathering Characteristics

3.3.4.1 Heavy Fuel Oil

Characteristics of Heavy Fuel Oil (HFO) were specified from the ADIOS oil database, and are summarised in Table 3-6. HFO is manufactured as a blend of highly volatile hydrocarbons, present in low proportions, and residues from oil distillation, hence the oil is largely composed of compounds that have low volatility or are resistant to evaporation altogether. HFOs have a high relative density, and although they will tend not to sink when in salt water, they have a tendency to sit low on the water surface and may be overwashed. The blend also has high viscosity (>20,000 cSt at 15 °C). As a consequence, the oil does not tend to spread rapidly when spilled onto the sea and only small reductions in the spilled oil volume will occur over time (< 20% over days). More-over, HFO has a tendency to take up water droplets to form a water in oil emulsion that may result in 30-70% increase in volume for the emulsified material with this emulsification resulting in an increase in the volume of oily waste compared to the original spill volume. Emulsification will also lead to a further increase in viscosity. The pour point of most HFO blends (~7 C) would be high relative to water temperatures in Western Port Bay during winter so that the oil may coagulate to a semisolid on the water although liquidise when heated by the sun and air on a warmer shoreline.

Table 3-6: Characteristics of the HFO oil used in this study.

Oil Type	Density (g/cm^3) (at 15 °C)	Viscosity (cP) (at 25 °C)	Component	Volatile (%)	Semi-Volatile (%)	Low Volatility (%)	Residual (%)
			BP (°C)	<180	180-265	265-380	>380
Heavy Fuel Oil	0.9749	3,180	% of total	1.0	4.9	11.3	82.8

An example forecast for the weathering of HFO under varying wind and current speeds, for a water temperature of 15 °C reveals the relatively small proportion of the oil volume that would likely evaporate, leaving a residual volume exceeding 80% of the initial spill. A low potential for this oil to entrain is also indicated, which can be attributed to the high viscosity of HFO.

HFO tends to contain low proportions of soluble aromatic hydrocarbons but the residual components will include poly-aromatic hydrocarbons with 4 or more carbon ring structures that have low water solubility. These will remain in the residual unless biodegraded over the longer term.

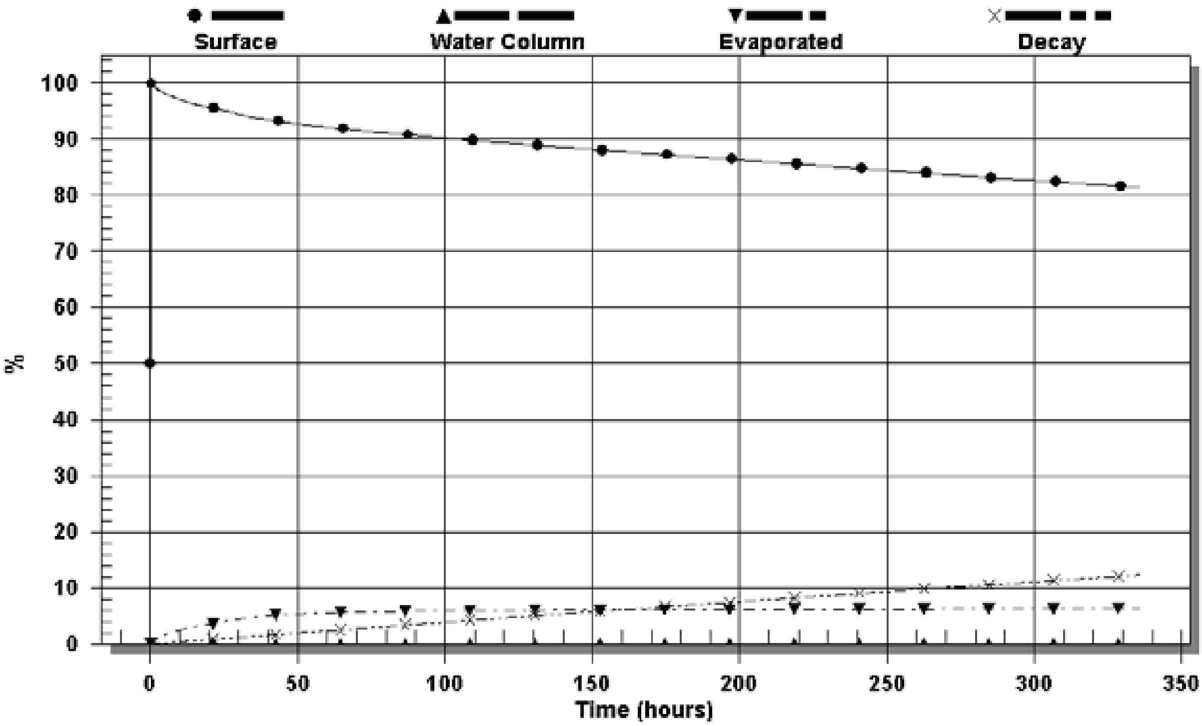

Figure 3-12: Proportional mass balance plot representing weathering of HFO on water at 15 °C, for varying tide and wind conditions.

3.3.4.2 Diesel Fuel

Diesel oil is also a manufactured blend and characteristics for marine diesel were derived from the ADIOS database for a blend suited to similar operational temperatures to Western Port Bay. Diesel oil has low viscosity and spreads rapidly to thin sheens when spilled onto seawater. Because this fuel oil is blended as a mixture of volatile and more persistent hydrocarbons (Table 3-7), the oil will undergo evaporation at rates that will vary over time. The most rapid evaporation, over the first hours, will result in the evaporation of the low percentage (6%) of highly volatile components, followed by the evaporation of the semi-volatile components. Evaporation will then slow markedly. The fate of the residual oil will then tend to vary with the prevailing conditions. Under calm mixing energy (calm wind and low tidally generated turbulence) the oil will evaporate further over the next 24 hours leaving a residual (~5%) of long carbon chain compounds. However, under moderate winds that generate wind-waves, diesel oil will tend to physically entrain into the water column as fine oil droplets. These droplets will tend to occur in the upper water column due to their positive buoyancy and may re-float when mixing decreases under calm conditions.

The proportion of soluble aromatic hydrocarbons in diesel is relatively low (approximately 3%).

Table 3-7: Characteristics of the diesel used in this study

Oil Type	Density (g/cm³) (at 25 °C)	Viscosity (cP) (at 25 °C)	Component	Volatile (%)	Semi-Volatile (%)	Low Volatility (%)	Residual (%)
			BP (°C)	<180	180-265	265-380	>380
Diesel Fuel Oil	0.8291	4.0	% of total	6	34.6	54.4	5

Predictions for the weathering of a marine diesel spill under representative ambient conditions are shown in Figure 3-13. In this example, an initial rapid evaporation of the volatile compounds is predicted for the first three days following the spill, resulting in 40% of the spilled mass evaporating. The residual oil mixture is then forecasted to physically entrain under conditions that generate wind waves (> ~12 knots). Note that this calculation sums the oil mass over all areas and that the spreading of the mass may decrease local concentrations.

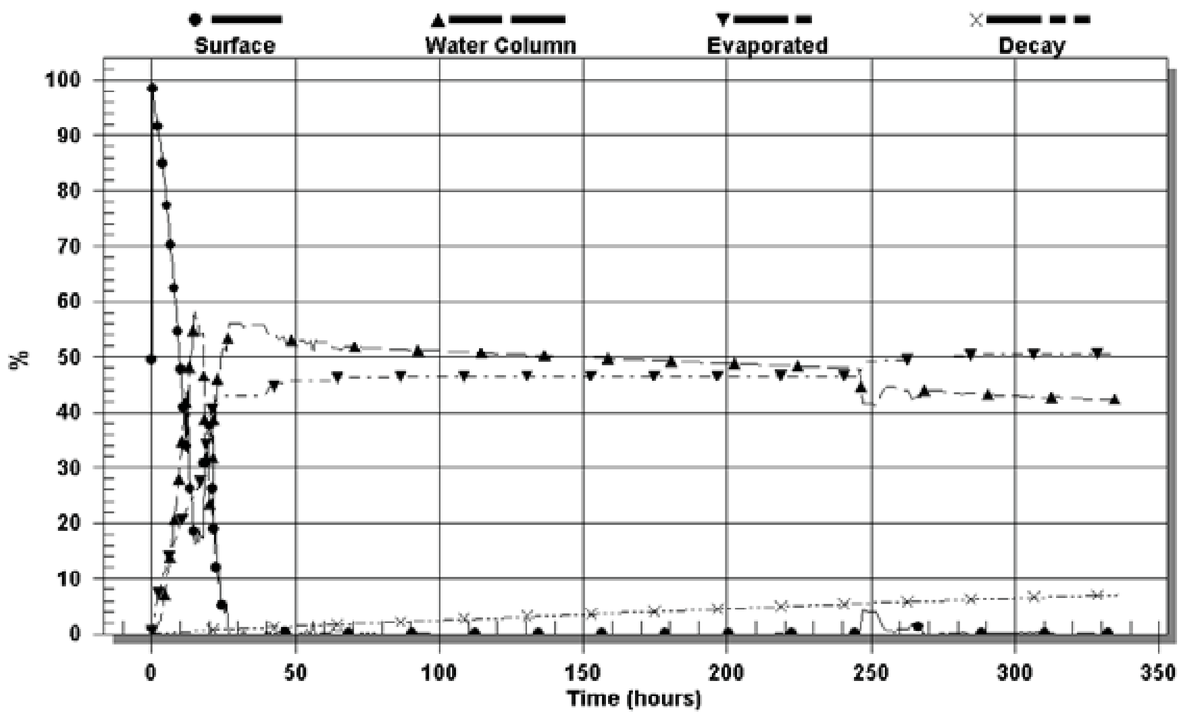

Figure 3-13: Proportional mass balance plot representing weathering of diesel over 14 days. Predictions are an example only, produced for a particular time-sequence of environmental conditions where wave action is present, resulting in entrainment of the heavier components

It can be noted from this analysis that HFO spills would have the greater likelihood of generating negative effects from oil on the water surface, or accumulating onto shorelines, while diesel presents the additional risk of exposure to entrained oil for organisms on the seabed or in the water column.

3.3.5 Replication and Simulation Lengths

One hundred replicate simulations were completed for each combination of spill scenario and season. Simulations were run for a period of 14 days from the spill start times to allow ample time for oil to migrate and redistribute within the study area due to washing off from areas that would not retain oil over subsequent tidal high periods or with shifts in the wind direction. Thus the assessment considers potential risks of contamination within the first 2 weeks of a spill and not the potential for subsequent contamination over the longer term.

4 RESULTS

4.1 Overview

Predictions for the probability of contact by oil concentrations exceeding defined thresholds are provided to summarise the results of the stochastic modelling. Results are presented separately for the surface, entrained and aromatic components of the oil given spills commencing within each season.

Recall that the probability contours summarise the outcomes of multiple replicate spills, with each potentially exposing a different area over the duration of the spill event. Hence, the wider extent of the contours summarise the collective area swept by many spill events, while the internal details designate the probability that a given location would be swept by oil (exceeding the defined threshold) during a single event. The large distribution of the probability contours can be attributed to the large variability and high complexity of the currents interacting with wind patterns, which would tend to transport different portions of the oil along different trajectories. The simulations indicated that floating oil will tend to oscillate along the channels over multiple tidal cycles, but will be subject to winds blowing towards shorelines over an extended period (days to weeks).

As an illustration of this phenomenon, a time sequence is presented to show forecasts for the movement of oil components from a single simulated spill event, involving a spill of HFO at Long Island Point Jetty (Figure 4-1). In this example, tracers representing the floating slick streamed upstream initially with the flooding tide and returned on the ebbing tide where a westerly wind diverted some of the oil tracers onto the shoreline of French Island. The volume still floating was then directed upstream and towards the western shore before migrating again with the ebb tide past Cribb Point towards the western entrance. Portions of the floating oil returning with the flooding tide are forecasted to strand on the northern side of Phillip Island with the remainder breaking up and migrating as oil patches into each of the estuary arms.

Summary tables are provided to summarise the probability of oil arriving at particular sections of shoreline that are designated as marine parks and conservation reserves (Figure 4-2), at specified threshold concentrations or greater. Estimates are also provided for the minimum elapsed time before floating oil may drift onto these shorelines. These estimates are based on the arrival of floating oil on at least one time step. As an alternative way of considering exposure risks, estimates are also provided for the potential concentrations of oil that might accumulate on shorelines over time. The maximum estimate is the highest accumulation predicted for any point on the shoreline during any replicate simulation and hence is an extreme estimate. The mean expected maximum is the highest accumulation predicted for any point on the shoreline after averaging among the replicate simulations and is therefore representative of a more typical outcome. Note that minimum thresholds of concentration are applied to instantaneous estimates of floating oil concentrations to calculate the probability of oil arriving at shorelines as floating oil; however, because it is possible that thinner films may accumulate onto sections of shoreline over the course of a spill event, the mean and maximum concentrations of accumulated oil can exceed these thresholds. Hence, it is possible for the modelling to detect situations where the probability of arrival at a threshold is less than 1% but a maximum local concentration is reported after allowing for accumulation of oil.

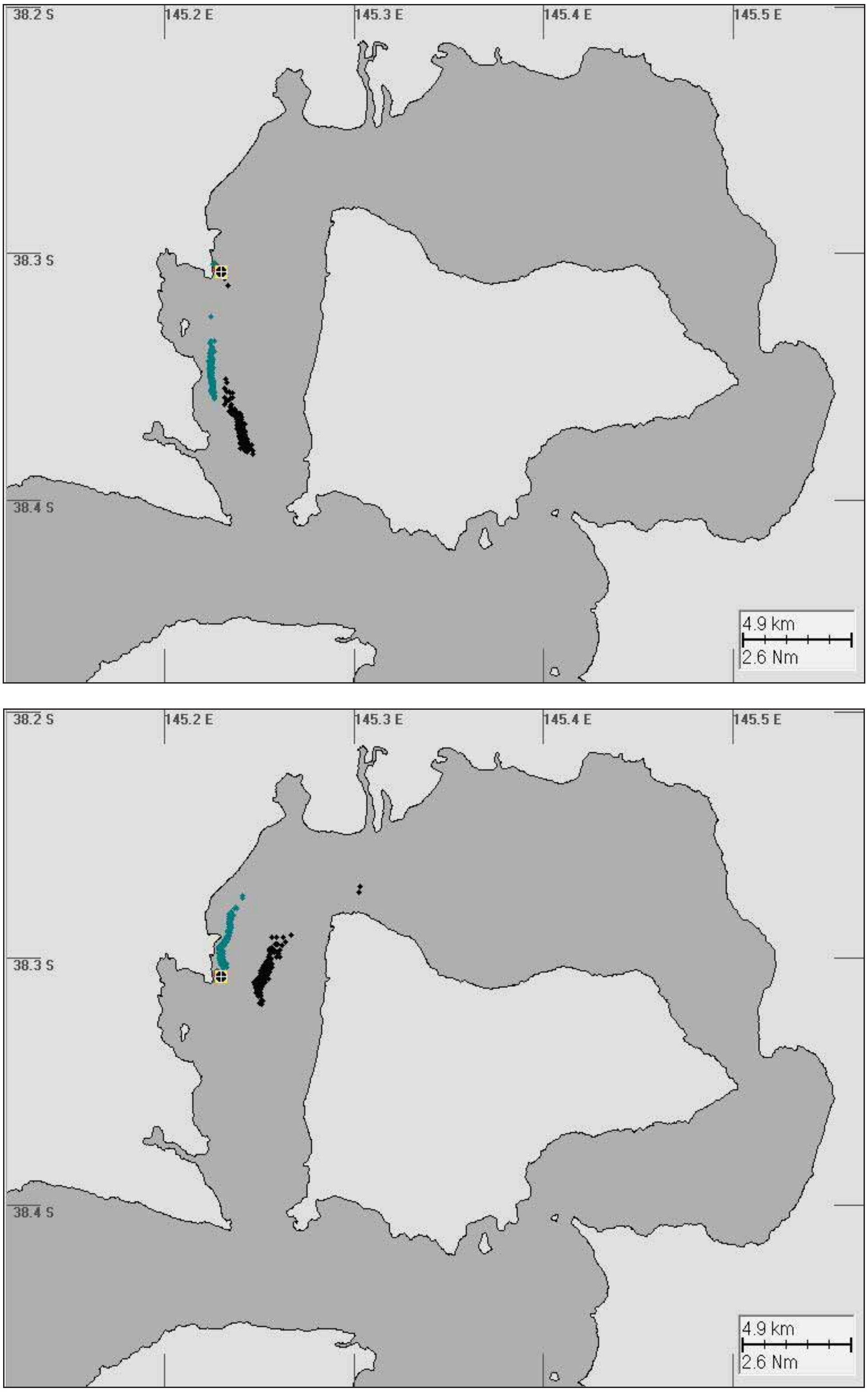

Figure 4-1: Example of a forecast for the trajectory of tracers representing components of an HFO spill at Long Point Jetty (Scenario 1). Black markers designate floating oil, green markers designate entrained oil, red markers designate oil stranded on shorelines

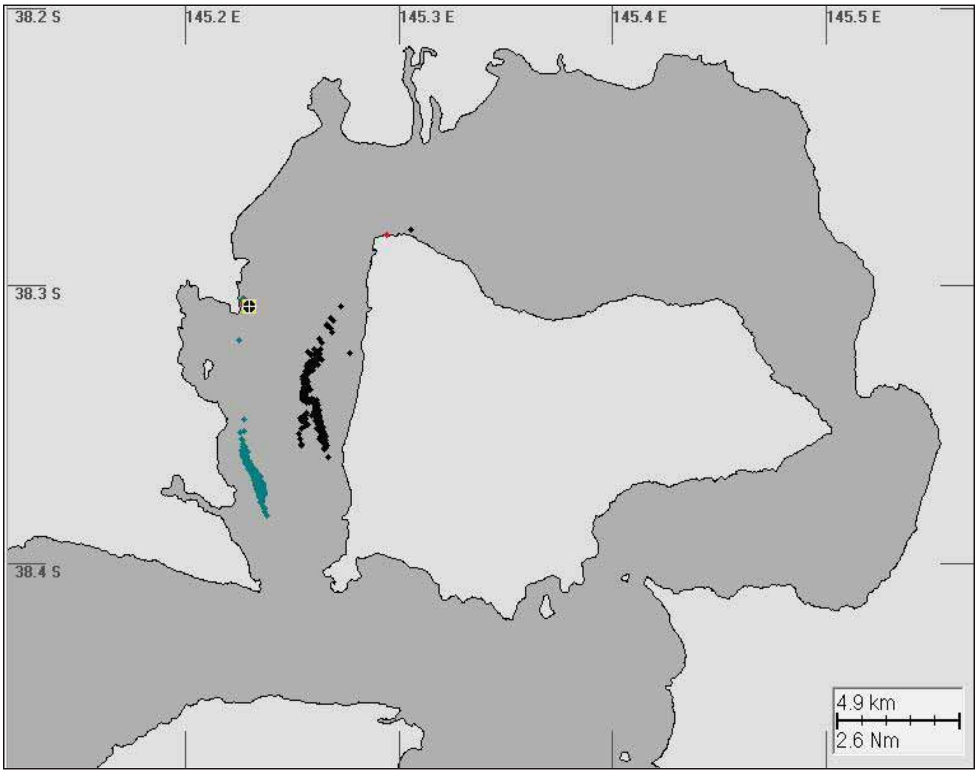

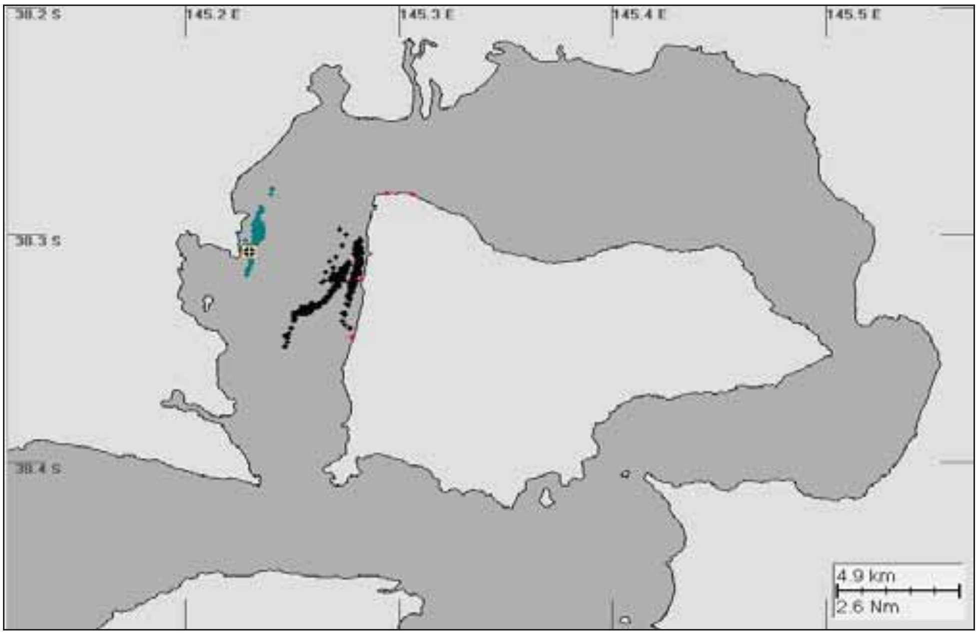

Figure 4-1 (Continued)

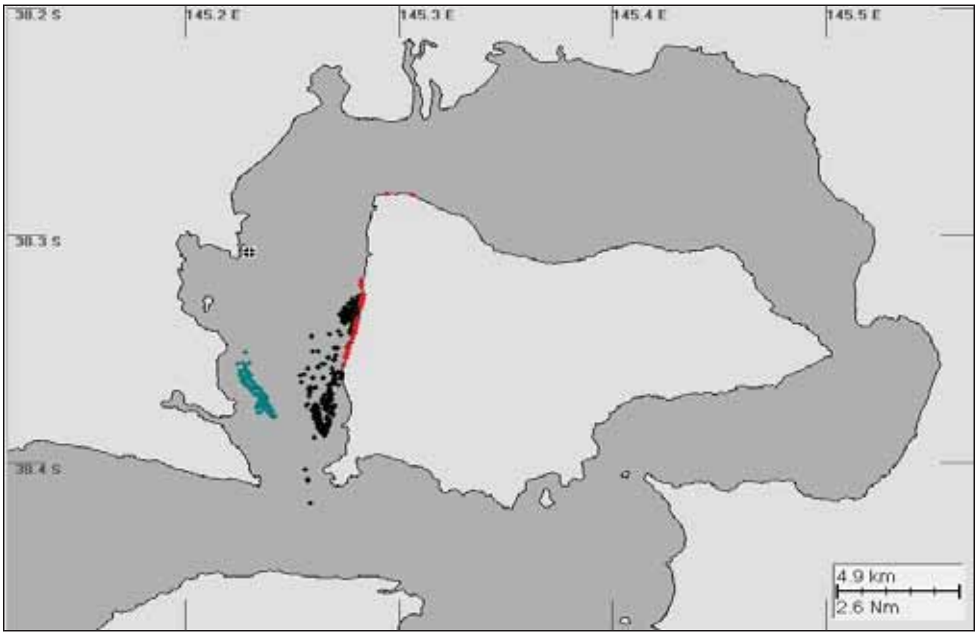

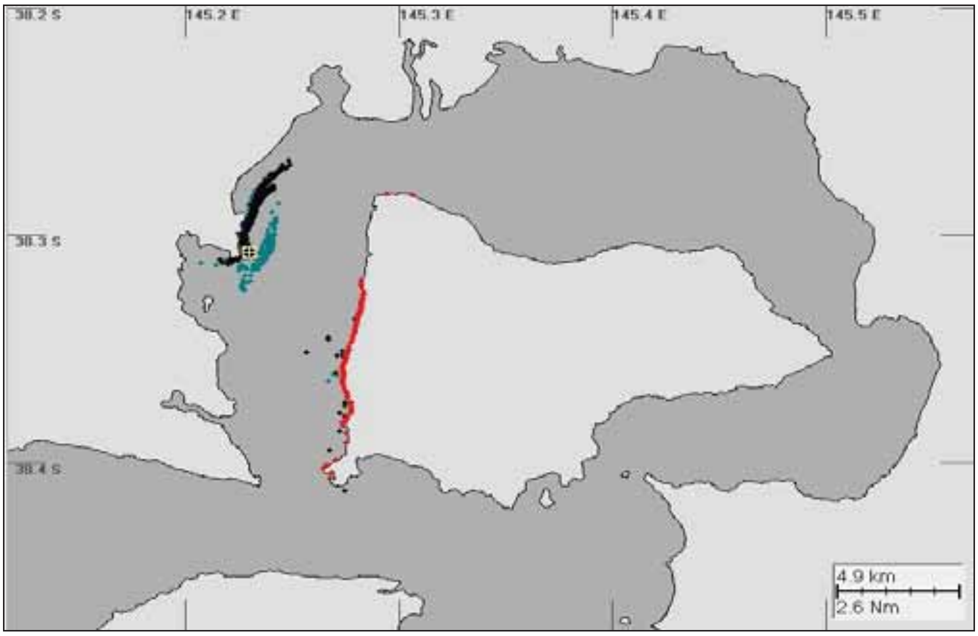

Figure 4-1 (Continued)

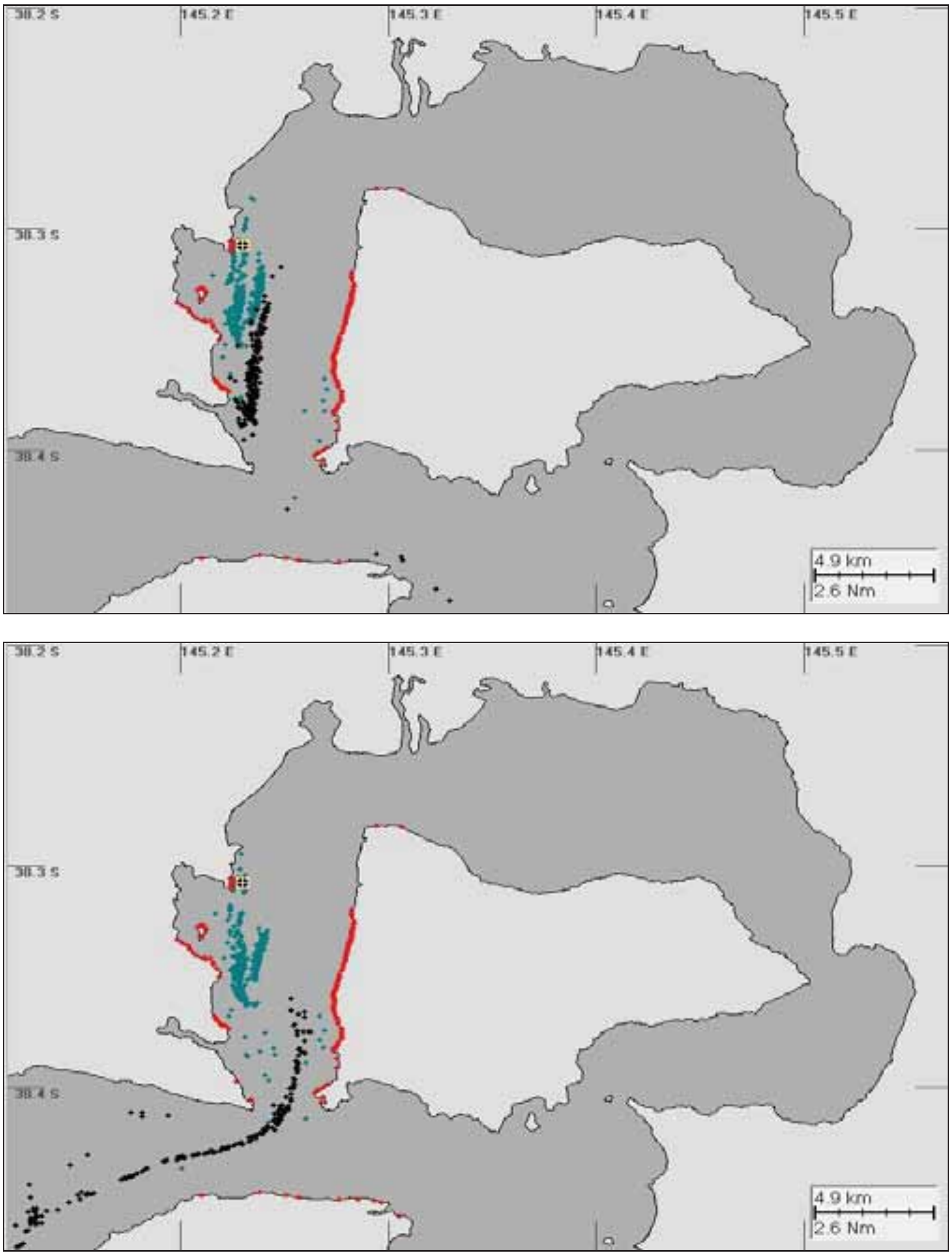

Figure 4-1 (Continued)

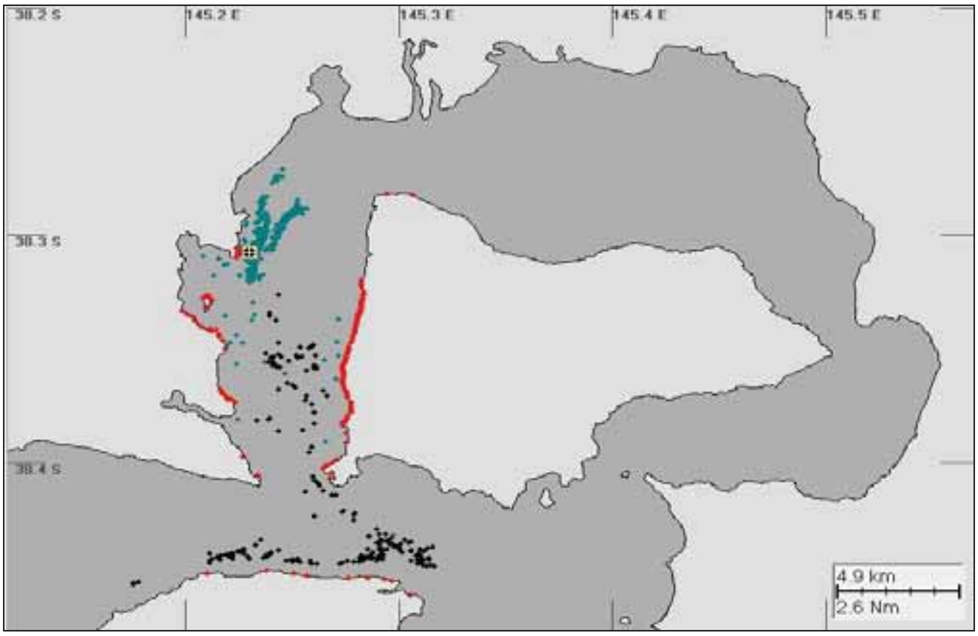

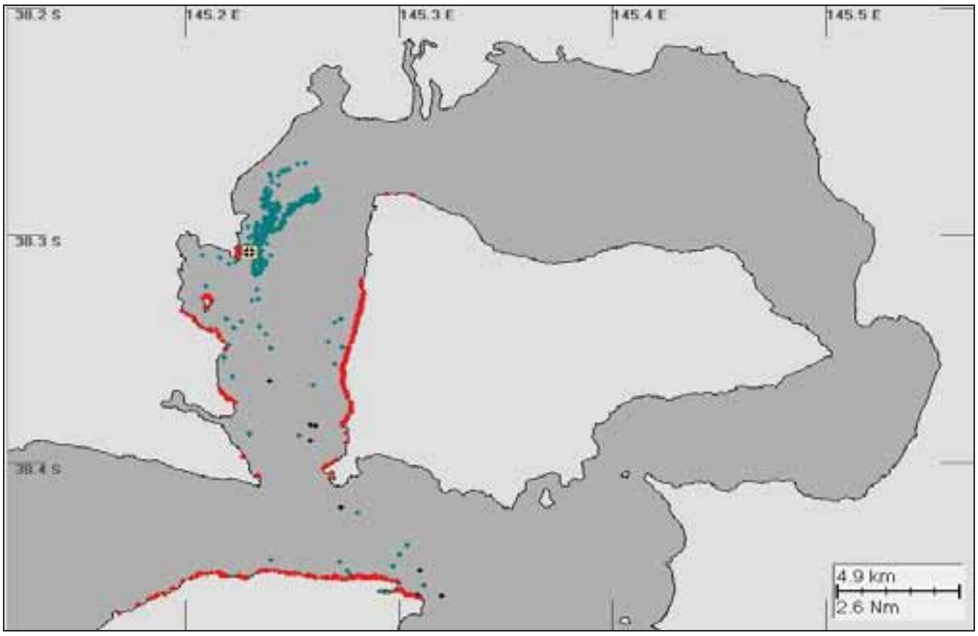

Figure 4-1 (Continued)

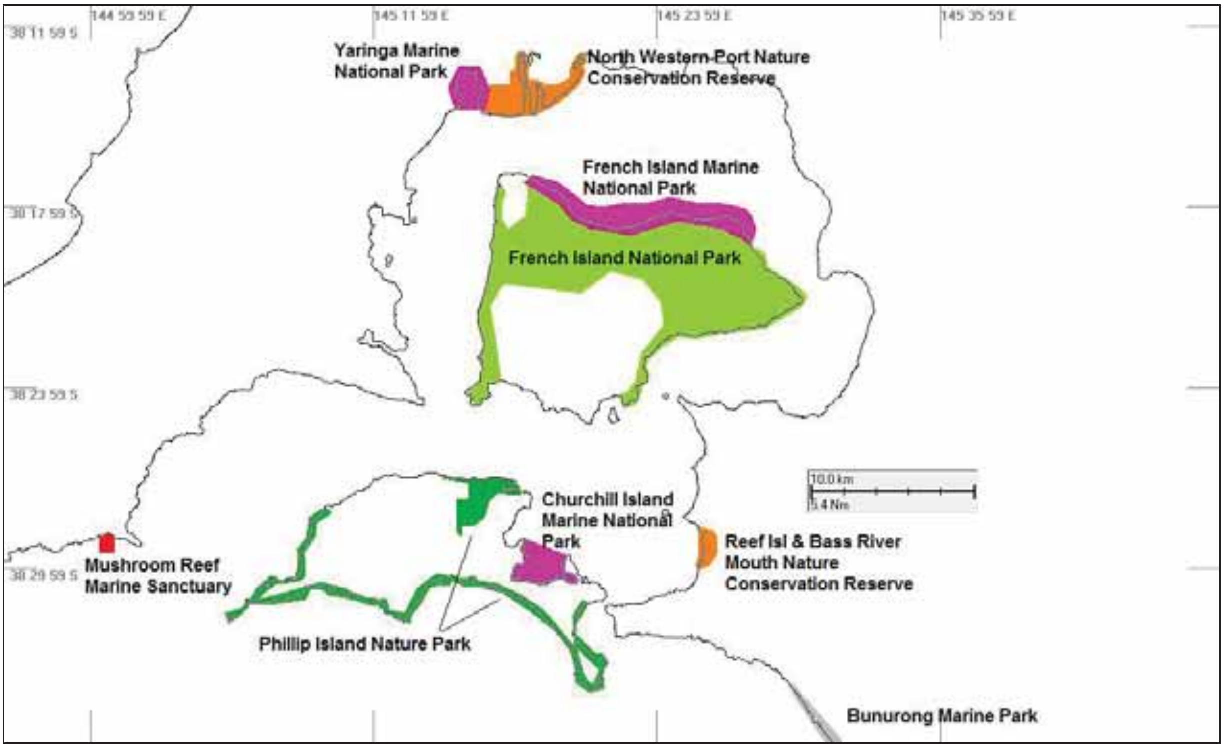

Figure 4-2: Distribution of national parks and marine reserves that have been established in Western Port Bay.

4.2 Simulation of a 200 Metric Tonne HFO spill at Long Point Jetty

This scenario investigated risks of contact for surrounding shorelines from a 200 MT spill of HFO over 3 days at Long Point Jetty.

Simulations of this spill scenario indicated that a high proportion of the oil mass would likely strand on shorelines at some point. Estimates as high as 85-90% of the volume were reported by the model, with this exposure occurring over a large part of the bay in a high proportion of cases.

The exposure probability contours calculated for this spill scenario commencing in summer indicate that floating oil is most likely to occur at concentrations > 10 g/m^2 within Lower North Arm but with the probability exceeding 30% of oil drifting into Northern North Arm. Probabilities of oil > 10 g/m^2 decrease to < 10% towards the Embayment Head and through the confluence zone between the Western Entrance Segment and the Rhyll Segment. The highest probability of contact (>50%) is forecasted along the tidal axis within 4 km of the jetty in both the ebb and flood direction. It is notable that the contours calculated for > 1 g/m^2 and > 10 g/m^2 are very similar for this spill scenario due to the forecast that the oil type will not spread but will be present as relatively thick layers of viscous oil.

Risks of contact with shorelines are indicated to be highest along the western shoreline, with > 30% probability of stranding indicated for the section of coastline extending from the Port of Hastings to Yaringa Marine Park (Quail Island Marine Reserve), at concentrations > 25 g/m^2. Probability of contact with North Western Port Nature Conservation Reserve are also indicated at > 30 % for concentrations > 25 g/m^2. The minimum time forecasted for floating oil to reach these locations is 6 to 7 hours – which would correspond with a single flood tide period. The potential concentrations of oil that could accumulate on any part of the shorelines in these areas was estimated at greater than 17 kg/m^2 (as oil, not inclusive of the mass of water in emulsified form) under the worst case simulation but averaged just over 1 kg/m^2 among the replicate simulations. Sections of shoreline along French Island National Park were forecasted to have > 20% probability of exposure at > 25 g/m^2 with extreme concentrations also forecasted to exceed 17 kg/m^2 and with similar durations (~ 8 hrs) required before exposure might occur. Churchill Island Marine National Park and Phillip Island nature park are forecasted to have relatively low risk of contact for this scenario in this season (~ 2%) with minimum drift times before exposure calculated at about 3 days.

The simulations indicated a low risk that oil would drift as far as the eastern or western entrances if the spill occurred in summer.

The exposure probability contours generated for spill simulations under winter conditions varied markedly from those calculated for spills in summer. While the contours still indicated > 10% probability that floating oil would occur at > 25 g/m^2 within Northern North Arm and Quail Island Marine Reserve, and > 30% probability of impinging on the western coastline of North Arm, the contours indicate a higher probability that floating oil at this concentration or greater would drift onto the western coastline of French Island, with the highest likelihood around Tortoise Island and into the confluence zone north of Phillip Island. The contours for winter indicate >20% probability that oil > 25 g/m^2 would extend across the Rhyll Segment and into the Churchill Island Marine National Park as well as along the Western Entrance Channel. At least 5% probability is indicated that concentrations > 25 g/m^2 would drift through the Eastern Entrance Channel to potentially affect shorelines along Cape Woolamai State Faunal Reserve and shorelines flanking the eastern side of this entrance.

The shoreline of French Island National Park is forecasted to have > 50% probability of contact at > 25 g/m^2, with the potential for over 17 kg/m^2 to occur under the worst case conditions. The shortest drift time to this shoreline indicated at ~ 6 hrs under winter conditions. Phillip Island Nature Park is forecasted to have 25% probability of exposure at > 25 g/m^2 with a similar potential concentration forecasted for the worst case but requiring about 1 day as a minimum elapsed duration. North Western Port Nature Conservation Reserve is forecasted to have 8% probability of exposure to oil > 25 g/m^2, with the potential for oil to arrive within 12 hours and accumulate to > 17 kg/m^2.

Table 4-1: Summary of shoreline risks for different locations resulting from a 200 MT spill of HFO at Long Point Island Jetty commencing during Summer.

	Probability (%) of films arriving at shorelines at > 1.0 g/m^2	Probability (%) of films arriving at shorelines at > 10.0 g/m^2	Probability (%) of films arriving at shorelines at > 25.0 g/m^2	Minimum time to shoreline (hours) for films at > 1.0 g/m^2	Minimum time to shoreline (hours) for films at > 10.0 g/m^2	Minimum time to shoreline (hours) for films at > 25.0 g/m^2	Maximum local accumulation (g/m^2)averaged among replicate spills	Maximum local accumulation (g/m^2) in the worst replicate spill
Yaringa Marine National Park	37	37	37	6	6	6	1,151	17,322
North Western Port Nature Conservation Reserve	34	34	34	7	7	7	1,218	17,322
French Island Marine National Park	14	14	14	8	8	8	38	2,138
Reef Island and Bass River Mouth Nature Conservation Reserve	1	1	1	231	231	231	2.6	257
Churchill Island Marine National Park	2	2	2	74	74	74	8.0	803
French Island National Park	24	24	24	8	8	8	904	17,322
Phillip Island Nature Park	2	2	2	68	68	68	53	2,862
Bunurong Marine Park	NC	NC	NC	NC	NC	NC	NC	NC
Mushroom Reef Marine Sanctuary	NC	NC	NC	NC	NC	NC	NC	NC

NC: No contact to shorelines indicated at > threshold

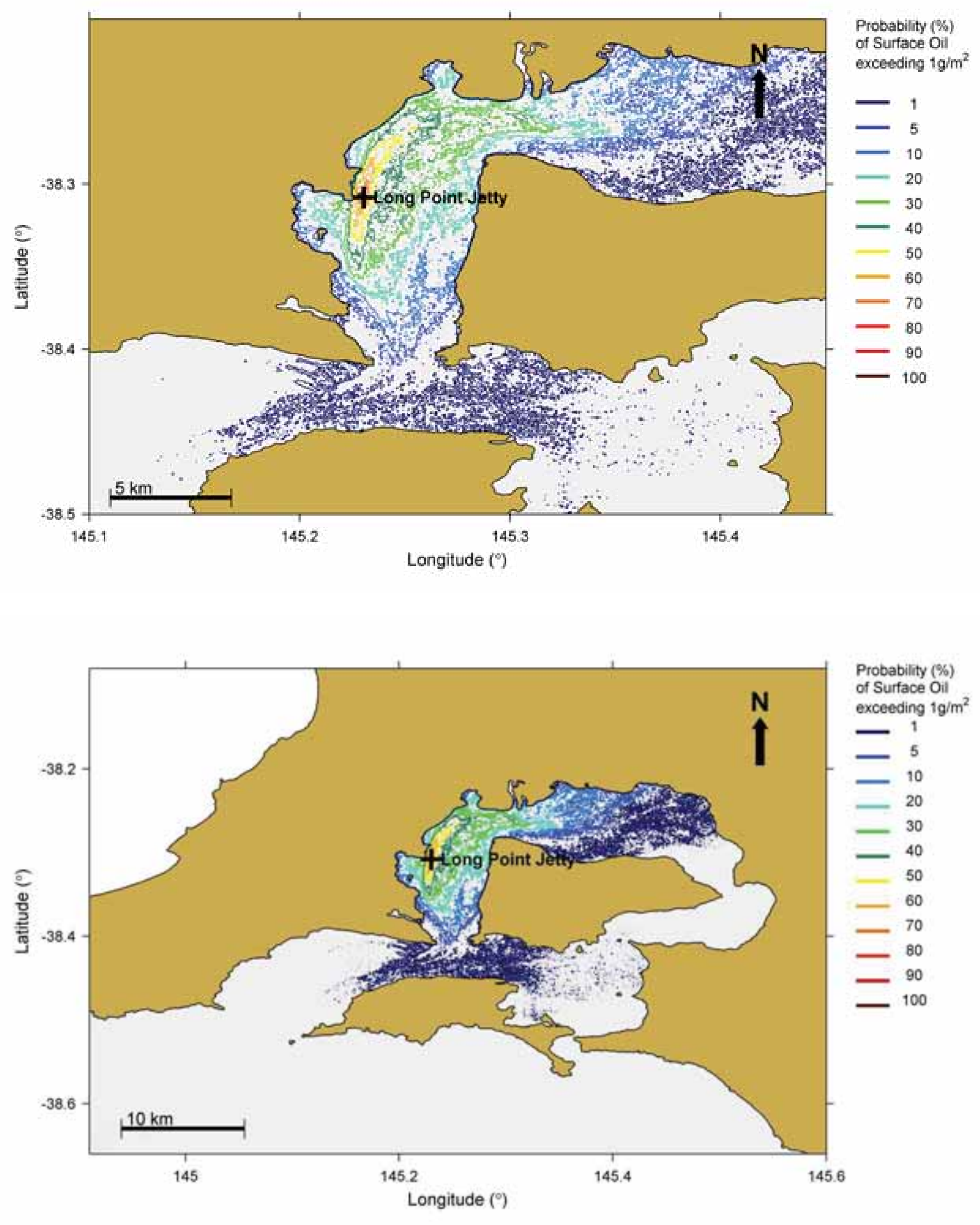

Figure 4-3: Probability contours for sea surface contact to concentrations above 1 g/m^2 resulting from a 200 MT HFO spill commencing during Summer.

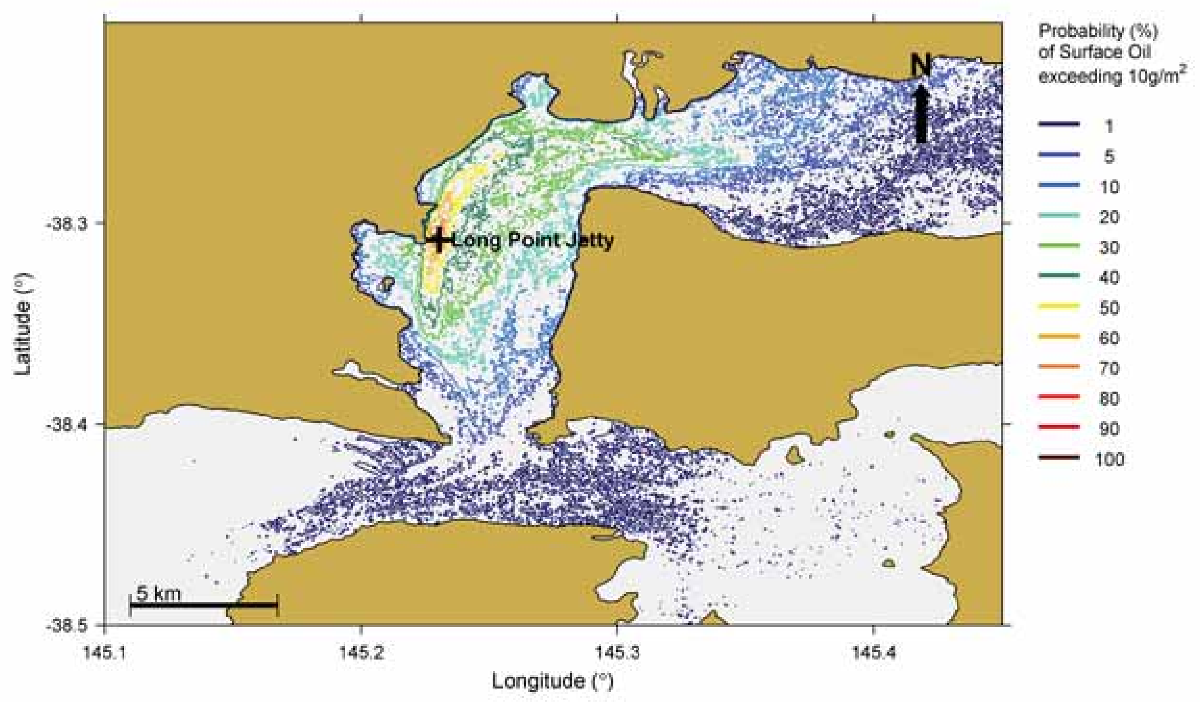

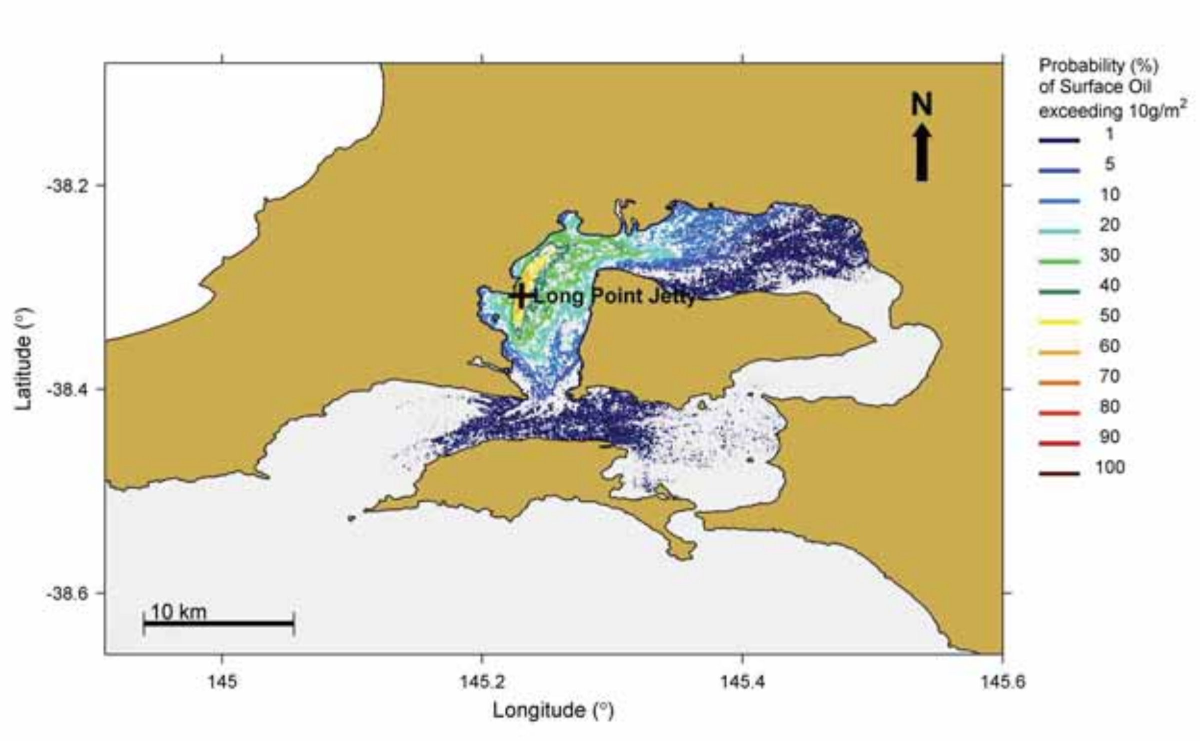

Figure 4-4: Probability contours for sea surface contact to concentrations above 10 g/m^2 resulting from a 200 MT HFO spill commencing during Summer.

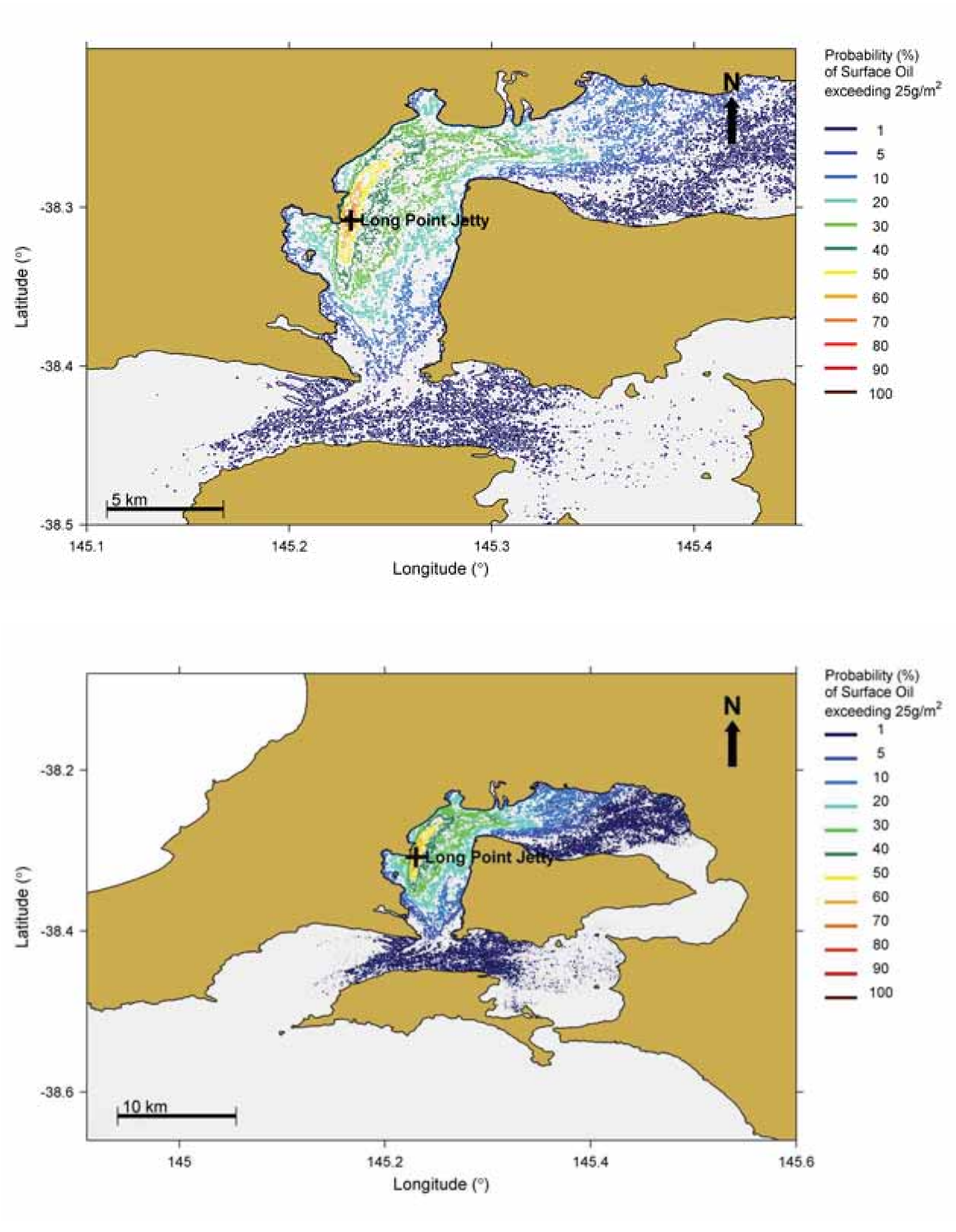

Figure 4-5: Probability contours for sea surface contact to concentrations above 25 g/m^2 resulting from a 200 MT HFO spill commencing during Summer.

Table 4-2: Summary of shoreline risks for different locations resulting from a 200 MT spill of HFO at Long Point Island Jetty commencing during Winter.

	Probability (%) of films arriving at shorelines at > 1.0 g/m^2	Probability (%) of films arriving at shorelines at > 10.0 g/m^2	Probability (%) of films arriving at shorelines at > 25.0 g/m^2	Minimum time to shoreline (hours) for films at > 1.0 g/m^2	Minimum time to shoreline (hours) for films at > 10.0 g/m^2	Minimum time to shoreline (hours) for films at > 25.0 g/m^2	Maximum local accumulation (g/m^2)averaged among replicate spills	Maximum local accumulation (g/m^2) in the worst replicate spill
Yaringa Marine National Park	12	12	12	7	7	7	260	9,921
North Western Port Nature Conservation Reserve	8	8	8	12	12	12	315	17,321
French Island Marine National Park	14	14	14	7	7	7	144	7,950
Reef Island and Bass River Mouth Nature Conservation Reserve	4	4	4	51	51	51	38	3,252
Churchill Island Marine National Park	11	11	11	34	34	34	122	3,785
French Island National Park	51	51	51	6	6	6	1,807	17,322
Phillip Island Nature Park	25	25	25	25	25	25	1,083	17,322
Bunurong Marine Park	1	1	1	177	177	177	NC	NC
Mushroom Reef Marine Sanctuary	NC	NC	NC	NC	NC	NC	NC	NC

NC: No contact to shorelines indicated at > threshold

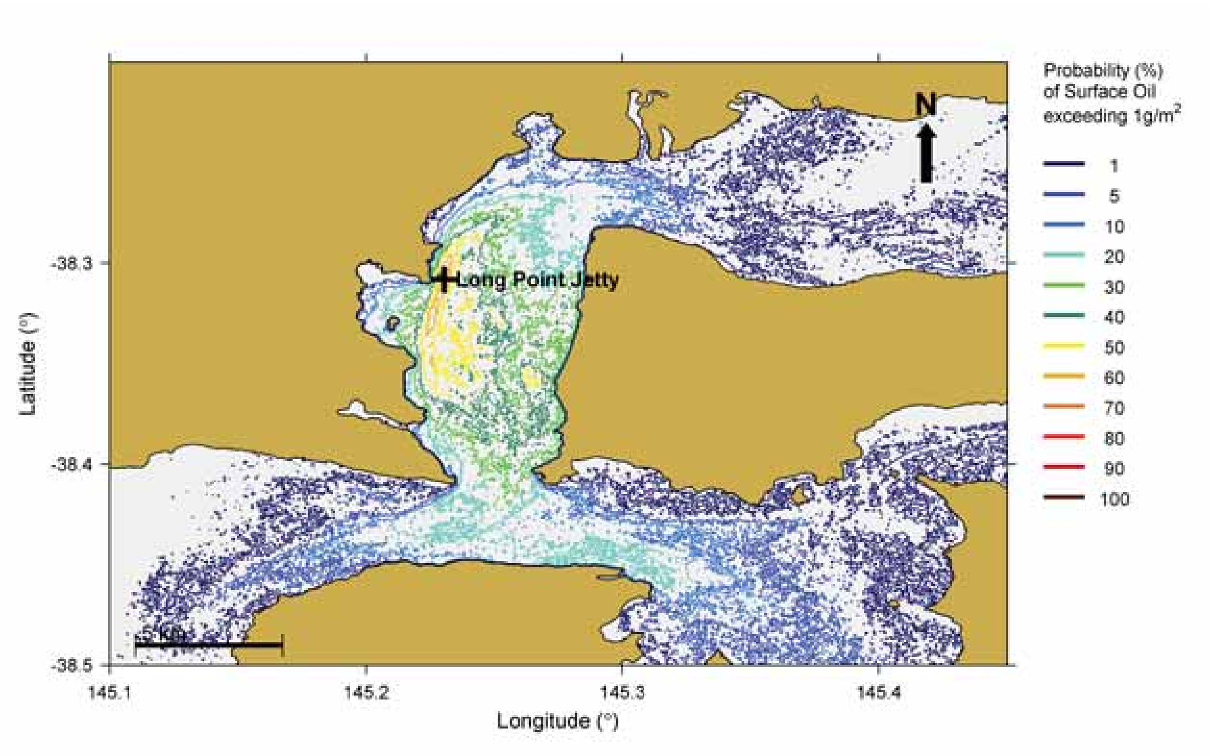

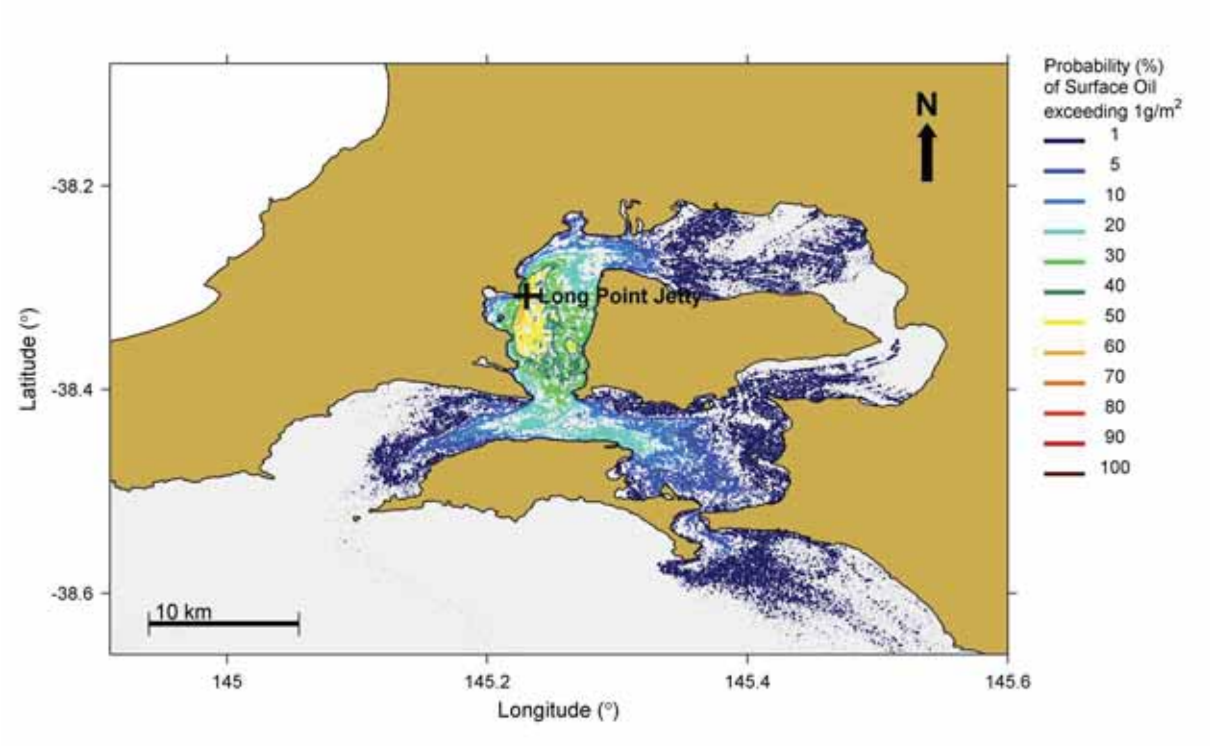

Figure 4-6: Probability contours for sea surface contact to concentrations above 1 g/m^2 resulting from a 200 MT HFO spill commencing during Winter.

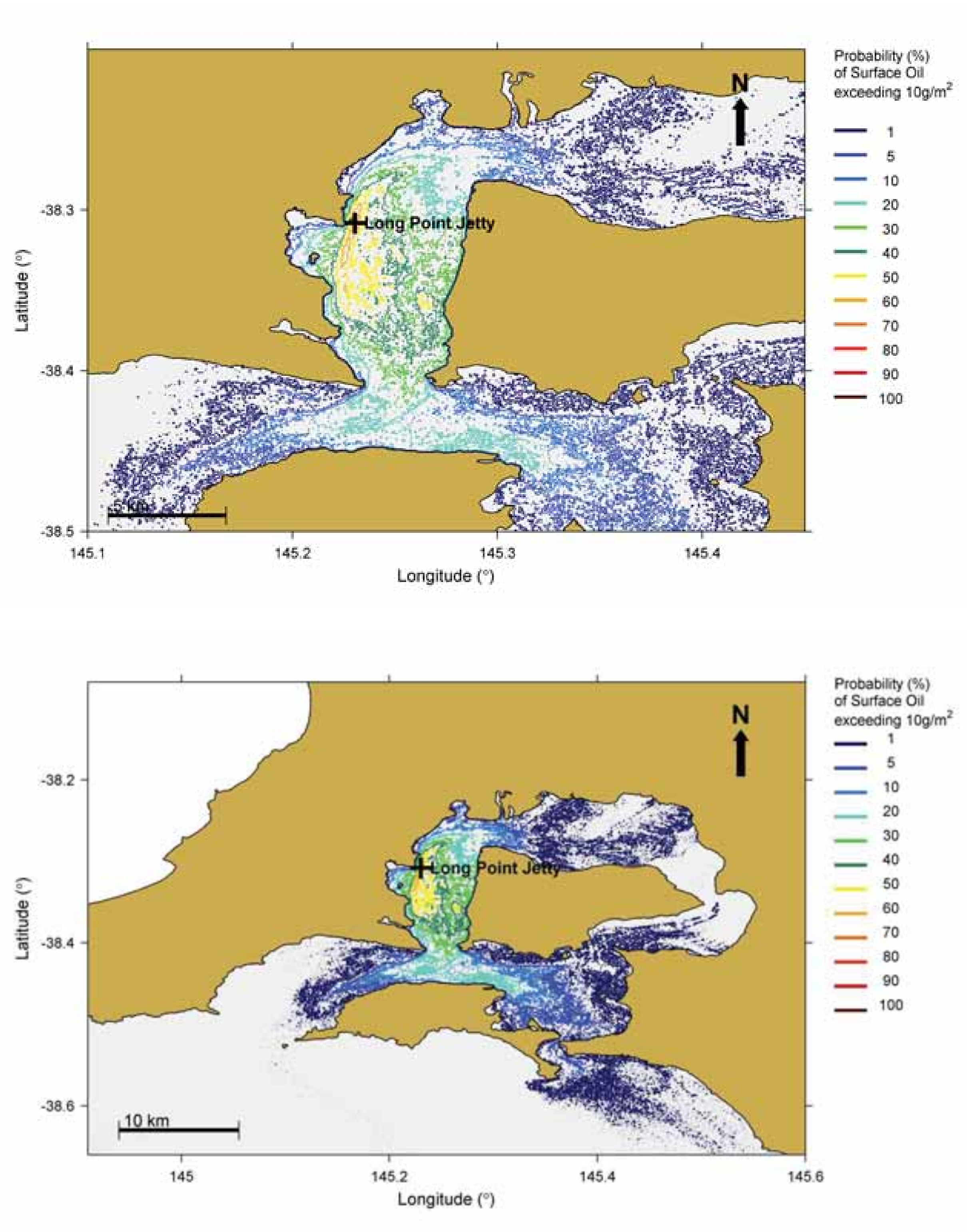

Figure 4-7: Probability contours for sea surface contact to concentrations above 10 g/m^2 resulting from a 200 MT HFO spill commencing during Winter.

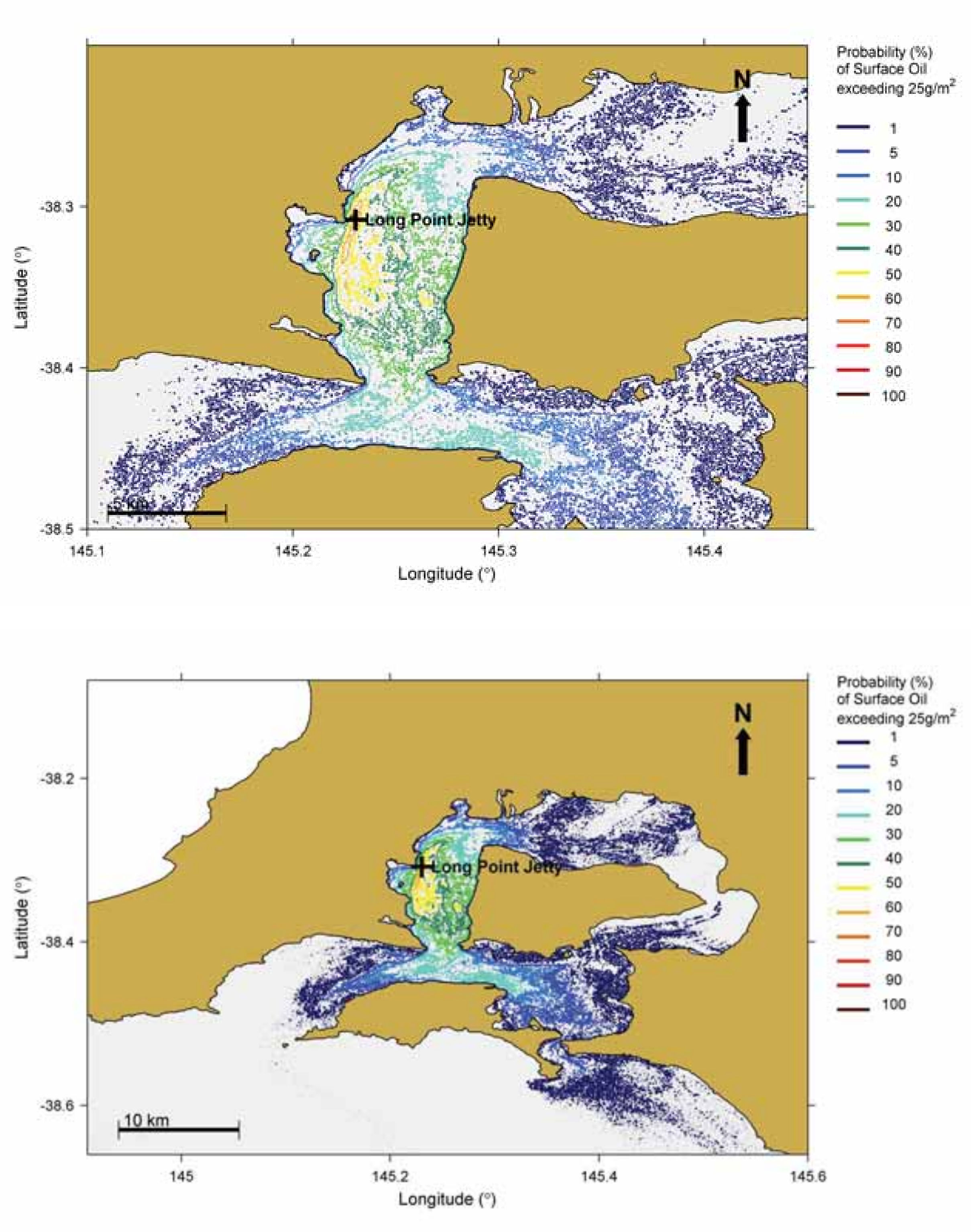

Figure 4-8: Predicted probability of sea surface contact to concentrations above 25 g/m^2 resulting from a 200 MT HFO spill commencing during Winter.

4.3 Simulation of a 200 Metric Tonne HFO spill at McHaffie's Reef

This scenario investigated risks of contact for surrounding shorelines from a 200 MT spill of HFO over 3 days at McHaffie's Reef, which lies along the shipping route to Port Hastings.

Repeated simulations of this spill scenario also indicated that a high proportion of the spill volume would eventually run aground, although this proportion is likely to be reduced compared to the same spill scenario at Long Point Jetty (~ 50-60%), with higher proportions likely during summer because a higher proportion is likely to be driven out to sea with offshore winds that are more frequent during winter.

Risk contours calculated from simulation of this spill scenario during summer indicated the highest probability that oil would drift along the Western Entrance Channel and spread over the Western Entrance Segment. The probability that concentrations > 25 g/m^2 would drift through the Confluence Zone and enter North Arm and East Arm is forecasted at 30-40%, with this contour impinging on Tortoise Point. The 30% probability contour is also forecasted to impinge on the northern coastline of Phillips Island. There is > 10% probability that concentrations of floating oil > 25 g/m^2 would drift out of the Western Entrance to potentially affect the southern coastline of Phillip Island and open coastlines to the east of the bay.

French Island National Park is forecasted to have > 35% probability of exposure at > 25 g/m^2 for this spill scenario in summer, with the minimum exposure time forecasted at ~ 6 hours and the potential for significant accumulation (> 17 kg/m^2) indicated. Phillip Island Nature Park is also forecasted as a potential site of high oil accumulation, but at a lower probability.

Probability contours generated from spill simulations under winter conditions indicate a markedly higher probability that floating oil > 25 g/m^2 would be constrained to oscillate through the Western Entrance Channel with the highest probability for oil to impinge onto McHaffie's Reef (>50%) and the northern coastline of Phillip Island.(> 30%). Oil concentrations > 25 g/m^2 are indicate to have > 10% probability of migrating from the bay at > 25 g/m^2. Oil concentrations > 25 g/m^2 are also indicated to have > 5% probability of entering Northern Arm and the Ryll Segment but relatively low probability of drifting further along North Arm and East Arm

Table 4-3: Summary of shoreline risks for different locations resulting from a 200 MT spill of HFO at McHaffie's Reef commencing during summer.

	Probability (%) of films arriving at shorelines at > 1.0 g/m^2	Probability (%) of films arriving at shorelines at > 10.0 g/m^2	Probability (%) of films arriving at shorelines at > 25.0 g/m^2	Minimum time to shoreline (hours) for films at > 1.0 g/m^2	Minimum time to shoreline (hours) for films at > 10.0 g/m^2	Minimum time to shoreline (hours) for films at > 25.0 g/m^2	Maximum local accumulation (g/m^2)averaged among replicate spills	Maximum local accumulation (g/m^2) in the worst replicate spill
Yaringa Marine National Park	8	8	8	34	34	34	51	1,875
North Western Port Nature Conservation Reserve	8	8	8	34	34	34	80	4,030
French Island Marine National Park	4	4	4	73	73	73	7.8	523
Reef Island and Bass River Mouth Nature Conservation Reserve	1	1	1	62	62	62	54	5,384
Churchill Island Marine National Park	3	3	3	49	49	49	47	2,988
French Island National Park	36	36	36	7	7	7	1,443	17,321
Phillip Island Nature Park	11	11	11	5	5	5	311	17,551
Bunurong Marine Park	3	3	3	69	69	69	16	1,055
Mushroom Reef Marine Sanctuary	NC	NC	NC	NC	NC	NC	NC	NC

NC: No contact to shorelines indicated at > threshold

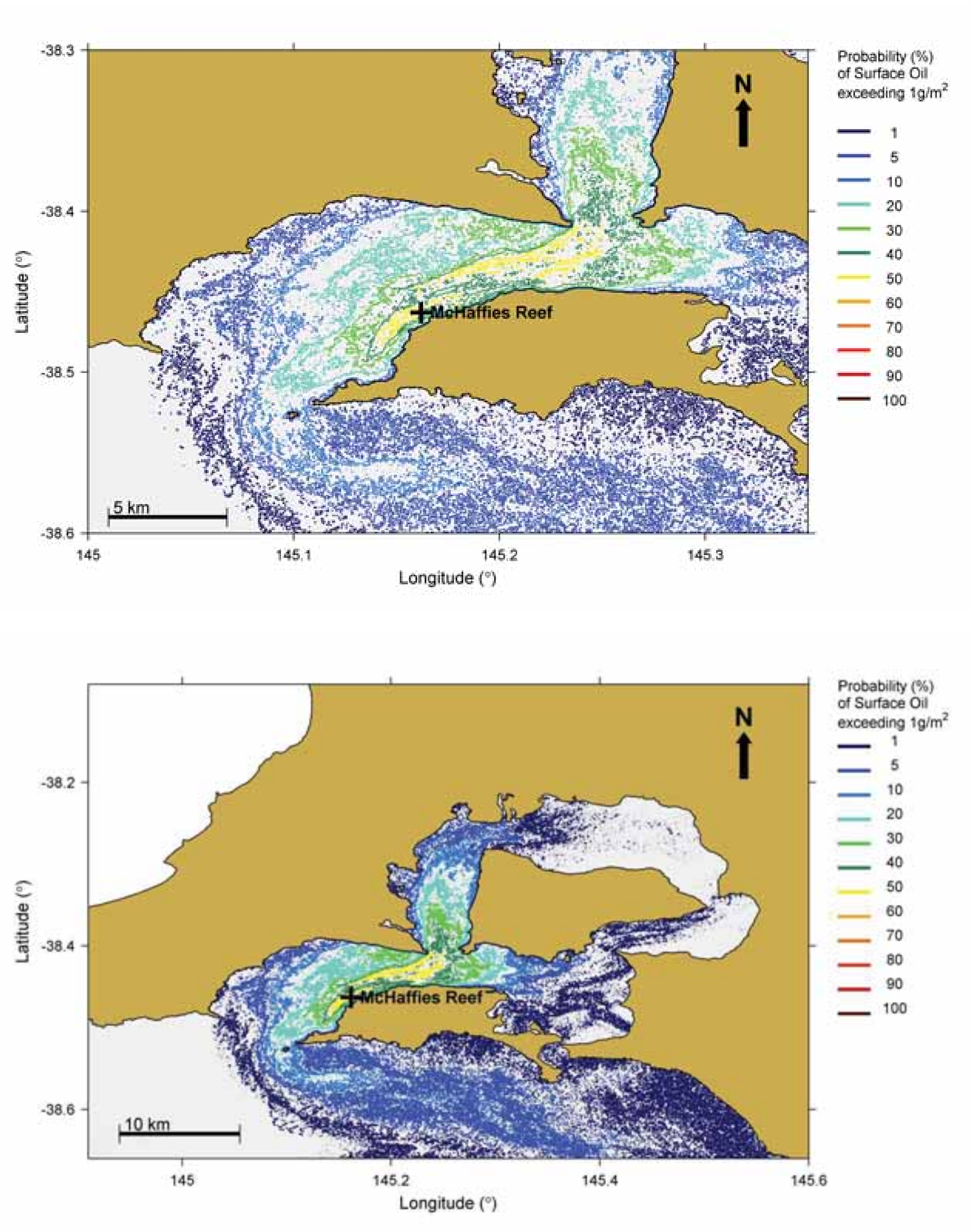

Figure 4-9: Probability contours for sea surface contact to concentrations above 1 g/m^2 resulting from a 200 MT HFO spill commencing during Summer.

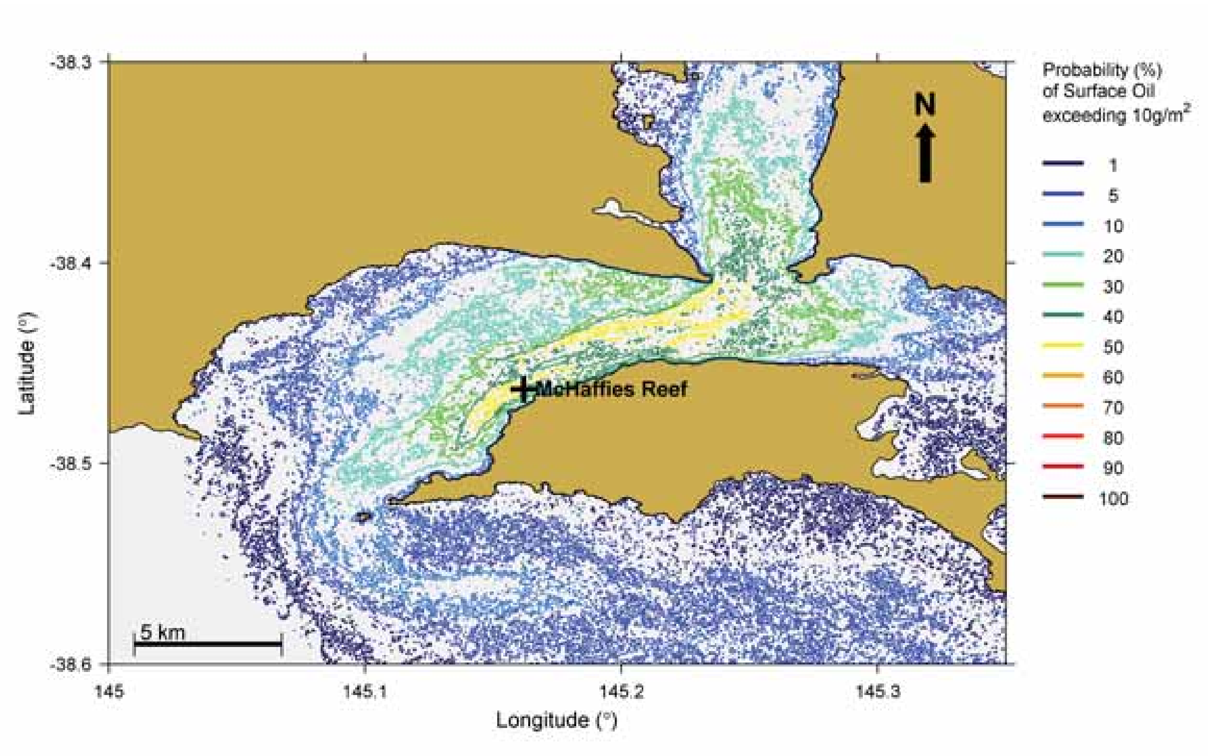

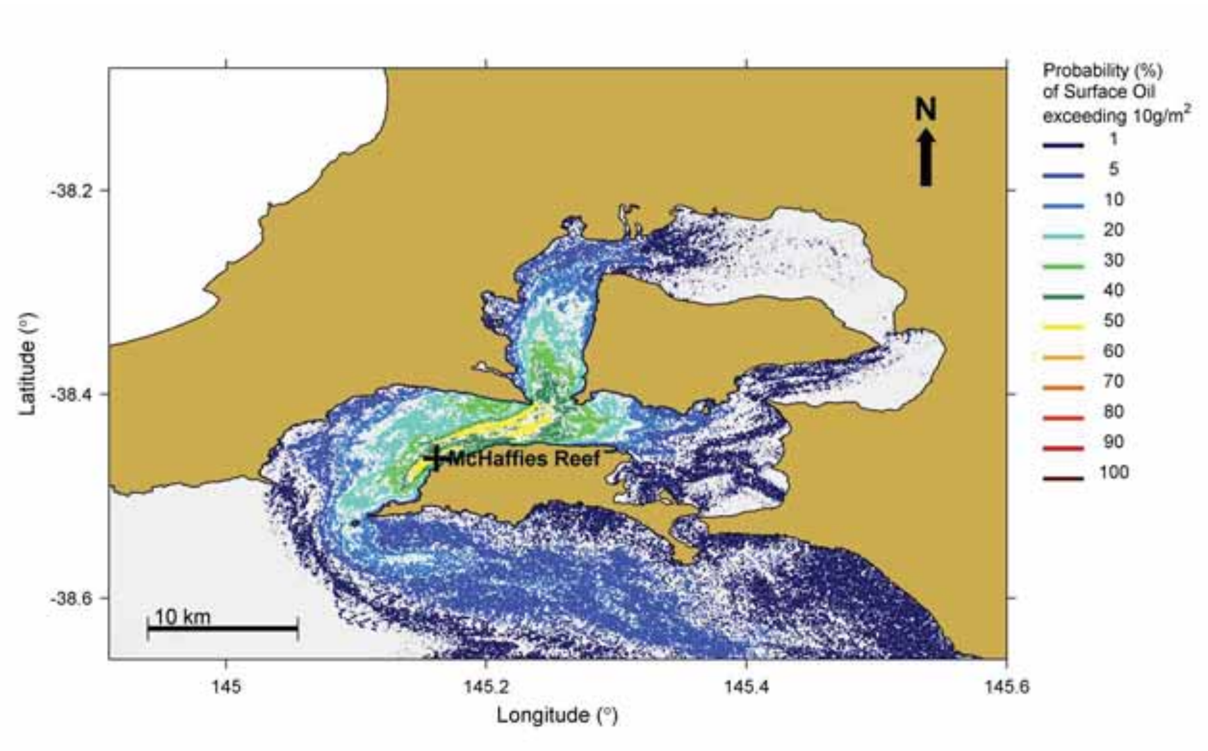

Figure 4-10: Probability contours for sea surface contact to concentrations above 10 g/m² resulting from a 200 MT HFO spill commencing during Summer.

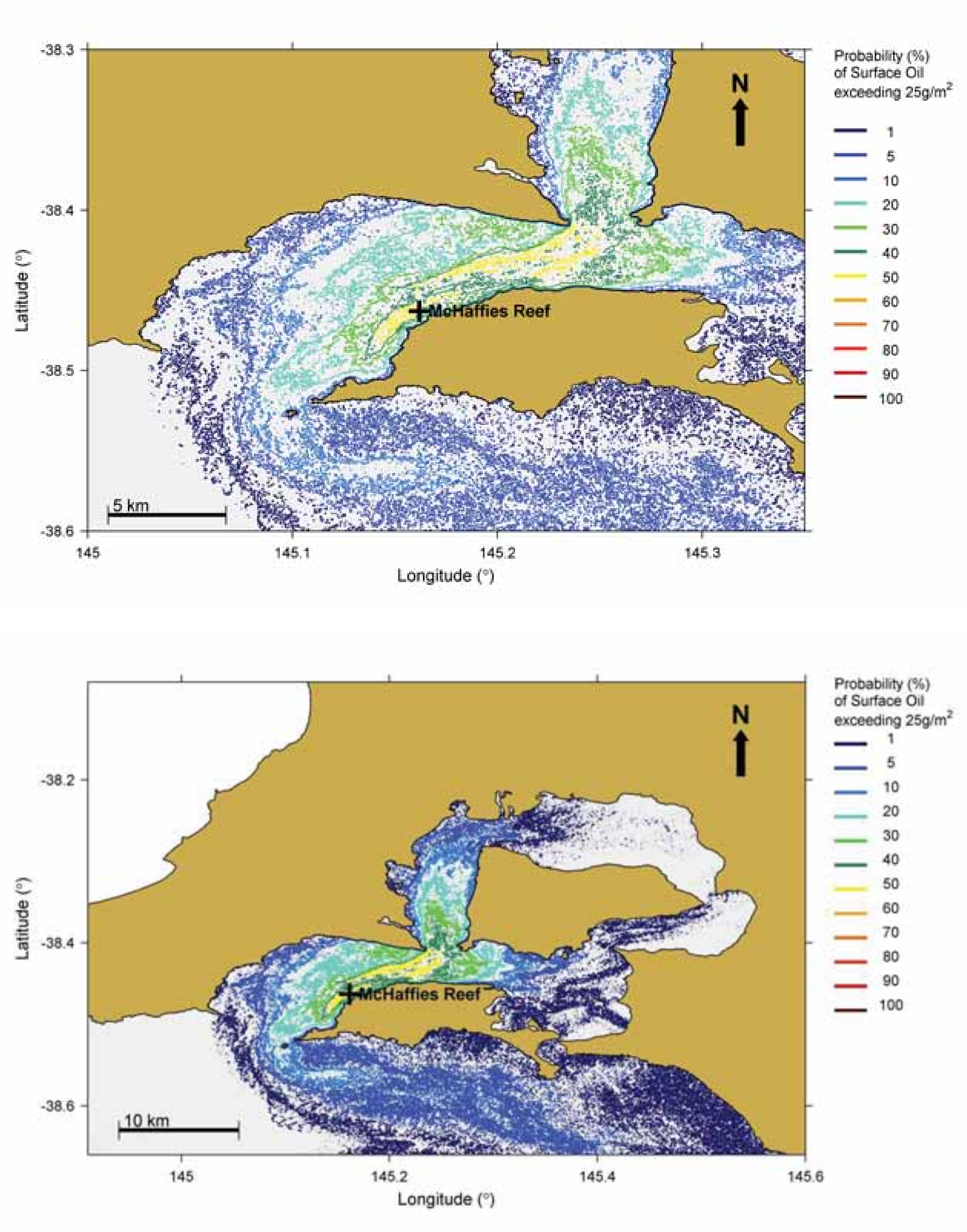

Figure 4-11: Probability contours for sea surface contact to concentrations above 25 g/m^2 resulting from a 200 MT HFO spill commencing during Summer.

Table 4-4: Summary of shoreline risks for different locations resulting from a 200 MT spill of HFO at Long Point Island Jetty commencing during Winter.

	Probability (%) of films arriving at shorelines at > 1.0 g/m^2	Probability (%) of films arriving at shorelines at > 10.0 g/m^2	Probability (%) of films arriving at shorelines at > 25.0 g/m^2	Minimum time to shoreline (hours) for films at > 1.0 g/m^2	Minimum time to shoreline (hours) for films at > 10.0 g/m^2	Minimum time to shoreline (hours) for films at > 25.0 g/m^2	Maximum local accumulation (g/m^2)averaged among replicate spills	Maximum local accumulation (g/m^2) in the worst replicate spill
Yaringa Marine National Park	1	1	1	106	106	106	14	1,350
North Western Port Nature Conservation Reserve	1	1	1	109	109	109	8.1	813
French Island Marine National Park	NC	NC	NC	NC	NC	NC	NC	NC
Reef Island and Bass River Mouth Nature Conservation Reserve	1	1	1	49	49	49	7.7	769
Churchill Island Marine National Park	2	2	2	102	102	102	61	5,213
French Island National Park	8	8	8	8	8	8	331	17,321
Phillip Island Nature Park	15	15	15	7	7	7	842	17,374
Bunurong Marine Park	1	1	1	198	198	198	5.2	519
Mushroom Reef Marine Sanctuary	NC	NC	NC	NC	NC	NC	NC	NC

NC: No contact to shorelines indicated at > threshold

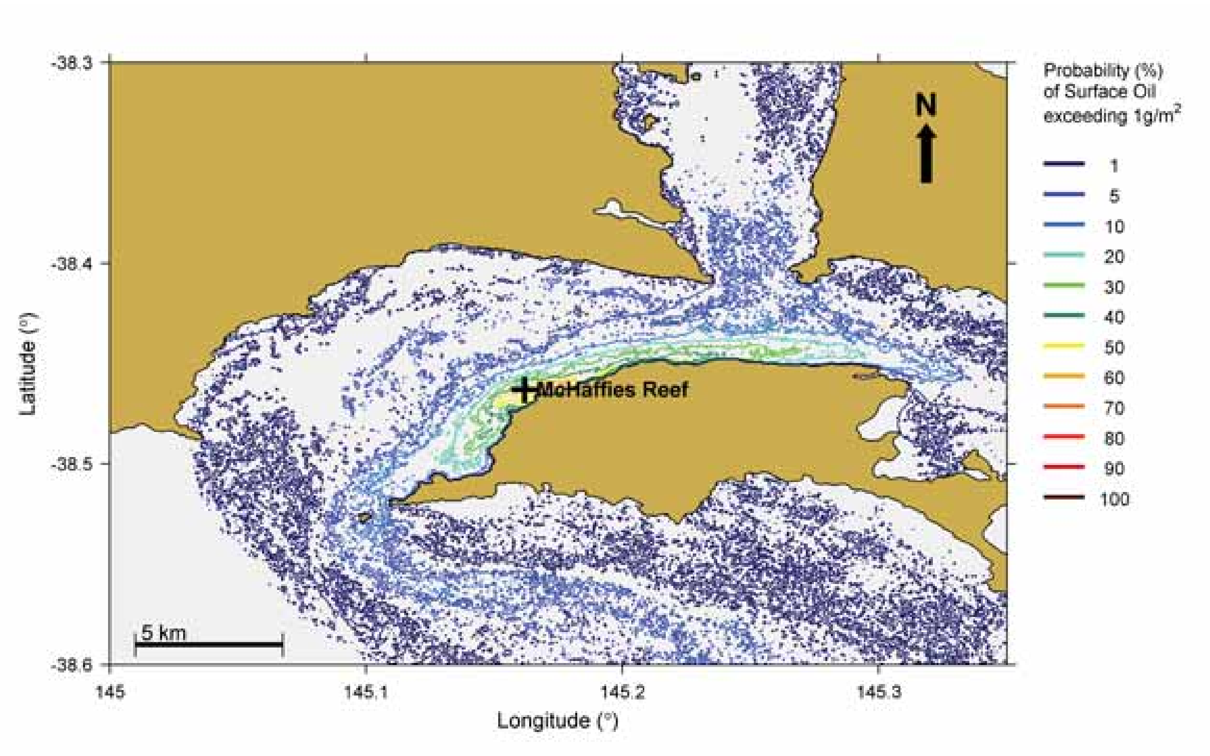

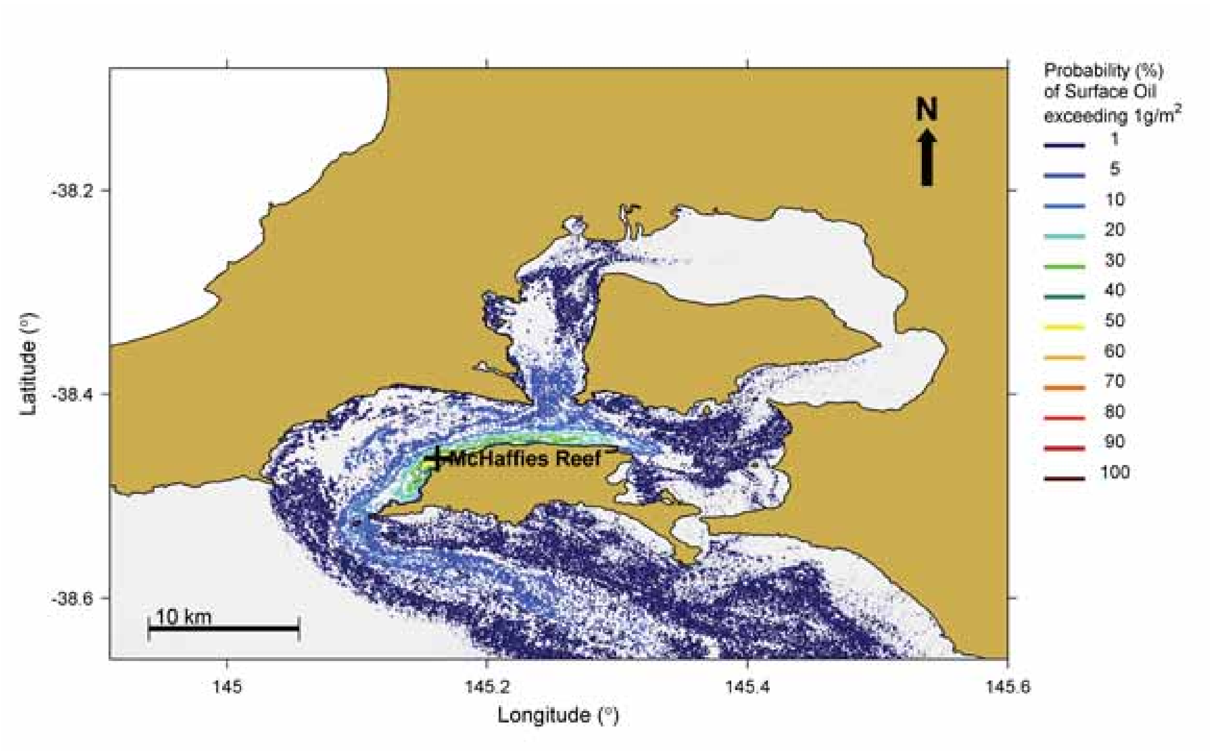

Figure 4-12: Probability contours for sea surface contact to concentrations above 1 g/m^2 resulting from a 200 MT HFO spill commencing during Winter.

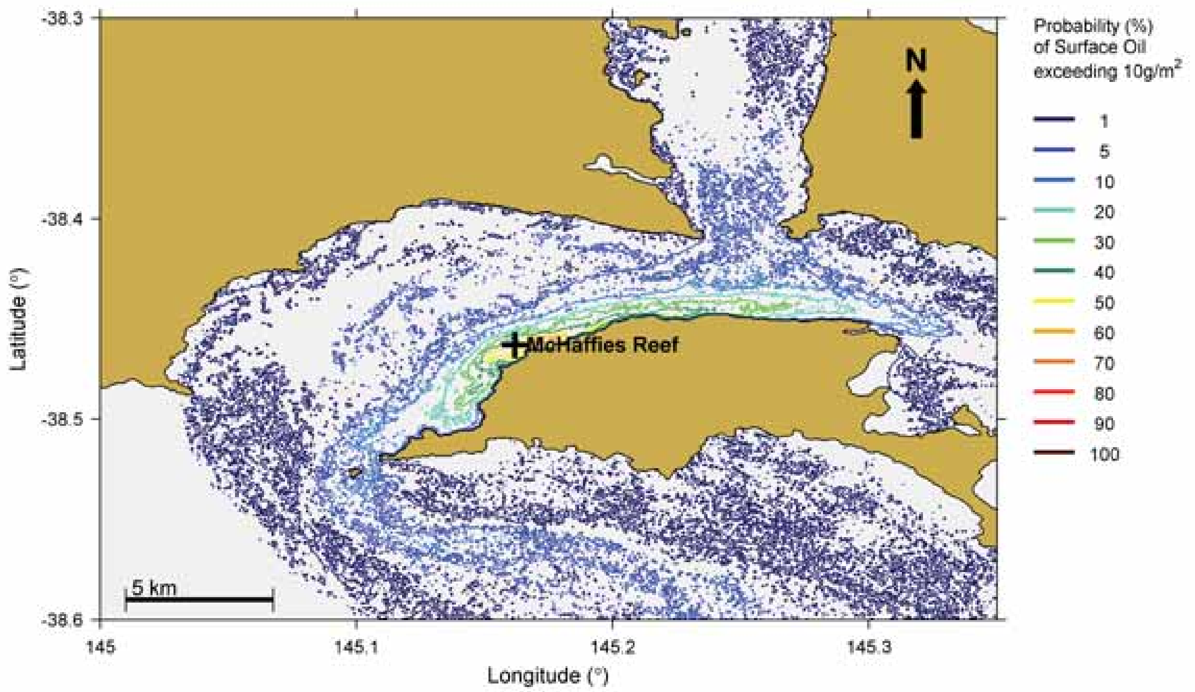

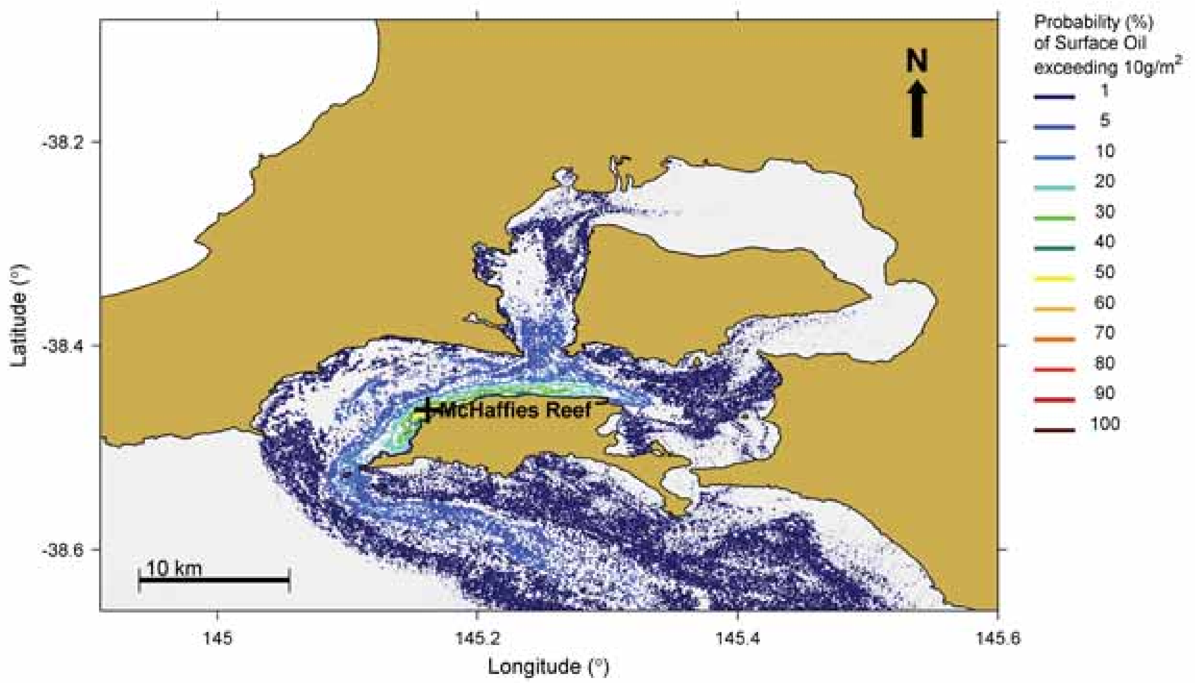

Figure 4-13: Probability contours for sea surface contact to concentrations above 10 g/m^2 resulting from a 200 MT HFO spill commencing during Winter.

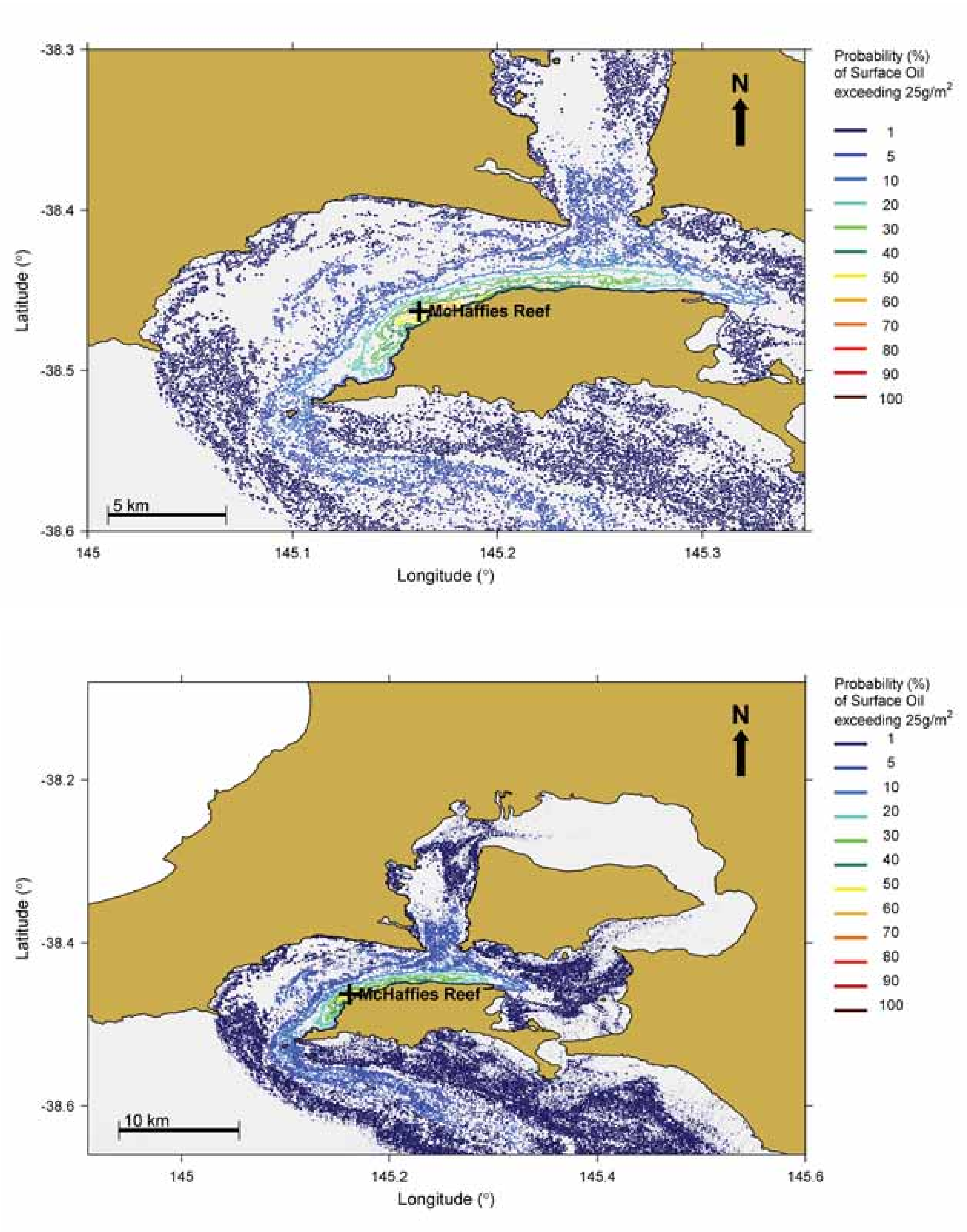

Figure 4-14: Predicted probability of sea surface contact to concentrations above 25 g/m^2 resulting from a 200 MT HFO spill commencing during Winter.

4.4 Simulation of an 80 m^3 diesel spill at Long Point Jetty

This scenario investigated risks of contact for surrounding shorelines from a 80 m^3 spill of diesel fuel at Long Point Jetty.

Risk contours calculated for spills of floating diesel during summer show similar seasonal trends to the HFO spill scenario but indicate that floating slicks will most likely be constrained within North Arm at > 25 g/m^2 but could extend to the mudflats in the Northern sector of North Arm at > 5% at > 1 g/m^2. Similar minimum concentrations are forecasted to potentially migrate south into the Confluence Zone but at low probability (1%). The highest probability of exposure (> 50%) over open water is indicated for a distance of 4-5 km along the tidal axis around Long Point Jetty and > 30% probability of exposure to shorelines on both the western and eastern coastline of North Arm is indicated.

Summary tables for the quantification of exposure risk for sensitive resources indicates a marked decrease in exposure probability at increasing concentration thresholds, which is attributed to the high spreading rate, the evaporation rate of volatile components and the tendency for diesel to entrain (hence reducing surface concentrations). High probabilities (>70%) of exposure are indicated for a number of the resources at the low threshold but probabilities of contact are forecasted at < 20% at > 25 g/m^2. Similar minimum drift times are indicated for oil to reach sensitive resources, compared to the HFO scenario from this location. The highest potential concentrations on shorelines are forecasted at > 12 kg/m^2, for French Island Marine National Park.

In contrast to the HFO scenarios, simulation of the diesel spills indicate that concentrations > 100 ppb have a high probability (> 50%) of occurring over a wide part of North Arm, with > 30% probability of exposure along the eastern and western shorelines of this arm. The mudflats in the north-east section of the bay have > 5% probability at > 100 ppb. Highest short term concentrations of entrained oil forecasted for any of the sensitive resource areas is around 3 ppm.

Exposure probability contours calculated from simulation of the diesel spill under winter conditions indicated a higher probability that diesel would drift south or south-east, with thin sheens (>1 g/m^2) forecasted to have > 30% probability of drifting into the confluence zone. A low probability is indicated for surface films to persist at > 25 g/m^2 in this area. French Island National Park and Phillip Island Nature Park are indicated to have the highest probability of exposure for surface films.

Exposure contours forecasted for physically entrained diesel indicate that concentrations > 500 ppb could occur throughout North Arm, with higher probabilities (> 20%) to the south of Long Point Island Jetty. Concentrations > 100 ppb are indicated to potentially occur into the Northern sector of North Arm, and through the Eastern Channel and Rhyll segment. French Island National Park is forecasted to have the highest probability of exposure (19% at > 500 ppb) and highest potential concentration (> 23 ppm).

Table 4-5: Summary of shoreline risks for different locations resulting from a 80 m^3 spill of diesel commencing during Summer.

	Probability (%) of films arriving at shorelines at > 1.0 g/m^2	Probability (%) of films arriving at shorelines at > 10.0 g/m^2	Probability (%) of films arriving at shorelines at > 25.0 g/m^2	Minimum time to shoreline (hours) for films at > 1.0 g/m^2	Minimum time to shoreline (hours) for films at > 10.0 g/m^2	Minimum time to shoreline (hours) for films at > 25.0 g/m^2	Maximum local accumulation (g/m^2)averaged among replicate spills	Maximum local accumulation (g/m^2) in the worst replicate spill
Yaringa Marine National Park	33	18	8	6	6	6	168	3,312
North Western Port Nature Conservation Reserve	33	18	8	7	7	7	220	3,314
French Island Marine National Park	15	6	4	8	8	8	12	1,194
Reef Island and Bass River Mouth Nature Conservation Reserve	NC	NC	NC	NC	NC	NC	NC	NC
Churchill Island Marine National Park	1	NC	NC	74	NC	NC	0.5	49
French Island National Park	24	15	7	8	8	8	255	3,313
Phillip Island Nature Park	1	NC	NC	63	NC	NC	2.6	263
Bunurong Marine Park	NC	NC	NC	NC	NC	NC	NC	NC
Mushroom Reef Marine Sanctuary	NC	NC	NC	NC	NC	NC	NC	NC

NC: No contact to shorelines indicated at > threshold

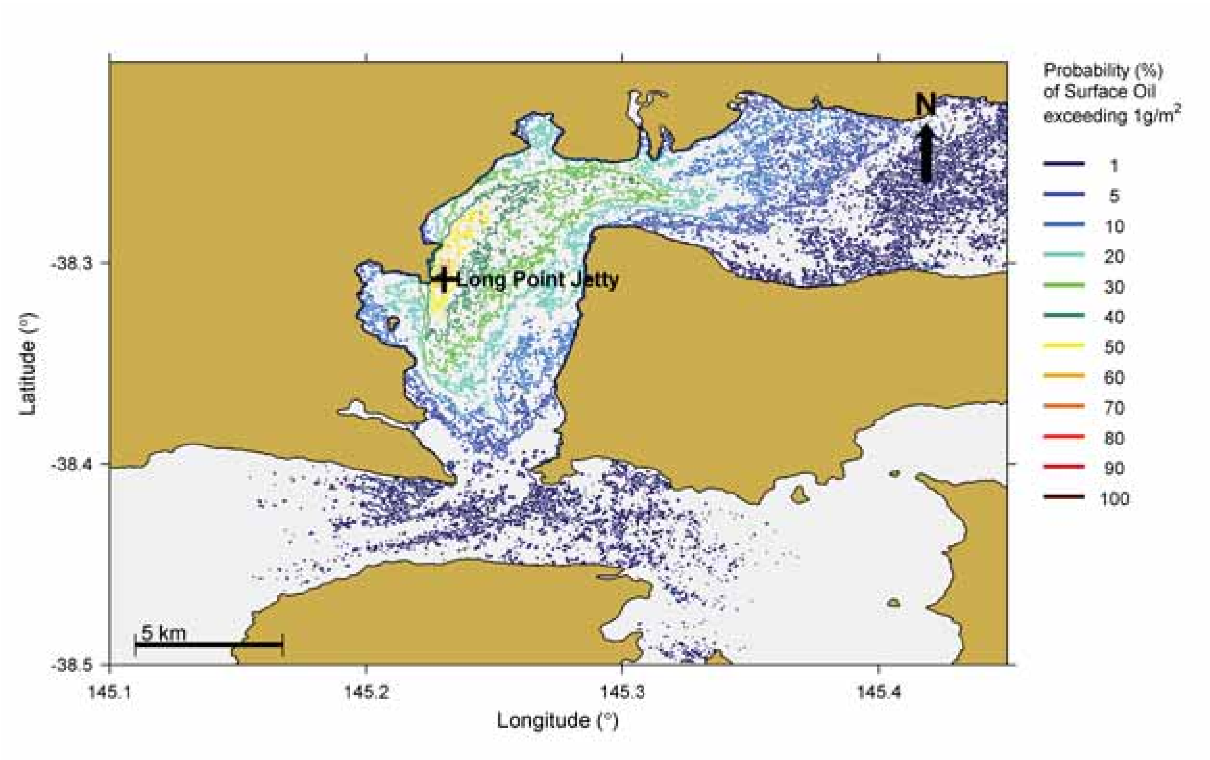

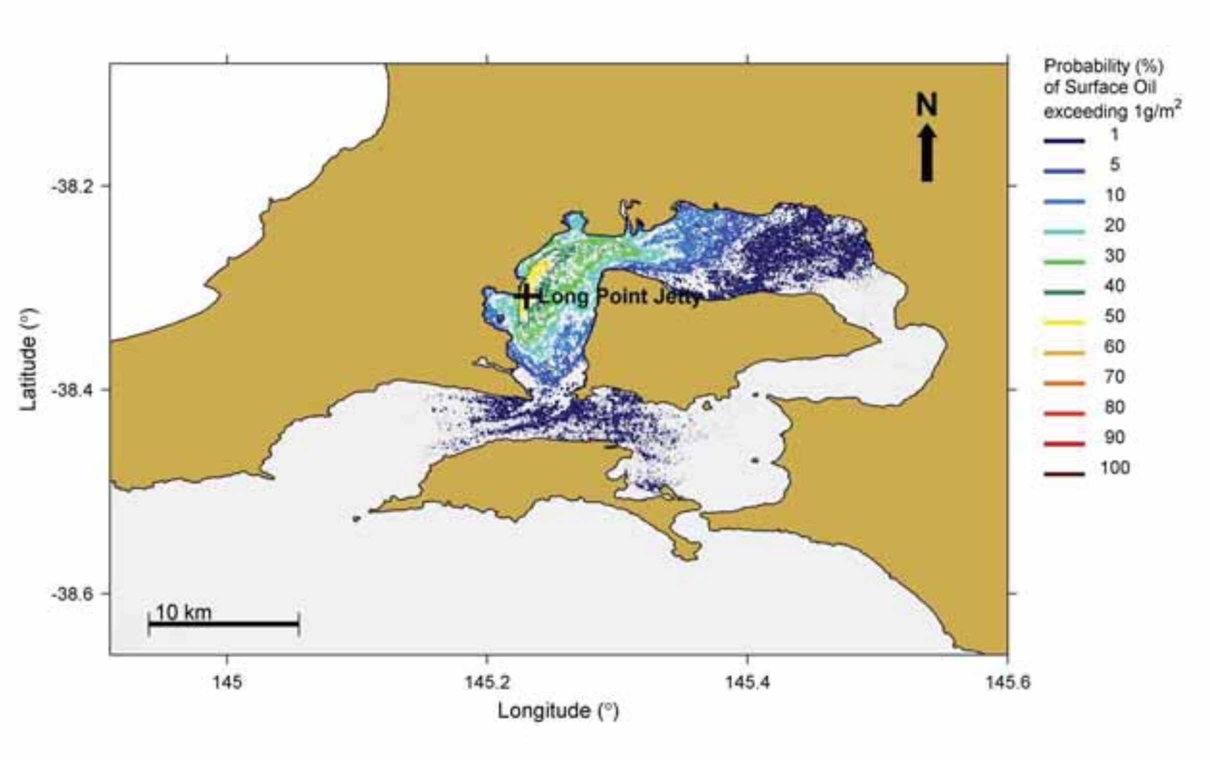

Figure 4-15: Probability contours for sea surface contact to concentrations above 1 g/m^2 resulting from a 80 m^3 diesel spill commencing during Summer. Dashed black line denote state/commonwealth boundary.

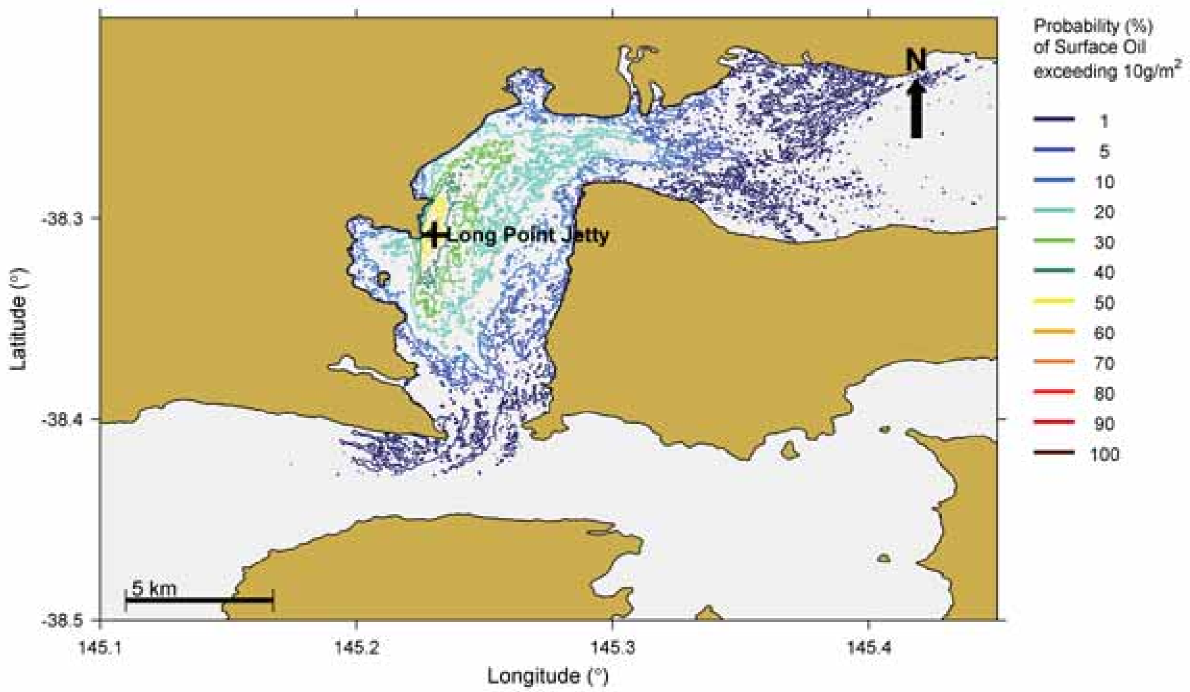

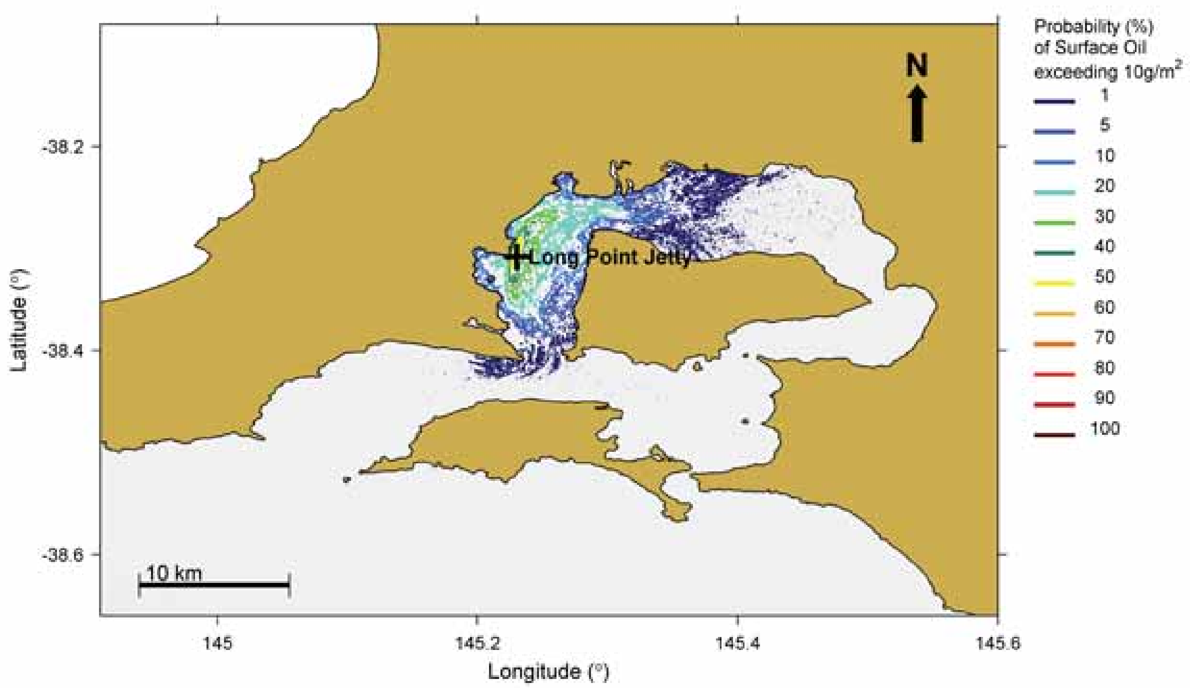

Figure 4-16: Probability contours for sea surface contact to concentrations above 10 g/m^2 resulting from a 80 m^3 diesel spill commencing during Summer. Dashed black line denote state/commonwealth boundary.

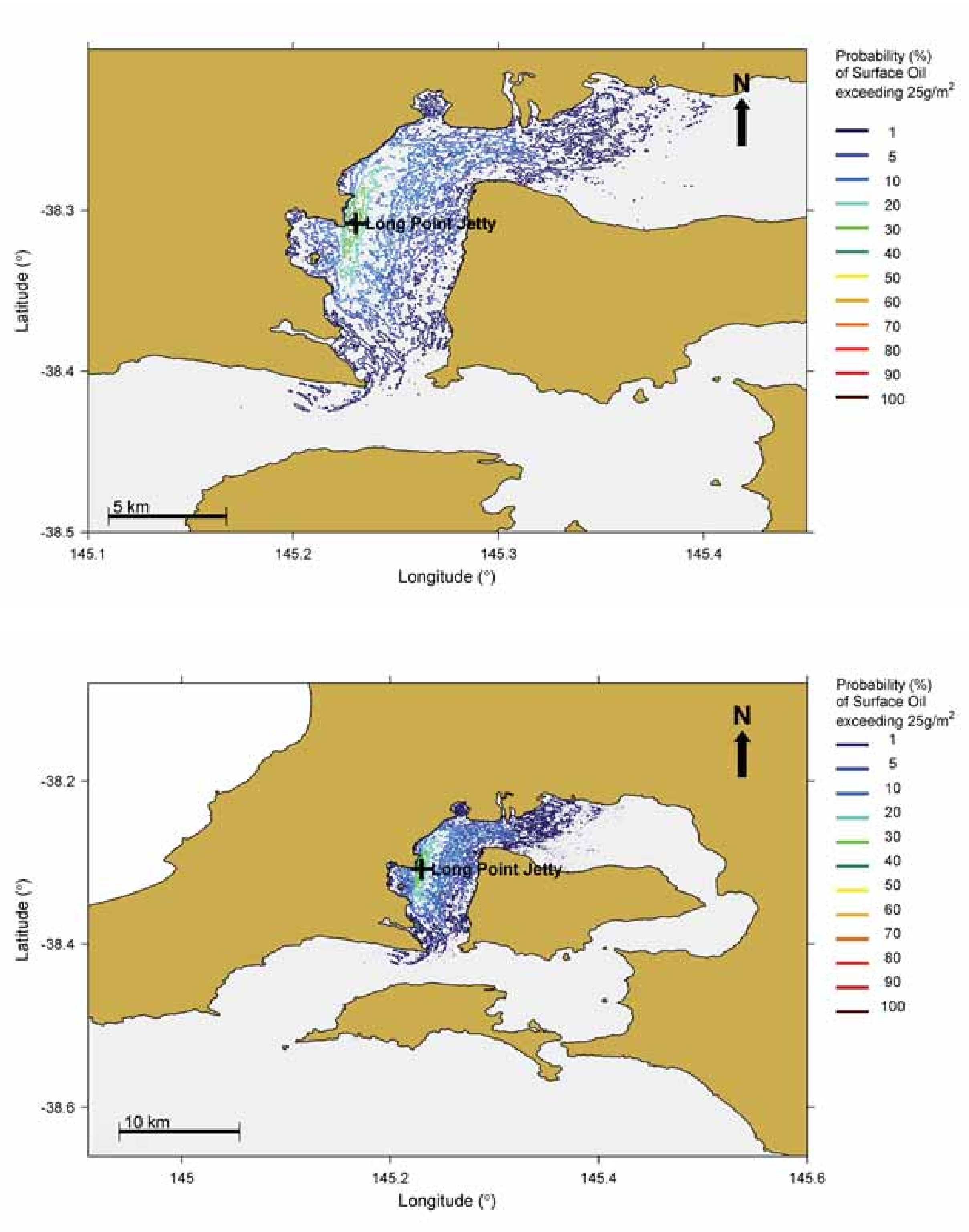

Figure 4-17: Probability contours for sea surface contact to concentrations above 25 g/m^2 resulting from a 80 m^3 diesel spill commencing during Summer. Dashed black line denote state/commonwealth boundary.

Table 4-6: Summary of risks for entrained oil concentrations in shallow waters resulting from a 80 m^3 spill of diesel commencing during Summer.

	Probability (%) of entrained hydrocarbon concentration > 10 ppb	Probability (%) of entrained hydrocarbon concentration > 100 ppb	Probability (%) of entrained hydrocarbon concentration > 500 ppb	Minimum time to shoreline (hours) at > 10 ppb	Minimum time to shoreline (hours) at > 100 ppb	Minimum time to shoreline (hours) at > 500 ppb	Maximum entrained hydrocarbon concentration (ppb) averaged among replicate spills	Maximum entrained hydrocarbon concentration (ppb) in the worse replicate
Yaringa Marine National Park	73	41	9	6	6	6	186	6,257
North Western Port Nature Conservation Reserve	73	43	12	5	5	7	230	9,496
French Island Marine National Park	74	49	19	7	11	13	330	12,685
Reef Island and Bass River Mouth Nature Conservation Reserve	1	NC	NC	214	NC	NC	<1	15
Churchill Island Marine National Park	1	NC	NC	153	NC	NC	<1	23
French Island National Park	78	52	20	6	6	6	331	12,914
Phillip Island Nature Park	5	2	1	66	84	210	22	1,970
Bunurong Marine Park	NC	NC	NC	NC	NC	NC	NC	NC
Mushroom Reef Marine Sanctuary	NC	NC	NC	NC	NC	NC	NC	NC

NC: No contact to shorelines indicated at > threshold

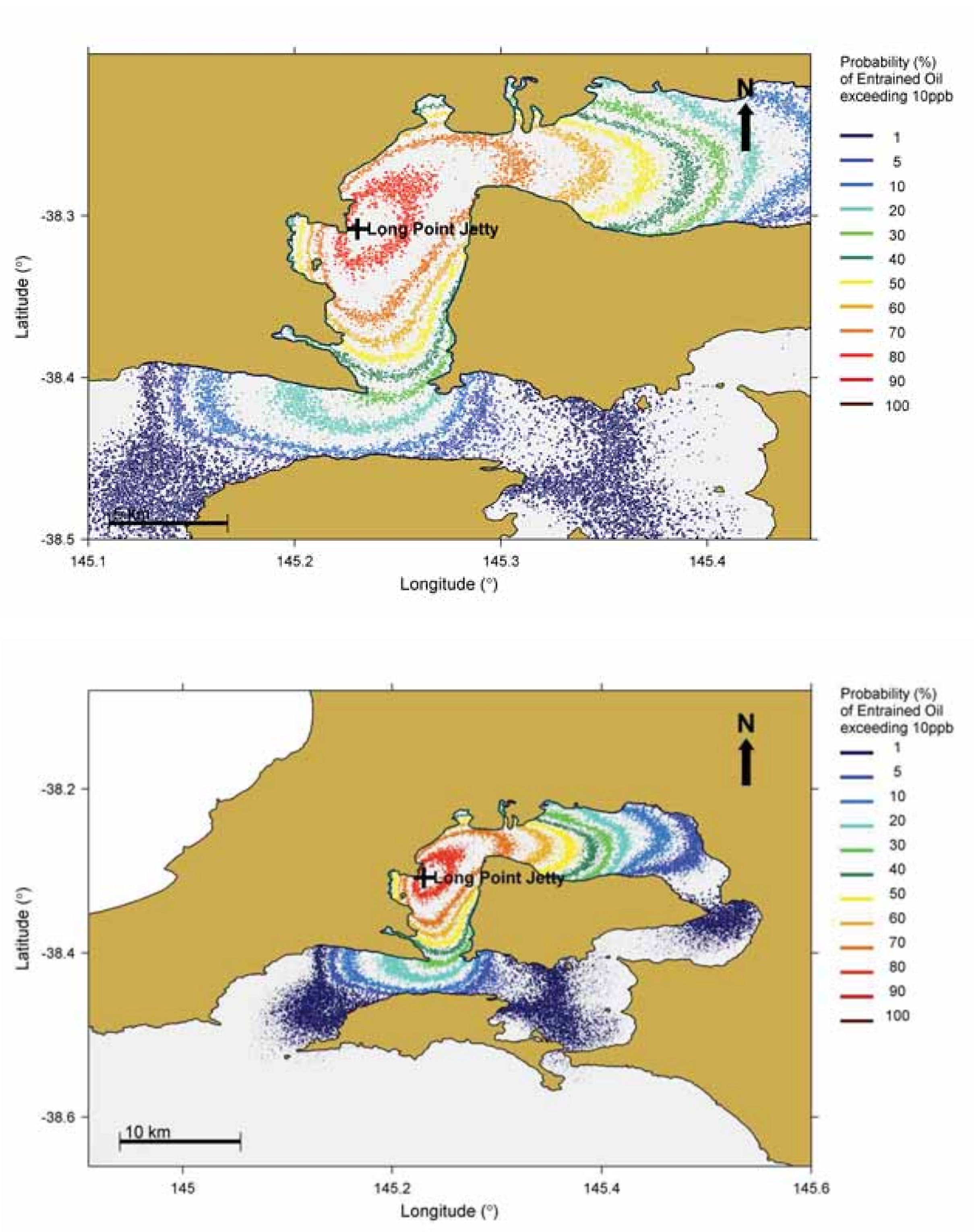

Figure 4-18: Probability contours for contact by entrained diesel exceeding 10 ppb resulting from a 80 m^3 spill of diesel commencing during Summer.

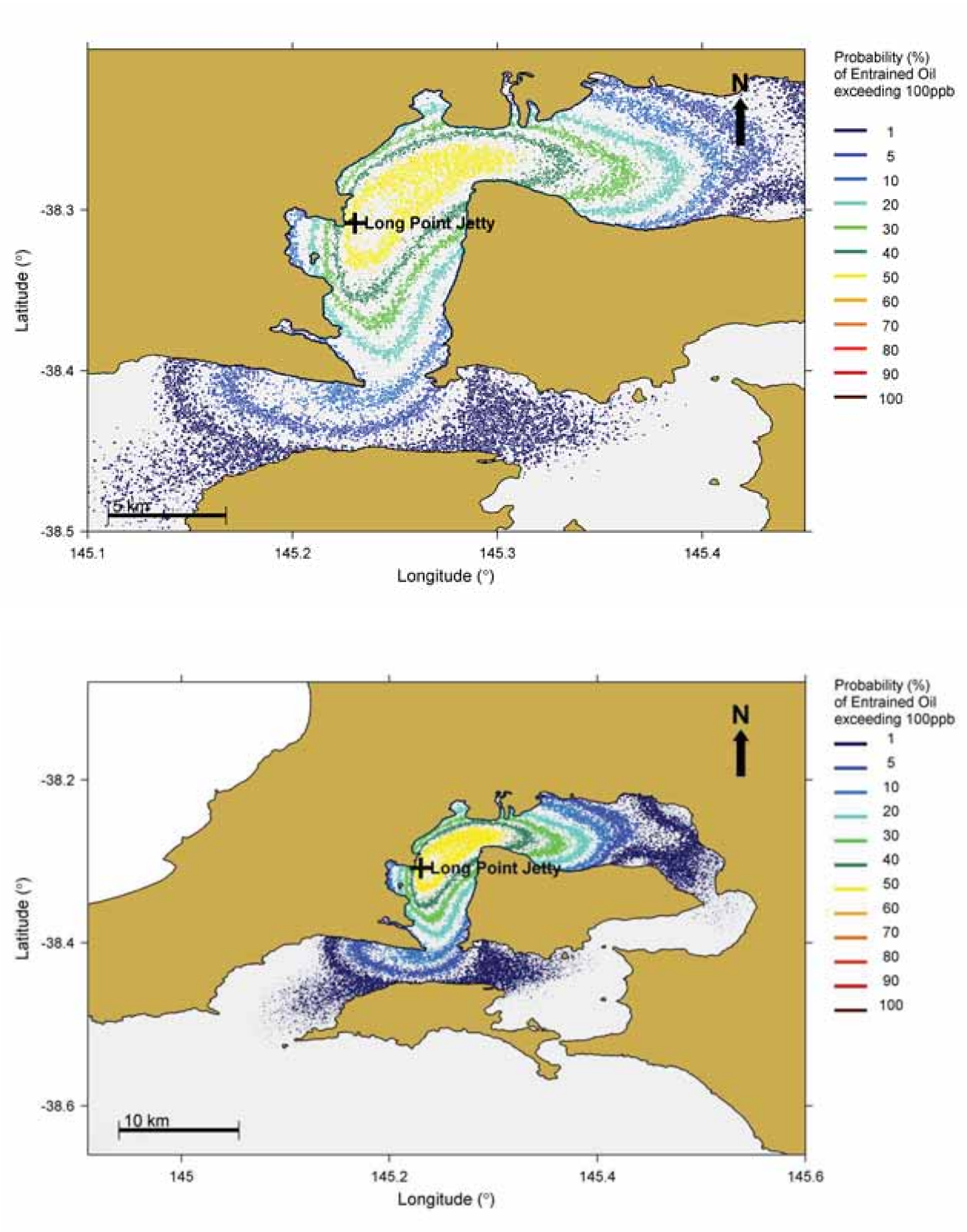

Figure 4-19: Probability contours for contact by entrained diesel exceeding 100 ppb resulting from a 80 m^3 spill of diesel commencing during Summer.

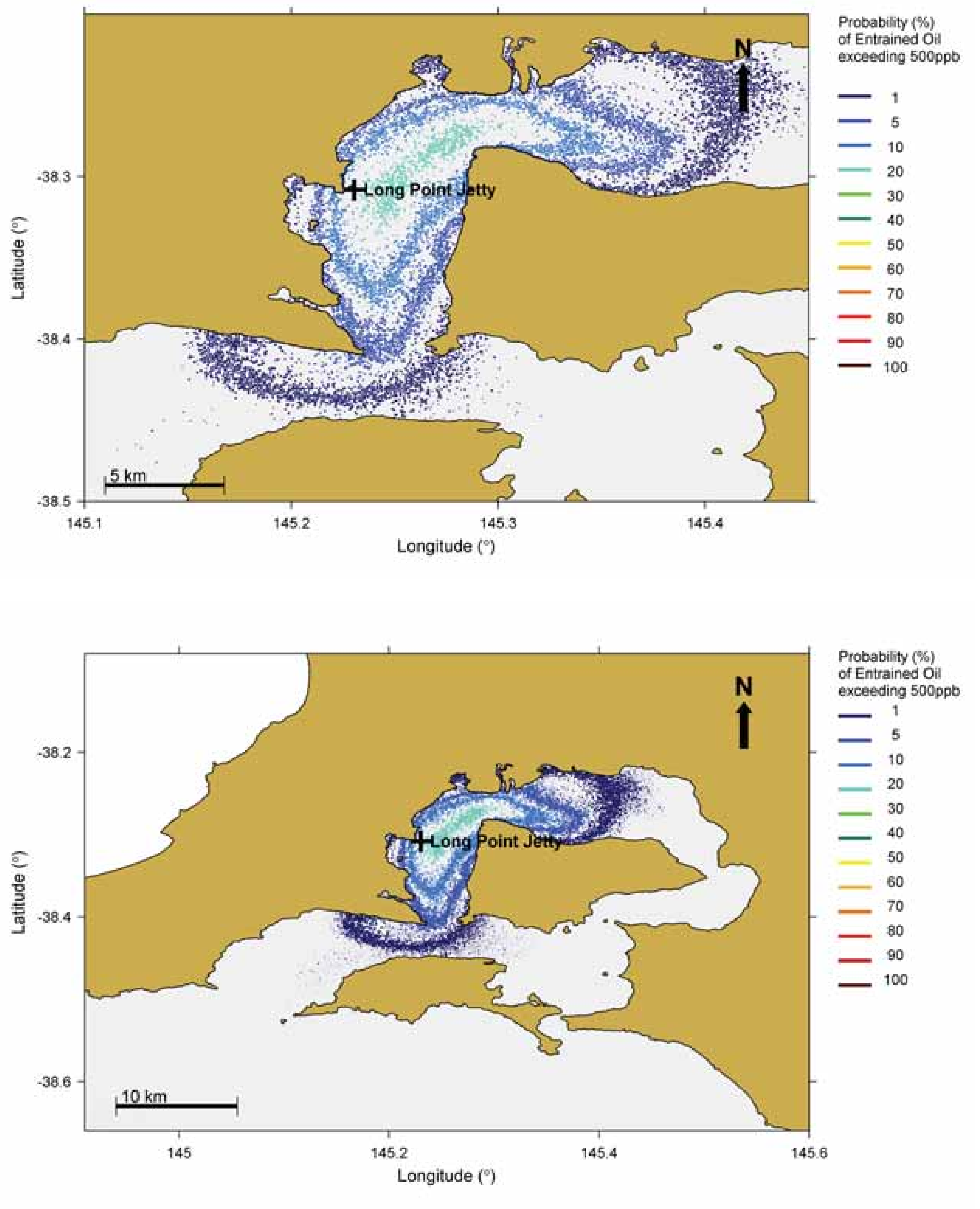

Figure 4-20: Probability contours for contact by entrained diesel exceeding 500 ppb resulting from a 80 m^3 spill of diesel commencing during Summer.

Table 4-7: Summary of shoreline risks for different locations resulting from a 80 m^3 spill of diesel commencing during Winter.

	Probability (%) of films arriving at shorelines at > 1.0 g/m^2	Probability (%) of films arriving at shorelines at > 10.0 g/m^2	Probability (%) of films arriving at shorelines at > 25.0 g/m^2	Minimum time to shoreline (hours) for films at > 1.0 g/m^2	Minimum time to shoreline (hours) for films at > 10.0 g/m^2	Minimum time to shoreline (hours) for films at > 25.0 g/m^2	Maximum local accumulation (g/m^2)averaged among replicate spills	Maximum local accumulation (g/m^2) in the worst replicate spill
Yaringa Marine National Park	9	5	2	7	7	7	40	3,062
North Western Port Nature Conservation Reserve	6	4	2	12	12	13	45	3,312
French Island Marine National Park	11	7	4	7	7	7	36	1,476
Reef Island and Bass River Mouth Nature Conservation Reserve	2	1	1	50	95	173	1.7	132
Churchill Island Marine National Park	6	2	1	34	41	41	6.9	550
French Island National Park	43	27	11	6	6	7	377	3,314
Phillip Island Nature Park	24	7	3	25	28	33	132	2,162
Bunurong Marine Park	NC	NC	NC	NC	NC	NC	NC	NC
Mushroom Reef Marine Sanctuary	NC	NC	NC	NC	NC	NC	NC	NC

NC: No contact to shorelines indicated at > threshold

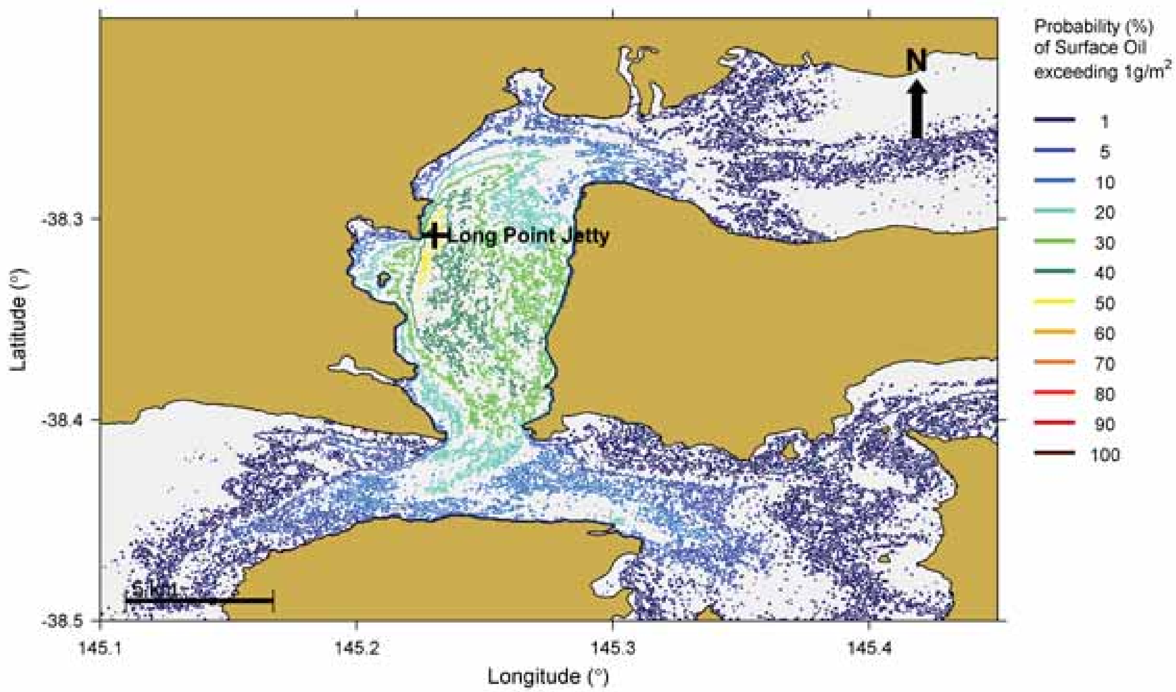

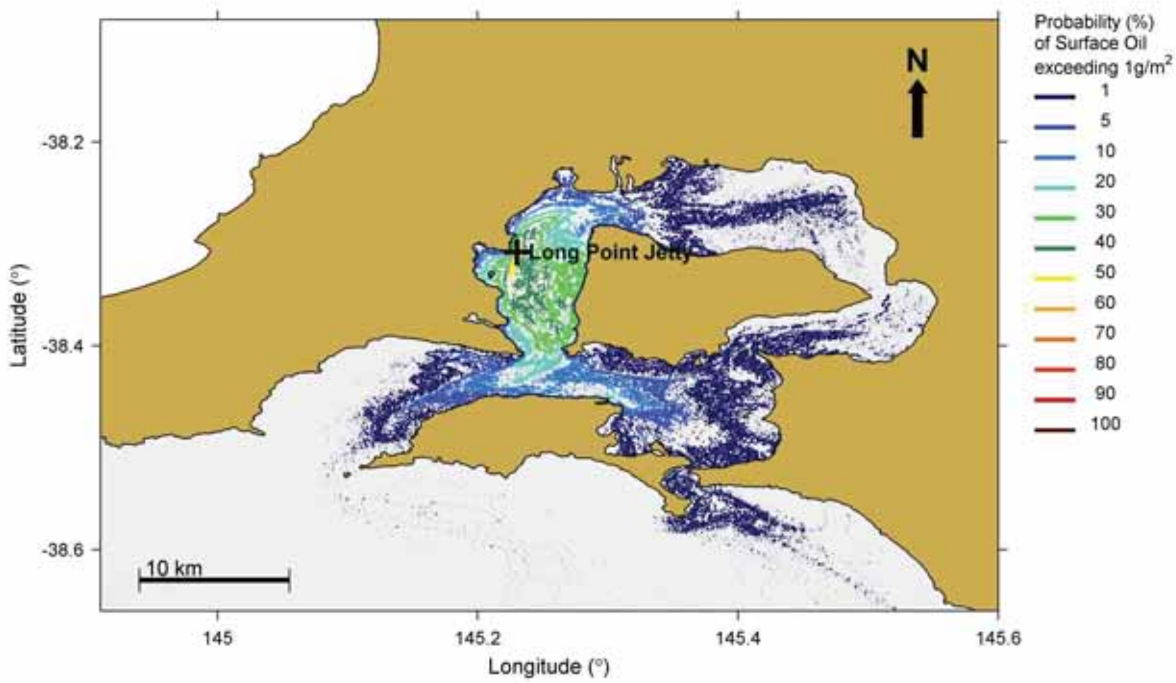

Figure 4-21: Probability contours for sea surface contact to concentrations above 1 g/m^2 resulting from a 80 m^3 diesel spill commencing during Winter. Dashed black line denote state/commonwealth boundary.

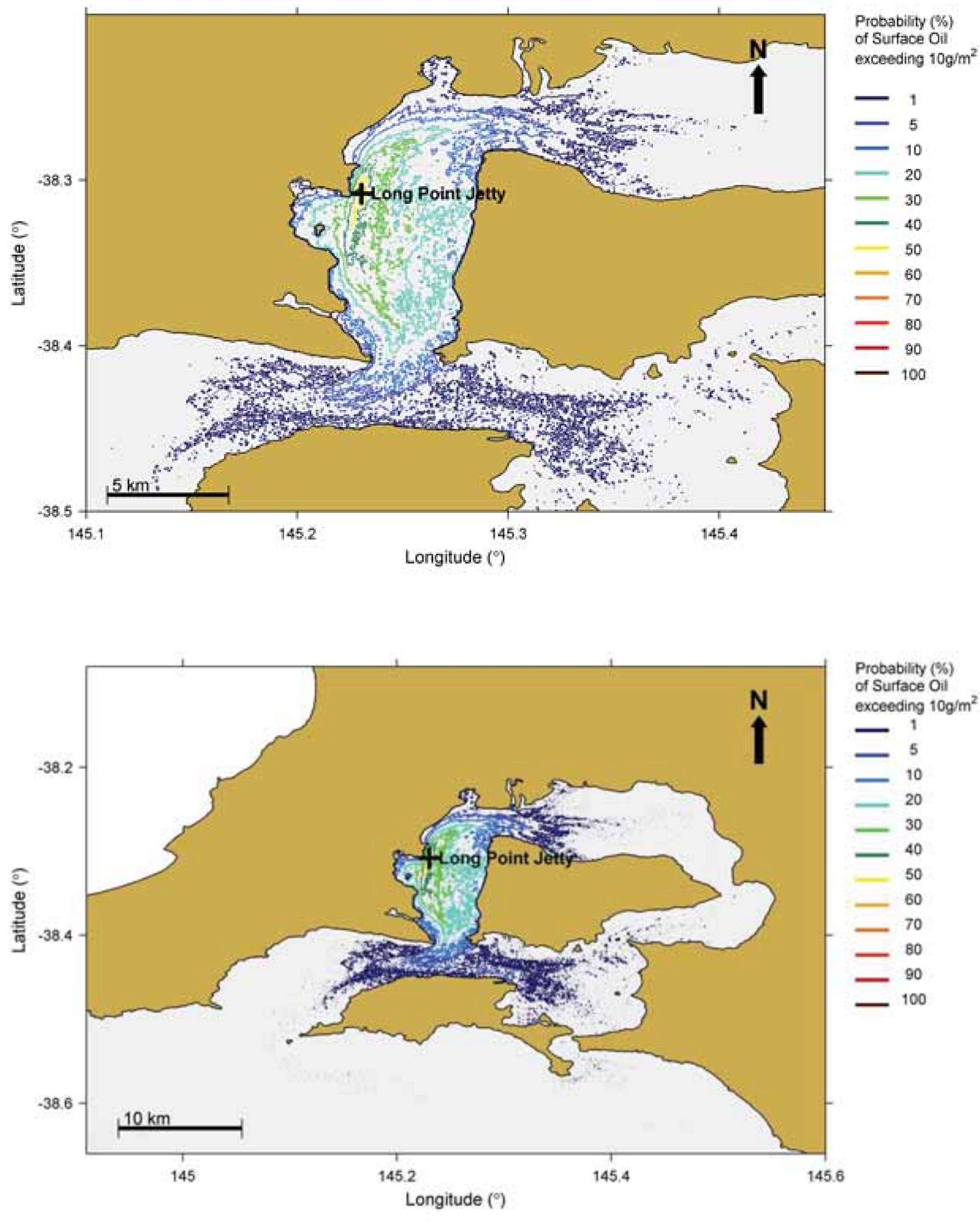

Figure 4-22: Probability contours for sea surface contact to concentrations above 10 g/m^2 resulting from a 80 m^3 diesel spill commencing during Winter. Dashed black line denote state/commonwealth boundary.

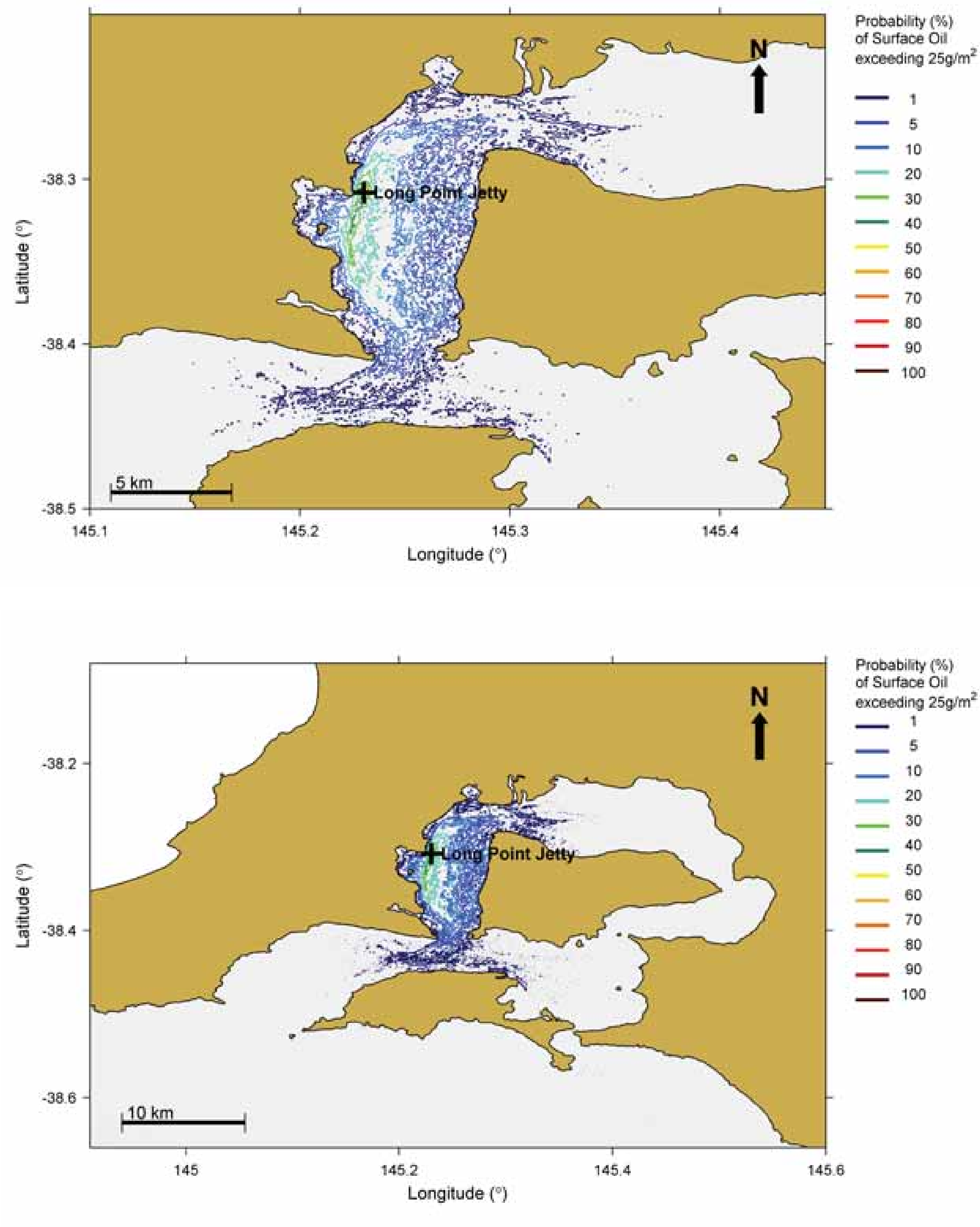

Figure 4-23: Probability contours for sea surface contact to concentrations above 25 g/m² resulting from a 80 m³ diesel spill commencing during Winter. Dashed black line denote state/commonwealth boundary

Table 4-8: Summary of risks for entrained oil concentrations in shallow waters resulting from a 80 m^3 spill of diesel commencing during Winter.

	Probability (%) of entrained hydrocarbon concentration > 10 ppb	Probability (%) of entrained hydrocarbon concentration > 100 ppb	Probability (%) of entrained hydrocarbon concentration > 500 ppb	Minimum time to shoreline (hours) at > 10 ppb	Minimum time to shoreline (hours) at > 100 ppb	Minimum time to shoreline (hours) at > 500 ppb	Maximum entrained hydrocarbon concentration (ppb) averaged among replicate spills	Maximum entrained hydrocarbon concentration (ppb) in the worse replicate
Yaringa Marine National Park	44	15	2	6	7	9	48	1,826
North Western Port Nature Conservation Reserve	48	17	3	9	9	57	56	1,389
French Island Marine National Park	57	30	7	6	7	14	174	6,489
Reef Island and Bass River Mouth Nature Conservation Reserve	12	3	NC	60	104	NC	11	496
Churchill Island Marine National Park	22	6	2	33	34	49	20	938
French Island National Park	74	47	19	5	5	5	432	23,366
Phillip Island Nature Park	52	22	6	27	27	27	118	4,020
Bunurong Marine Park	1	NC	NC	124	NC	NC	<1	49
Mushroom Reef Marine Sanctuary	NC	NC	NC	NC	NC	NC	NC	NC

NC: No contact to shorelines indicated at > threshold

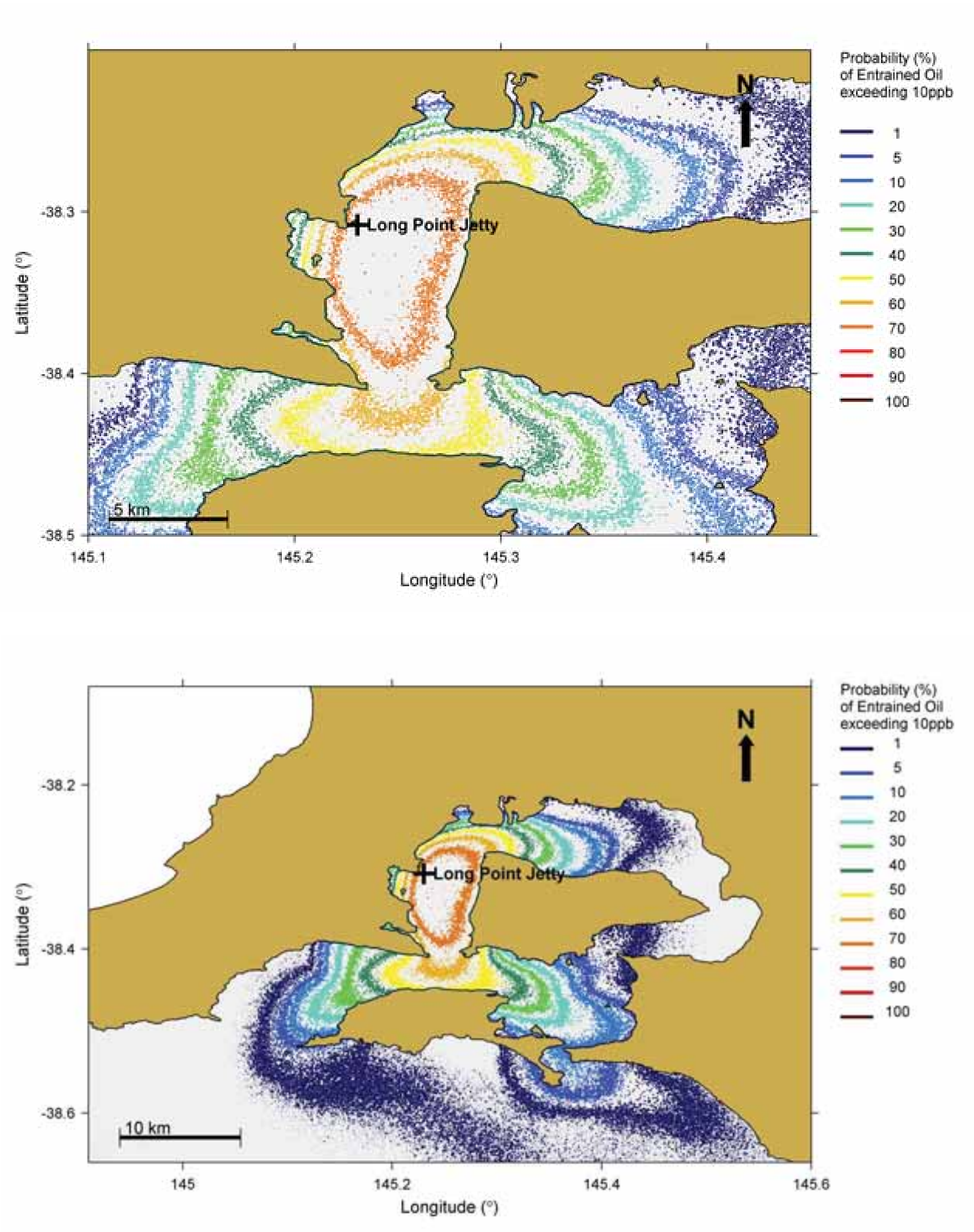

Figure 4-24: Probability contours for contact by entrained diesel exceeding 10 ppb resulting from a 80 m^3 spill of diesel commencing during Winter months.

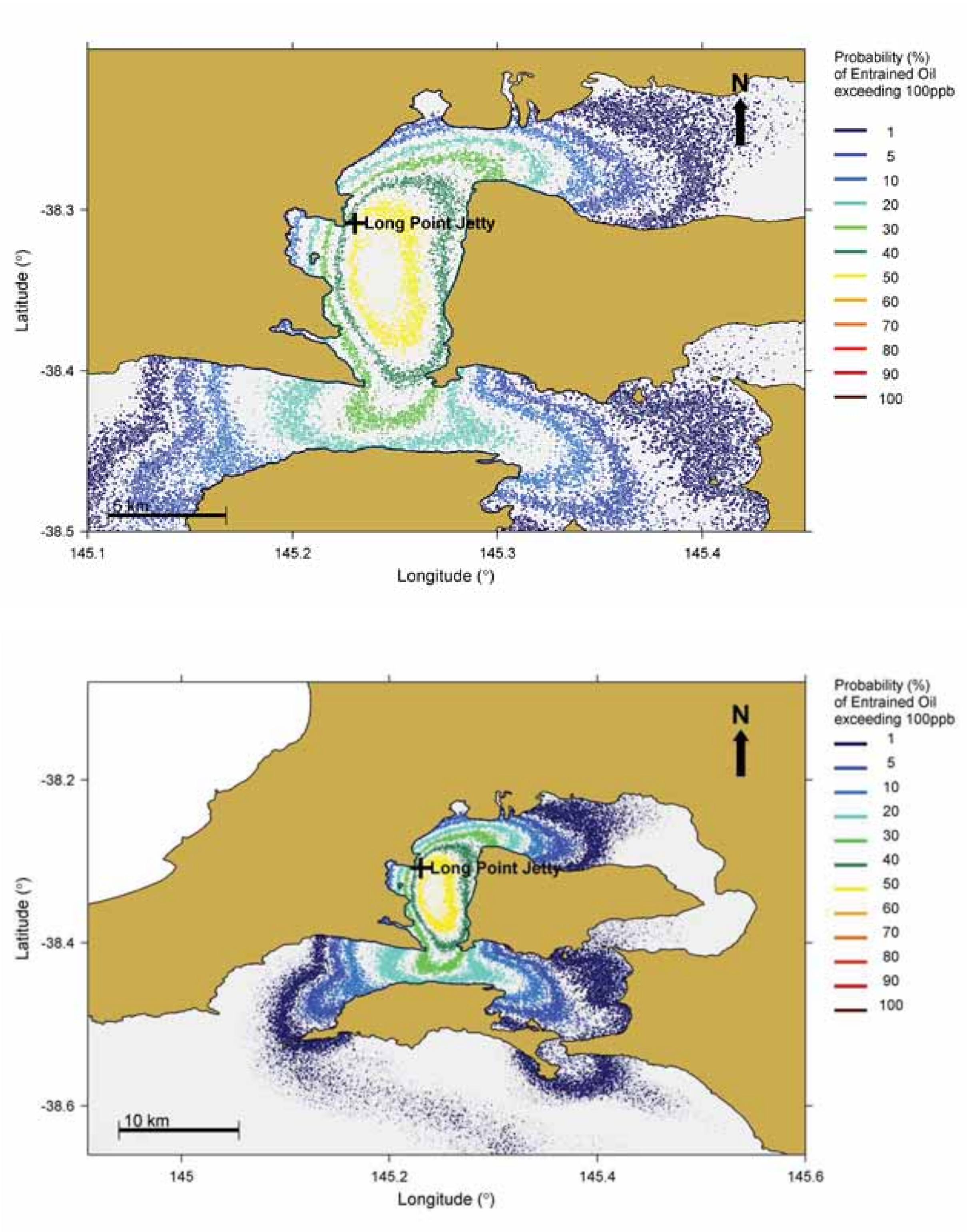

Figure 4-25: Probability contours for contact by entrained diesel exceeding 100 ppb resulting from a 80 m^3 spill of diesel commencing during Winter months.

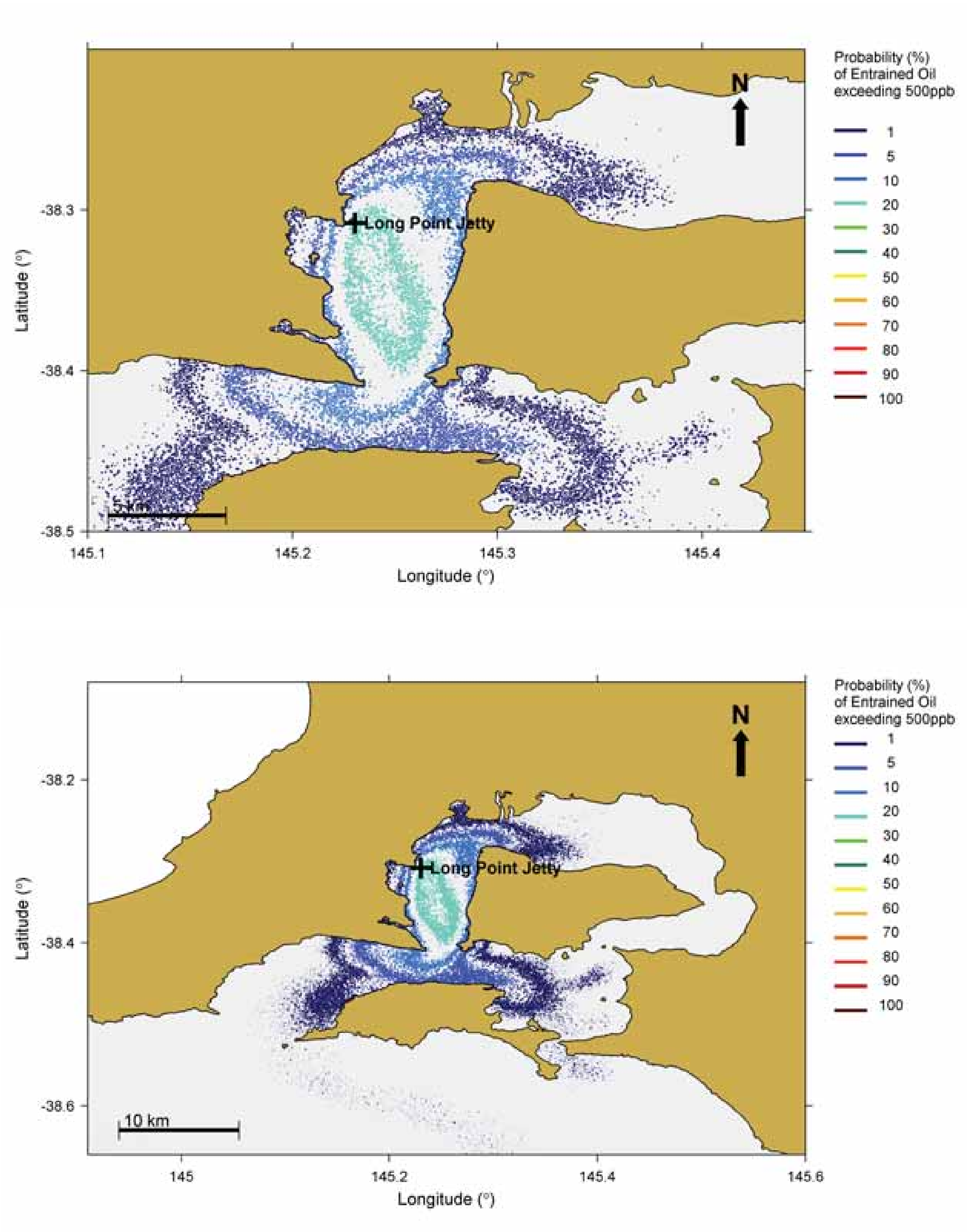

Figure 4-26: Probability contours for contact by entrained diesel exceeding 500 ppb resulting from a 80 m^3 spill of diesel commencing during Winter months

5 DISCUSSION & CONCLUSIONS

This risk assessment provides guidance on the potential outcomes of oil spills that might occur from shipping operations associated with the Port of Hastings, which is located in Western Port Bay, Victoria. The assessment considers the likely and possible outcomes of a number of defined spill scenarios involving the release of conservatively low volumes of fuel oil, relative to the size of some of the major oil spills that have occurred from shipping accidents in Australia (AMSA undated) and other countries (ITOPF undated). The assessment specifically quantifies the probability of exposure for surrounding shorelines and intertidal areas, the potential concentrations that could occur and the minimum potential response times that would be available to mount some form of response for specific locations along the shoreline.

The assessment is based on stochastic modelling of the transport and weathering processes that would affect the trajectory and fate of fuel oils spilled at Long Island Point Jetty or at McHaffie's Reef, which lies adjacent to the shipping channel used by ships approaching or leaving Port Hastings. Stochastic modelling involves repeated computer-simulation of the same spill scenario many times, using a different sequence of wind and current conditions in each simulation, to determine the likelihood of particular outcomes. By randomly selecting these sequences of wind and current data from a suitably long (multiple year) sample of the local wind and current conditions, the modelling will reveal both the more likely outcomes of a defined spill scenario (those generated by the more typical conditions) and the possible but less likely outcomes (those generated by less common conditions) that reflect variability in local conditions.

Spill scenarios were defined by the unique characteristics of the oil involved, the spill location, the volume of oil involved and the release duration. Spill modelling considered spills of two oil types commonly carried by ships and/or support craft: Heavy Fuel oil and diesel fuel. Because spill scenarios were chosen to represent potential spills from shipping operations, all spills were assumed to involve discharge at or onto the water surface. However, a fully three-dimensional oil spill model (SIMAP) was applied to the study to indicate the potential for exposure from floating oil, oil that strands on shorelines, oil that becomes physically entrained (mixed) within the water column and oil compounds that dissolve into the water column.

Representation of current forcing within Western Port Bay and approaches was provided by a detailed, three-dimensional, hydrodynamic model that represented the tidal wetting and drying of the extensive intertidal areas within the bay. Variations in current patterns over time and space were represented by simulation of three-dimensional current fields (i.e. varying vertically and horizontally) over a 3 year sample period (2009-2011, inclusive). Hourly records of the wind speeds and directions measured at Cerberus and Rhyll for the same 3 year period provided representation of the wind forces that would act on the water surface and floating oil. Hind-casts from this hydrodynamic model were well validated against the movement of drogues placed at a number of locations in Western Port Bay on a number of occasions, indicating good reliability in the prediction of current movement in the bay.

The main findings of this modelling study are as follows:

- The outcomes of a given spill scenario will depend strongly upon the oil type, spill location and the current and wind patterns that prevail over the post-spill period.
- Complex tidal currents are active within Western Port Bay. Higher speed tidal flows, which would exert the highest influence on the transport of spilled oil, are restricted to a complex of channels that link through the various sub areas of the estuary system, while generally weaker currents occur over broad areas of shallower water. Spills into or adjacent to major shipping channels are likely to result in floating oil slicks repeatedly migrating along the main tidal channels over a series of flood and ebb tides. However, moderate to strong wind acting at an angle across the tidal channels will tend to displace the slicks from the main tidal channels into areas where there is a decreased tidal influence and an increased influence of wind forcing. Under the influence of wind acting across the tidal channels, slicks will tend to drift from the channels to expose lee shores.
- A large proportion of an HFO spill would not evaporate and the residual oil may take up quantities of water to form an oil in water emulsion. Consequently, the residual will continue to migrate over the short to medium term (hours to days) as surface slicks, moving under the changing influence of the tidal migrations and wind forces until the oil strands onto shorelines. In contrast, diesel oil spilled onto the water will spread rapidly and a higher proportion (~ 40-50 %) would evaporate over a period of < 12 hrs. leaving a residual component that will be distributed both on and in the water column
- Due to the length of the tidal migrations and the connectivity of the channels, slicks will tend to break up over time and portions of the oil may enter different sections of the bay depending upon the source location, the timing of the spill relative to the tidal phase (e.g. spring versus neap tides) and the wind conditions over the period. This has implications for the extent of locations that might be affected by oil contamination, with a higher probability that exposure would be widespread rather than localised.
- The predominance of southerly winds during summer and northerly winds during the winter is forecasted to result in higher likelihoods that floating oil will drift northward at a greater rate during summer - the wind impeding the speed of movement due to the prevailing tidal currents over ebbing tides and increasing the speed of movement over flooding tides. The reverse trend is indicated for spills that occur in winter.

Spills from Long Point Island Jetty have the potential to affect all shorelines within North Arm, extending to the mudflats in the north-eastern sector of Western Port Bay. Most of the areas designated as National Parks or marine reserves within Western Port Bay are indicated to be at risk of contamination, at varying probabilities, with higher probabilities of significant concentration accumulating along the western and north western shoreline during summer. Potential loads into Yaringa Marine National Park around Quail Island are forecasted to be very high (> 17 kg/m^3 as oil), for a moderate HFO spill and also high (> 3 kg/m^3) for a relatively large diesel spill. Because the mode of negative effects for these two oil types are likely to be different – smothering and direct contact toxicity in the case of HFO and toxicity for diesel, both concentrations are likely to result in extensive impacts to the local fauna and flora. Considerations of environmental effects should also consider the longer-term outcomes, particularly for HFO residues that have the potential to contaminate the extensive mudflats and wetland sediments to become a source of leaching hydrocarbons for decades.

Moderate (80 m^3) spills of diesel at Long Point Island Jetty are also forecasted to present a high probability of exposure to entrained diesel at concentrations > 500 ppb for intertidal and shallow subtidal zones (< ~ 3 m depth) throughout Northern Arm, with plumes likely to oscillate with the tidal currents to affect multiple dosages for habitats. Concentrations are expected to decrease substantially beyond the Confluence Zone between Eastern Channel and Western Channel.

Spills of HFO at McHaffie's Reef are most likely to drift with the strong tidal currents that migrate along the Eastern Entrance Channel, with proportions of the oil likely to move into the Confluence Zone and into both North Arm and the Eastern Arm through the Rhyll Segment. Seasonal wind patterns are also likely to affect the outcomes, with a high likelihood that oil will accumulate on the north west and north coast of Phillip Island and considerable concentrations if a spill occurs in winter but oil more likely to spread over the Eastern Arm and potentially strand on shorelines of North Arm and East Arm if the spill occurs in summer.

Of particular note, the modelling indicated that exposure to designated marine reserves and national parks could occur within about 6 hours or less, providing a short time for any effective response to be made to reduce levels of contamination in these locations. Consideration must also be given to the effectiveness of available response techniques and equipment. While the forecast for slicks to most likely stream along the tidal channels with the tides, at least over the first day, would improve the potential for oil slicks to be contained, the hydrodynamic modelling indicates that the speed of the tidal streams would be too great for booming equipment that is currently available – which is limited to about 0.3-0.4 m/s (0.7 knots). Oil would tend to entrain under booms that were fixed in place as barriers across the tidal streams as current speeds exceed these performance limits.

Spills of HFO have historically proven to result in greater persistence and environmental consequences, both short-term and long term, compared to lighter oils due to their low volatility and high viscosity/stickiness, and they present particular challenges for effective response (Gunter, undated). Practical difficulties include fouling of booming equipment, entrainment under booms, difficulties in pumping waste oil and handling of emulsified oils. The high viscosity of the residuals also makes it difficult to isolate from contaminated sediment, forcing removal of contaminated sediment with associated disturbance of the habitat. HFOs are also considered difficult to treat with chemical dispersants, due to their high viscosity, although some modern dispersants can be effective on some blends. However, this treatment would increase the dispersion of oil into the water column, increasing exposure to subtidal habitats. Previous modelling assessments have indicated that the use of chemical dispersant on oil spills in Western Port Bay would yield a net negative environmental effect because dispersant application, if it could be conducted in time, because this treatment would not effectively reduce the concentrations of untreated oil that could drift ashore but would markedly increase the concentration of entrained oil and soluble hydrocarbons within the water column and over the shallow intertidal fringes of the waterway – increasing the potential for deleterious effects on intertidal and subtidal organisms (Zigic et al. 2011). These considerations indicate that response efforts would be limited to attempts to deflect oil and to remove oil from contaminated shorelines after oil comes ashore, likely requiring removal of contaminated sediment. Previous attempts to conduct such clean-ups after major spills of heavy oils that resulted in contamination of soft-sediment habitats and other shorelines have proven to be limited in effectiveness, even with very high resourcing and associated costs (Bryner 2010). Past events of a similar nature to those represented in the modelling also indicate the high potential for long term legacy effects lasting multiple decades due to slow leaching of oil from contaminated sediments that remain despite these efforts (e.g. Peterson 2003).

The indications from the modelling that large areas of shoreline might be affected by a single spill event suggests that the effort and cost of this effort would also be high in the setting of Western Port Bay, while the nature of the sensitive habitats suggest that long term contamination of areas that receive heavy fuel oil would be highly likely.

Spills of diesel are more likely to have greater shorter term consequences for organisms on and in the water column, because of the tendency of a large proportion of this fuel to entrain into through the water column. Entrainment will be increased under increased wave action over the open water and against shorelines. The churning of diesel into the water at shorelines has been observed to cause high mortality of invertebrate epifauna and megafauna as well as fish that occupy shoreline habitats (French 1998).

Figure 5-1: Diesel leaking from the Lady Cheryl*, which sunk in Port Phillip Bay in 2012, showing the dispersion of the fuel into the water as a white milky cloud (Source: www.abc.net.au).*

6 REFERENCES

Andres B.A (1999) Effects of persistent shoreline oil on breeding success and chick growth in black oystercatchers. The Auck, vol. 116, No. 3 July 1999.

AMSA (2002). *National Marine Oil Spill Contingency Plan*. Australian Maritime Safety Authority, Canberra, ACT, Australia.

AMSA (undated) Major Oil Spills in Australia. Australian Maritime Safety Authority. http://www.amsa.gov.au/marine_environment_protection/major_oil_spills_in_australia/

BA (2003). *Extended Guidelines for the Use of the Bonn Agreement Oil Appearance Code (BAOAC)*. Bonn Agreement Secretariat, London, UK.

Bryner, J (2010) Experts: Most of the Gulf oil spill won't be cleaned up. Live Science 29 April 2010

Deltares (2011). "Delft3d-FLOW User Manual", Deltares. Delft, The Netherlands. V 3.15.

Egbert, G.D and Erofeeva, S.Y (2002): "Efficient inverse modeling of barotropic ocean tides", J. Atmos. Oceanic Technol., 19(2), 183-204.

Flater, D (1998). *XTide Harmonic Tide Clock and Tide Predictor*. (www.flaterco.com/xtide/)

French, D.P (1998). Modelling the impacts of the North Cape oil spill. *Proceedings of the 21st Arctic and Marine Oil Spill Program Technical Seminar*, June 1998, Edmonton, Alberta, Canada (387-430).

French, D.P (2000b). Estimation of oil toxicity using an additive toxicity model. *Proceedings of the 23rd Arctic and Marine Oil Spill Program Technical Seminar*, June 2000, Vancouver, British Columbia, Canada (561-600).

French, D. P (2001) Modelling Oil Spill Impacts. In State of the Art in Oil Modelling and Processes, Garcia-Martinez, R and Brebbia, R (eds.), WIT Press, Ashurst Lodge, Ashurst, Southampton, UK, 2001.

French, D.P, Brown, G, MacDonald, E, Quirk, J, Natzke S and Ingram B.S, Bishop, R, Welsh, M and Phillips, M (1996). The CERCLA type a natural resource damage assessment model for coastal and marine environments (NRDAM/CME), Technical Documentation, Vol. V, Economic Databases. Final Report, Submitted to the Office of Environmental Policy and Compliance, U.S. Dept. of the Interior, Washington, DC, April, 1996, Contract No. 14-01-0001-91-C-11.

French, D, Howlett E and Mendelsohn D (1994). Oil and chemical spill impact model system description and application. Pp. 815-835. In *Proceedings of 17th Arctic and Marine Oil Spill Program (AMOP) Technical Seminar*, Ottawa, Canada.

French, D.P & Rines, H.M (1997). Validation and use of spill impact modelling for impact assessment. *Proceedings of the 1997 International Oil Spill Conference*, April 1997, Fort Lauderdale, FL, USA (829-834).

French, D.P, Schuttenberg, H & Isaji, T (1999). Probabilities of oil exceeding thresholds of concern: examples from an evaluation for Florida Power and Light. *Proceedings of the 22nd Arctic and Marine Oil Spill Program Technical Seminar*, June 1999, Calgary, Alberta, Canada (243-270).

French, D. P, (1998) Estimate of Injuries to Marine Communities Resulting from the North Cape Oil Spill Based on Modeling of Fates and Effects. Report to US Department of Commerce, National Oceanic and Atmospheric Administration (NOAA), Damage Assessment Center, Silver Spring, MD, January 1998. Available in Administrative Record, North Cape Restoration Plan, NOAA Damage Assessment Center, Silver Spring, MD, 101p plus appendices.

French-McCay, D.P (2002). Development and application of an oil toxicity and exposure model, OilToxEx. *Environmental Toxicology and Chemistry* Vol. 21, pp. 2080–2094.

French McCay, D.P (2004) Oil spill impact modelling: development and validation. *Environmental Toxicology and Chemistry*: Vol. 23, no. 10, pp. 2441-2456.

Gerritsen, H, de Goede, E.D, Platzek, F.W, Genseberger, M, van Kester, J.A.Th.M and Uittenbogarrd, R.E (2007). Validation Document Delft3D-FLOW. Report X0356, M3470. Delft Hydraulics.

Gunter, P (undated). The particularities of Heavy Fuel Oil. *Interspill* Conference. http://www.interspill.com/previous-events/2009/13-May/pdf/1530_gunter.pdf

Goodman, R (2007). *Oil on Water Sheens*. Innovative Ventures Ltd., Cochrane, Alberta, Canada.

Gordon, R (1982). *Wind driven circulation in Narragansett Bay*. Ph.D. Thesis. Department of Ocean Engineering, University of Rhode Island, Kingston, RI, USA.

Gerritsen, H, de Goede, E.D, Platzek, F.W, Genseberger, M, van Kester, J.A.Th.M. and Uittenbogaard, R.E (2007) “Validation Document Delft3D-FLOW”. Deltares. Delft, The Netherlands. V 1.0.

Harris, J.E, Hinwood, J.B, Marsden, M.A.H & Sternberg, R.W (1979), ‘Water movement, sediment transport and deposition, Western Port, Victoria’, *Marine Geology*, vol. 30, 131–61.

Harris, J.E, Robinson, J.B (1979), ‘Circulation in Western Port, Victoria, as deduced from salinity and reactivesilica distributions’, *Marine Geology*, Vol. 30 101–16.

Hinwood, J.B (1979), ‘Hydrodynamic and transport models of Western Port, Victoria’, *Marine Geology*, vol. 30, 117–30.

Hinwood, J.B & Jones, J.C.E (1979), ‘Hydrodynamic data for Western Port, Victoria’, *Marine Geology*, vol. 30, 47–63.

Isaji, T. & Spaulding, M.L (1984). A model of the tidally induced residual circulation in the Gulf of Maine and Georges Bank. *Journal of Physical Oceanography* **14**: 1119-1126.

Isaji, T. & Spaulding, M.L (1986). A numerical model of the M_2 and K_1 tide in the northwestern Gulf of Alaska. *Journal of Physical Oceanography* **17**: 698-704.

Isaji, T, Howlett, E, Dalton, C and Anderson, E (2001). Stepwise-continuous-variable-rectangular grid. *Proceedings of the 24th Arctic and Marine Oil Spill Program Technical Seminar*, June 2001, Edmonton, Alberta, Canada (597-610).

ITOPF (undated). Database of accidental spills from shipping. The International Tanker Owners Pollution Federation Limited

http://www.itopf.com/information-services/data-and-statistics/statistics/#major

Johansen, Ø, Rye, H and Cooper, C (2003). DeepSpill – field study of a simulated oil and gas blowout in deep water. *Spill Science & Technology Bulletin* **8** (5-6): 433-443.

King, B. & McAllister, F.A (1998). Modelling the dispersion of produced water discharges. *APPEA Journal* **38**: 681-691.

Koops, W, Jak, R.G and van der Veen, D.P.C (2004). Use of dispersants in oil spill response to minimize environmental damage to birds and aquatic organisms. *Interspill 2004*, June 2004, Trondheim, Norway (presentation 429).

NASA http://ntrs.nasa.gov/archive/nasa/casi.ntrs.nasa.gov/19990089548_1999150788.pdf

National Research Council (2005). *Oil Spill Dispersants: Efficacy and Effects*. Washington, DC: The National Academies Press.

NOAA (1982). *Climatological Atlas of the World Ocean*. National Oceanic and Atmospheric Administration, Rockville, MD, USA.

NRC 2005. Oil Spill Dispersants: Efficacy and effects. National Research Council of the National Academies. The National Academies Press. Washington, D. C. ISBN 030909562p

Oke, P.R, Brassington, G.B, Griffin, D.A and Schiller, A (2008). The Bluelink ocean data assimilation system (BODAS). *Ocean Modelling* **21**: 46-70.

Oke, P.R, Brassington, G.B, Griffin, D.A and Schiller, A (2009). Data assimilation in the Australian Bluelink system. *Mercator Newsletter* **34**: 35-44.

Okubo, A (1971). Oceanic diffusion diagrams. *Deep-Sea Research* **18**: 789-802.

Owen, A (1980). A three-dimensional model of the Bristol Channel. *Journal of Physical Oceanography* **10**: 1290-1302.

Owens, E.H & Sergy, G.A, (1994). *Field Guide to the Documentation and Description of Oiled Shorelines,* Environmental Technology Centre, Environment Canada, 66 p.

Pace, C.B, Clark, J.R and Bragin, G.E (1995). Comparing crude oil toxicity under standard and environmentally realistic exposures. *Proceedings of the 1995 International Oil Spill Conference*, American Petroleum Institute, Washington, DC (1003-1004).

Peterson, H, Rice, S.D, Short, J.W, Esler, D, Bodkin, J.L, Ballachey, B. E and Irons, D (2003). Long-Term Ecosystem Response to the Exxon Valdez Oil Spill. Science 19 Vol. 302 no. 5653 pp. 2082-2086

Schiller, A, Oke, P.R, Brassington, G.B, Entel, M, Fiedler, R, Griffin, D.A and Mansbridge, J.V (2008). Eddy-resolving ocean circulation in the Asian-Australian region inferred from an ocean reanalysis effort. *Progress in Oceanography* **76**: 334-365.

Solbakken, J.E, Knap, A.H, Sleeter, T.D, Searle, C.E & Palmork, K. H (1984) Investigation into the fate of 14C-labelled xenobiotics (naphthalene, phenanthrene, hexachlorobiphenyl, octachlorostyrene) in Bermudian corals. Marine Ecology – Progress Series. Vol. 16: 149-154.

Spaulding, M.L, Bishnoi, P.R, Anderson, E & Isaji, T (2000). An integrated model for prediction of oil transport from a deep water blowout. *Proceedings of the 23rd Arctic and Marine Oil Spill Program Technical Seminar*, June 2000, Vancouver, British Columbia, Canada (611-636).

Sternberg R.W (1979). 'Bottom-current measurements and circulation in Western Port, Victoria', *Marine Geology*, Vol. 30, 65–83.

Willmott, C.J (1981). On the Validation of Models. Physical Geography 2, 184-194.

Willmott, C.J (1982). Some comments on the evaluation of model performance, Bulletin of the American Meteorological Society, pp 1309 – 1313.

Willmott, C.J & Matsuura, K (2005). Advantages of the mean absolute error (MAE) over theroot mean square error (RMSE) in assessing average model performance, Journal of Climate Research, Vol 30, pp 79 – 82.

Yapa, P.D. & F. Chen (2004). Behaviour of oil and gas from deepwater blowouts. *Journal* of *Hydraulic Engineering* **130** (6): 540-553.

Zigic, S, Zapata, M, Isaji, T, King, B & Lemckert, C (2003). Modelling of Moreton Bay using an ocean/coastal circulation model. *Coasts and Ports Australasian Conference*, September 2003, Auckland, New Zealand (paper 170).

Zigic, S, King, B and Langtry, S (2011) Quantifying the net environmental benefit of using dispersant on oil spills in Western Port Bay, Victoria. Proceedings of the Coasts and Ports conference, 2011.